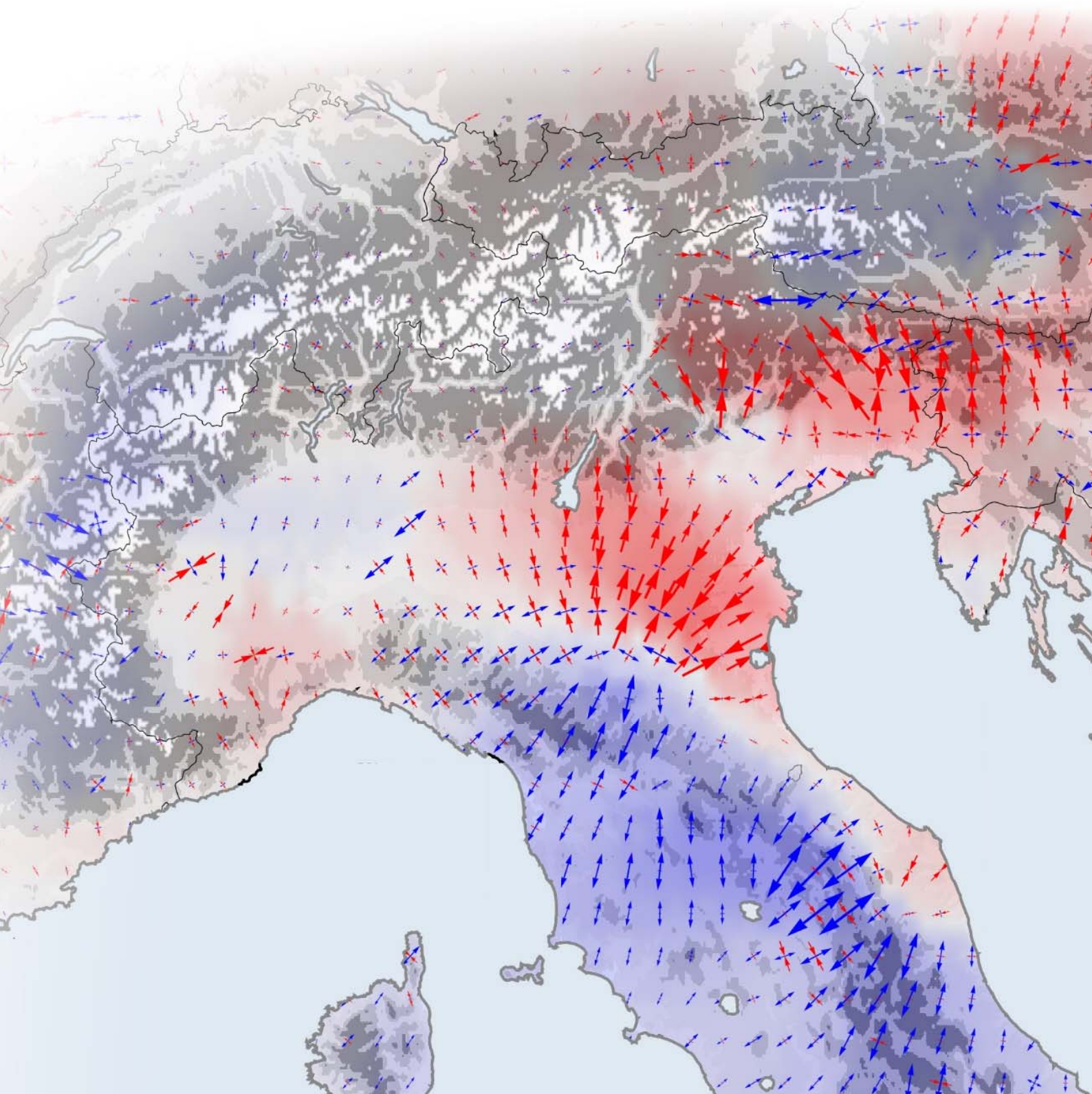


# Annual Report 2018

Deutsches Geodätisches Forschungsinstitut  
der Technischen Universität München  
(DGFI-TUM)



Front cover:

The picture displays the horizontal strain field of the Alpine and Apennine region, where red areas indicate compression, and blue areas indicate lateral spreading. These data are the result of an extensive analysis of observations that were collected by more than 300 GPS stations over a period of twelve years. A large number of the stations were set up in the EU project ALPS-GPSQUAKENET and are in part operated by the DGFI-TUM.

Through homogeneous processing of several billion observed data items, the position changes of the stations could be identified accurate down to fractions of a millimeter and thus make the movements of the mountain ranges visible on a comprehensive basis. The measured values were used to create a computer model that illustrates horizontal and vertical shifts as well as lateral spreading and compression over the entire Alpine and Apennine region at a resolution of 25 kilometers.

The model depicts visibly both large-scale patterns of movement and regional special factors. Each year the Alps grow an average of 1.8 millimeters in height and move to the northeast at a speed of up to 1.3 millimeters. These changes in the surface of the Earth serve as the basis for inferences regarding underground plate tectonics. The research was conducted in collaboration with the Geodesy and Glaciology project of the Bavarian Academy of Sciences and Humanities. Details on the data processing and the results of the study are presented in Section 1.1 of this report.

Technische Universität München  
Ingenieur fakultät Bau Geo Umwelt  
Deutsches Geodätisches Forschungsinstitut (DGFI-TUM)

Arcisstr. 21  
D - 80333 München

[www.dgfi.tum.de](http://www.dgfi.tum.de)

# Contents

<b>Preface</b>	<b>1</b>
<b>1 Research Area Reference Systems</b>	<b>5</b>
1.1 Analysis of Space-Based Microwave Observations . . . . .	6
1.2 Analysis of Satellite Laser Ranging Observations . . . . .	8
1.3 Computation of Satellite Orbits . . . . .	10
1.4 Determination of Reference Frames . . . . .	12
<b>2 Research Area Satellite Altimetry</b>	<b>22</b>
2.1 Multi-Mission Analysis . . . . .	22
2.2 Sea Surface . . . . .	23
2.3 Inland Altimetry . . . . .	33
<b>3 Cross-Cutting Research Topics</b>	<b>38</b>
3.1 Atmosphere . . . . .	38
3.2 Regional Gravity Field . . . . .	50
3.3 Standards and Conventions . . . . .	54
<b>4 Information Services and Scientific Transfer</b>	<b>57</b>
4.1 Internet representation . . . . .	57
4.2 Membership in scientific bodies . . . . .	60
4.3 Publications . . . . .	64
4.4 Posters and oral presentations . . . . .	66
4.5 Participation in meetings, symposia, conferences . . . . .	75
4.6 Guests . . . . .	79
<b>5 Projects</b>	<b>80</b>
<b>6 Personnel</b>	<b>81</b>
6.1 Lectures and courses at universities . . . . .	81
6.2 Lectures at seminars and schools . . . . .	81
6.3 Thesis supervision . . . . .	82
6.4 Conferral of Doctorates . . . . .	82
6.5 International Research Stays . . . . .	82



## Preface

### The Institute

The Deutsches Geodätisches Forschungsinstitut (DGFI-TUM) is a research institute of the Technical University of Munich (TUM) where it is part of the Chair of Geodetic Geodynamics within TUM's Faculty of Civil, Geo and Environmental Engineering (BGU).

The institute's scientific focus is on basic research in the field of Space Geodesy with the ambition to provide a comprehensive and long-term valid metric of the Earth system for science and practice at the highest level of precision and consistency. In strong international and interdisciplinary collaboration, DGFI-TUM processes, analyses and combines observations from all relevant space-geodetic observing systems and complementary data sources.

For almost seven decades, the institute has continuously been involved in a broad variety of national and international research activities of which many were of high significance for the scientific advancement of geodesy. A central aspect of the institute's research has always been the precise determination of the Earth's geometrical shape and its temporal changes. For the solid Earth, this involves in particular the realization of global and regional horizontal and vertical terrestrial reference systems and of the celestial reference system. With respect to water surfaces, the DGFI-TUM has a key focus on the precise determination of the changing sea level, the ocean's surface dynamics and water stages of inland water bodies using satellite altimetry.

DGFI-TUM's strategic focus is reflected by its organization into the two research areas *Reference Systems* and *Satellite Altimetry* (Fig. 1). The two research areas are complemented by three overarching research topics that cover the investigation of the state and dynamics of the atmosphere (with a strong focus on ionospheric disturbances and space-weather impacts), the determination of high resolution regional gravity fields, and the enhancement of consistency in geodetic data analysis by establishing unique standards and conventions in an international context.

In the frame of the Research Group Satellite Geodesy (Forschungsgruppe Satellitengeodäsie, FGS), the institute contributes to the scientific data processing of the Geodetic Observatories Wettzell (Germany) and AGGO (Argentina). Furthermore, it operates several worldwide distributed GNSS stations.

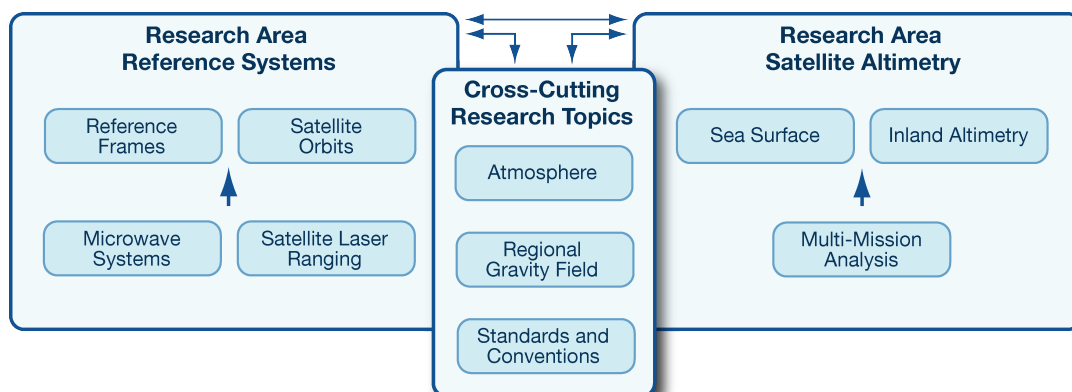


**Figure 1:** Research Areas of the DGFI-TUM

## National and international involvement

The institute was originally established in 1952 as an independent research facility at the Bavarian Academy of Sciences and Humanities (BAW) in Munich, and with effect from January 1, 2015 the DGFI became part of the TUM. The institute is intensively networked with renowned research institutions all over the world, and over its history it has been involved in a multitude of internationally coordinated scientific activities. During the first decades after its foundation, DGFI achieved outstanding results particularly in the fields of geodetic-astronomical observations and electro-optical distance measurements for the determination of the German and European triangulation as well as in gravimetric surveys for gravity networks. The DGFI was involved in the first worldwide network of satellite triangulation and played an important role in the development of dynamical methods of satellite geodesy for precise orbit determination, point positioning and gravity field modelling.

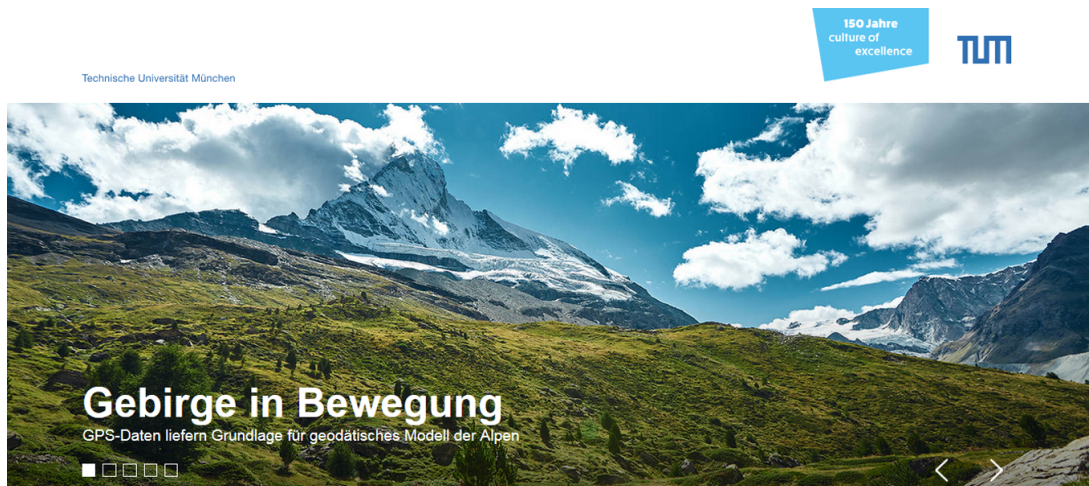
The DGFI-TUM collaborates at key positions in international scientific organizations, especially within the framework of the International Union of Geodesy and Geophysics (IUGG), the International Astronomical Union (IAU), and the International Association of Geodesy (IAG). In particular, the institute recognizes the outstanding role of IAG's Scientific Services that form the backbone of national and international spatial data infrastructure. In this context, the DGFI-TUM operates data centers, analysis centers and research centers, and it has taken leading roles and supporting functions in IAG's Commissions, Projects, Working and Study Groups. Scientists of DGFI-TUM occupy central positions in several international organizations (see Section 4.2) and thus contribute to shaping the future direction of international geodetic research. In IAG's Global Geodetic Observing System (GGOS) that coordinates the generation of high-quality science data products under predefined standards and conventions, the DGFI-TUM has a position of particular importance by chairing the GGOS Bureau of Products and Standards and two of the four GGOS Focus Areas (see Section 3.3).

The DGFI-TUM also participates in research programmes of the European Union (EU) and the European Space Agency (ESA), and it cooperates in activities of the United Nations (UN). In this regard, the institute is involved in the implementation of a UN Resolution for a Global Geodetic Reference Frame (GGRF) and provides an IAG representative to the UN Working Group for the Global Geodetic Reference Frame (GGRF).

## Research highlights of particular scientific and public interest

During the year 2018, several scientific results of the DGFI-TUM gained broad attention in the scientific community and in the public. The following activities and publications can be highlighted.

- Mountains in motion: A comprehensive model of the present-day surface-kinematics in the Alpine-Adriatic region was created by high-level data analysis of more than 300 continuously operating GNSS stations distributed over the entire chain of the Alps, its foreland and the Apennines (see title page). Based on the newest GNSS processing standards, measurement data over 12 years was homogeneously analyzed to determine the three-dimensional changes of the station coordinates with a mean precision of 0.2 mm/a in the horizontal direction, and 0.4 mm/a in the height. The model illustrates coherent patterns of on-going uplift processes and horizontal deformations with respect to the Eurasian Plate and will serve as the basis for inferences regarding underground plate tectonics (*Present-day surface deformation of the Alpine region inferred from geodetic techniques*, Earth System Science Data, 2018, doi:[10.5194/essd-10-1503-2018](https://doi.org/10.5194/essd-10-1503-2018)). See Section 1.1. for further details.



- Reference Systems – the Backbone for Positioning, Navigation and Earth System Research: Triggered by the need of a precise reference on Earth and in space, the DFG research unit “Space-Time Reference Systems for Monitoring Global Change and for Precise Navigation in Space” (FOR1503) aims at developing integrative methods and procedures for a consistent definition and realization of geodetic reference systems. DGFI-TUM is involved in the FOR1503 with two studies that were part of a special issue of the Journal of Geodesy (2018). The study *Consistent estimation of geodetic parameters from SLR satellite constellation measurements* (Journal of Geodesy, 2018, doi:[10.1007/s00190-018-1166-7](https://doi.org/10.1007/s00190-018-1166-7)) highlights the benefits of a consistent exploitation of satellite laser ranging (SLR) observations to a multi-satellite constellation for the joint estimation of reference frame parameters, satellite orbits, low-degree gravity field coefficients and Earth orientation parameters (EOP). The study *Consistent realization of celestial and terrestrial reference frames* (Journal of Geodesy, 2018, doi:[10.1007/s00190-018-1130-6](https://doi.org/10.1007/s00190-018-1130-6)) addresses the first combined solution of the global Terrestrial Reference Frame (TRF), the Celestial Reference Frame (CRF) and the EOP from different space-geodetic observing techniques. With this study, DGFI-TUM, for the first time, realized the IUGG Resolution R3 (2011) which urges that highest consistency between TRF, CRF and EOP should be a primary goal of all future realizations. See Section 1.4 for details.
- Virtual contact lenses for radar satellites: The observation of changes in sea level and ocean currents in the ice-covered regions of the Arctic and Antarctic is particularly challenging, as the radar signals of altimeter satellites are reflected by the ice. But where ocean wa-



ter passes through openings in the permanent ice, the water surface can now be measured using the newly developed analysis method ALES+ (Adaptive Leading Edge Subwaveform Retracker). This algorithm automatically identifies the portion of the radar signals that is reflected by water and derives sea level values. ALES+ has been developed in the frame of DGFI-TUM's involvement in the ESA Climate Change Initiative on Sea Level (*ALES+: Adapting a homogenous ocean retracker for satellite altimetry to sea ice leads, coastal and inland waters*, Remote Sensing of Environment, 2018, doi:10.1016/j.rse.2018.02.074). A press release was issued by TUM in 2018, addressing the importance of sea level observations in high latitude for the understanding of climate-related changes in ocean dynamics. Further details can be found in Section 2.2.

- Extension of ocean research from sea level to sea state: In 2018, the ESA Climate Change Initiative on Sea State was launched. DGFI-TUM is strongly involved in this international effort comprising 14 partner institutions. The initiative targets at the development of a consistent multi-decadal global record of sea state parameters to investigate wave heights and related wind fields as well as their temporal evolution in the context of climate change. DGFI-TUM is leading the algorithm development for the satellite altimetry part of the project. See Section 2.2. for more details.
- Upgrade of DGFI-TUM's *Database for Hydrological Time Series of Inland Waters (DAHITI)*: DAHITI provides water level time series of more than 1600 inland water bodies such as lakes and rivers from satellite altimetry. Now, along with the water levels, also time series of surface water extents are available for a variety of lakes. The water surfaces are extracted from optical Landsat and Sentinel-2 images using a newly developed algorithm. By combining the vertical changes in water level with the horizontal changes in surface area, also fluctuations of volume and water storage can be computed. More information is provided in Section 2.3.
- Successful completion and extension of the project OPTIMAP: For several years, OPTIMAP has been DGFI-TUM's flagship project in space-weather research. It is funded by the Bundeswehr GeoInformation Centre (BGIC) and aimed at the development of an operational system for near real-time (NRT) Vertical Total Electron Content (VTEC) maps with variable spectral resolution. A unique feature of the VTEC modelling in OPTIMAP is the implementation of a Multi-Kalman-Filter (MKF) procedure for NRT processing of various space-geodetic observations with different latencies. The MKF also allows for generating VTEC forecasts up to four days. The project was completed successfully in 2018. The developed procedure serves as the basis for a project extension of three years in which the NRT model shall be transferred to real-time applications; see Section 3.1.
- Committee on *Essential Geodetic Variables (EGVs)*: In 2018, the Committee on the definition of EGVs has been established as a GGOS component associated with the Bureau of Products and Standards (BPS) chaired by DGFI-TUM (see Section 3.3). The members of the Committee on EGVs comprise the GGOS Science Panel, representing the IAG Commissions, the Inter-Commission Committee on Theory, the four GGOS Focus Areas (Unified Height System, Geohazards, Sea Level, and Geodetic Space Weather Research), and representatives of the IAG Services. Examples for such EGVs are the position of reference objects (geodetic ground stations, radio sources), EOPs, ground- and space-based gravity measurements. EGVs will serve as a basis for a gap analysis to identify requirements concerning observational properties and networks, accuracy, as well as spatial and temporal resolution and latency.



# 1 Research Area Reference Systems

Research in the field of reference systems and the precise determination of global and regional reference frames has been a key focus of the institute for many years. The computation of reference frames relies on the space geodetic observation techniques Very Long Baseline Interferometry (VLBI), Satellite and Lunar Laser Ranging (SLR/LLR), Global Navigation Satellite Systems (GNSS), and Doppler Orbitography and Radiopositioning Integrated by Satellite (DORIS). The work in this research area involves a refined modelling and analysis of these observation techniques and the development of advanced combination methods. As a backbone for this work, DGFI-TUM employs the software package DOGS (DGFI Orbit and Geodetic parameter estimation Software) with the components DOGS-OC for SLR and DORIS data processing and precise orbit determination, DOGS-RI for the analysis of VLBI observations, and DOGS-CS for the combination of the different observations on the normal equation level (see Table 1.1). In 2018, the institute has started to enhance the DOGS-OC software for the analysis of DORIS observations. All the DOGS software packages are continuously updated to incorporate the latest developments and the state-of-the-art models for the data processing. The GNSS data are analysed with the Bernese software.

**Table 1.1:** Components of the DGFI Orbit and Geodetic parameter estimation Software (DOGS).

Component	Purpose
DOGS-OC	SLR and DORIS data processing and precise orbit determination
DOGS-RI	VLBI data processing
DOGS-CS	Combination of space-geodetic observations on the normal equation level

The work benefits from DGFI-TUM's engagement in international scientific organizations, in particular in the frame of the International Association of Geodesy (IAG) and the International Astronomical Union (IAU). Mostly by virtue of long-term commitments, DGFI-TUM operates data centres, analysis centres, and research centres. This ensures the direct access to the original data of the space-geodetic techniques and to the results and products generated by scientific services. Table 1.2 summarises the activities that are closely related to this research area.

**Table 1.2:** Long-term commitments of DGFI-TUM in international organizations related to this research area.

IAG Service	DGFI-TUM Commitments
International Earth Rotation and Reference Systems Service (IERS)	International Terrestrial Reference System (ITRS) ITRS Combination Centre
International GNSS Service (IGS)	Regional Network Associate Analysis Centre for SIRGAS (RNAAC-SIR), Tide Gauge Monitoring Working Group (TIGA)
International Laser Ranging Service (ILRS)	Global Data and Operation Centre (EDC), Analysis Centre
International VLBI Service for Geodesy and Astrometry (IVS)	Analysis Centre, Combination Centre (together with BKG)

The research in this field is supported by several projects funded by the Deutsche Forschungsgemeinschaft (DFG) and the European Space Agency (ESA). This funding and the contributions from these projects are gratefully acknowledged (see Section 5).

## 1.1 Analysis of Space-Based Microwave Observations

### VLBI data analysis

Very Long Baseline Interferometry (VLBI) has been part of DGFI-TUM's research activities since many years. In 2008, the institute became an operational Analysis Centre (AC) of the International VLBI Service for Geodesy and Astrometry (IVS), which organizes the world-wide collaboration in performing VLBI observations and analysis. An operational AC has to provide solutions (in the form of datum-free normal equations) for the most important 24-hour VLBI experiments on a regular and timely basis. In particular, these experiments comprise the twice-weekly rapid turnaround EOP (Earth Orientation Parameter) sessions.

2018 was the first year in which all of our contributions have been computed with DGFI-TUM's proprietary VLBI analysis tool DOGS-RI, the Radio Interferometry component of the DGFI Orbit and Geodetic parameter estimation Software (DOGS) package. It is based on the current standards as defined by the International Earth Rotation and Reference Systems Service (IERS) 2010 Conventions, and DGFI-TUM is continuously integrating the latest developments in VLBI modelling (e.g. new tropospheric mapping functions) to ensure a high quality of solutions. A comparison of our results to those of other ACs has been undertaken in the context of the IVS General Meeting 2018 and revealed a good agreement with the solutions of other VLBI analysis softwares (see Figure 1.1 and Table 1.3 and (Glomsda et al. 2018)). The major implementation effort in 2018 can be assigned to the change in storage format for VLBI observables and auxiliary data: since October 1st, the *vgosDB* format replaces the old *NGS/Mk3 cards*.

**Table 1.3:** WRMS of differences to the IERS 14 C04 EOP series per Analysis Centre (AC). "n/a" means that the corresponding parameter was not available in the IVS contribution. For each EOP, the WRMS of DGFI-TUM's solution is within the range of the other ACs, while the combined solution of the IVS (IVS CC) performs best.

EOP	AC1	AC2	AC3	AC4	IVS CC	DGFI-TUM
$x_{pol}$ [mas]	0.165	0.151	0.132	0.156	0.080	0.148
$\dot{x}_{pol}$ [mas/d]	0.296	0.258	0.273	0.317	0.232	0.291
$y_{pol}$ [mas]	0.194	0.162	0.135	0.176	0.076	0.157
$\dot{y}_{pol}$ [mas/d]	0.288	0.254	0.268	0.322	0.231	0.291
$\Delta UT1$ [ms]	0.015	0.018	0.015	0.016	0.010	0.014
$LOD$ [ms/d]	0.019	0.017	0.018	0.019	0.016	0.019
$\Delta X^{CIP}$ [mas]	n/a	n/a	n/a	0.168	0.033	0.137
$\Delta Y^{CIP}$ [mas]	n/a	n/a	n/a	0.153	0.036	0.138

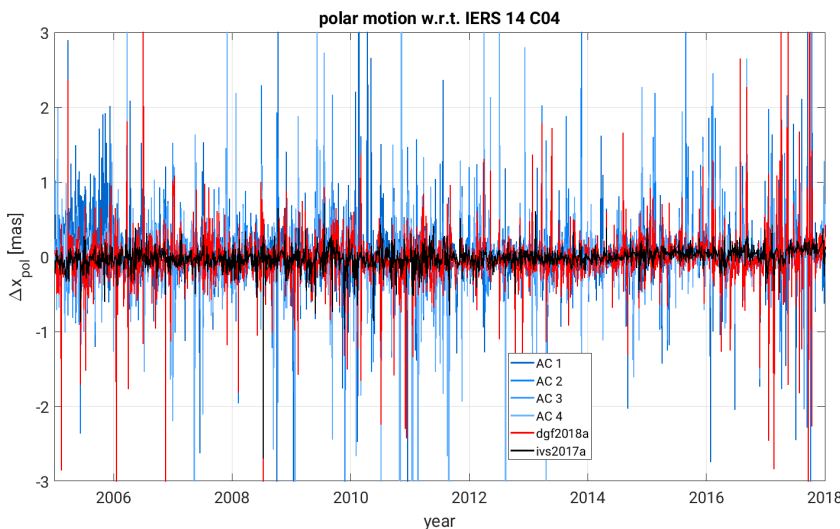


**Figure 1.1:** Deviations between the EOP  $x_{pol}$  as estimated by various IVS Analysis Centres (AC) and the corresponding value of the IERS C04 series. dgf2018a (red) is the solution of DGFI-TUM, ivs2017a (black) is the combination solution of the IVS Combination Centre.

## Monitoring of regional deformations with GNSS

DGFI-TUM has installed 21 continuously operating GNSS (CO-GNSS) stations in Europe and South America since 1998; 11 of these stations are still under the responsibility of DGFI-TUM, while the others were formally transferred to local institutions to facilitate their operability. Five stations were installed along the German Alps in the frame of the European Union's Territorial Cooperation (INTERREG III) Alpine Space Project for detection and control of crustal deformations in the Alpine region (ALPS-GPS QUAKENET). Although this project formally ended, four DGFI-TUM stations continue delivering measurements and are included in different European geodetic projects. The other CO-GNSS stations contribute to various international initiatives, especially to the IGS Tide Gauge Benchmark Working Group (TIGA), the IGS Multi-GNSS Experiment (MGEX), and the regional densification of the ITRF in Latin America (SIRGAS). Based on the analysis of precise station position time series, DGFI-TUM investigates the best possible strategy to model consistently three main components: (1) a linear component to derive horizontal and vertical displacement fields that serve as the basis for monitoring regional surface deformations; (2) earthquake-related discontinuities to identify deformation patterns associated to inter-seismic, co-seismic and post-seismic effects; and (3) seasonal components to infer transient surface deformations caused by atmospheric and hydrological loading.

A highlight in 2018 was the generation of a present day surface kinematics model across the Alpine region based on a high-level data analysis of about 300 GNSS stations continuously operating over more than 12 years. The processing of the daily GNSS observations was accomplished using the double-difference baseline approach and the least-squares adjustment implemented in the Bernese GNSS software V5.2 (Dach et al. 2015). The determination of precise station coordinates and velocities was performed within a multi-year solution (see Sánchez et al. 2018a). Figure 1.2 shows the horizontal and vertical surface kinematics across the Alpine region inferred from the continuous GNSS station network. Our results make evident that the horizontal deformation in the Alpine region is dominated by the counter-clockwise motion of the Adria microplate, causing compression in the Eastern Alps, dextral shear in the Central Alps and a very slow deformation in the Western Alps. The vertical motion shows an averaged uplift of 1.8 mm/a of the entire mountain chain, with exception of the southern part of the Western Alps, where no significant uplift is detected. The fastest uplift rates (more than 2 mm/a) occur in the central area of the Western Alps, in the Swiss Alps, and in the Southern Alps in the boundary region between Switzerland, Austria and Italy. This kinematics model was determined under a strong cooperation between DGFI-TUM and "Erdmessung und Glaziologie der Bayerische Akademie der Wissenschaften" (see Sánchez et al. 2018a).

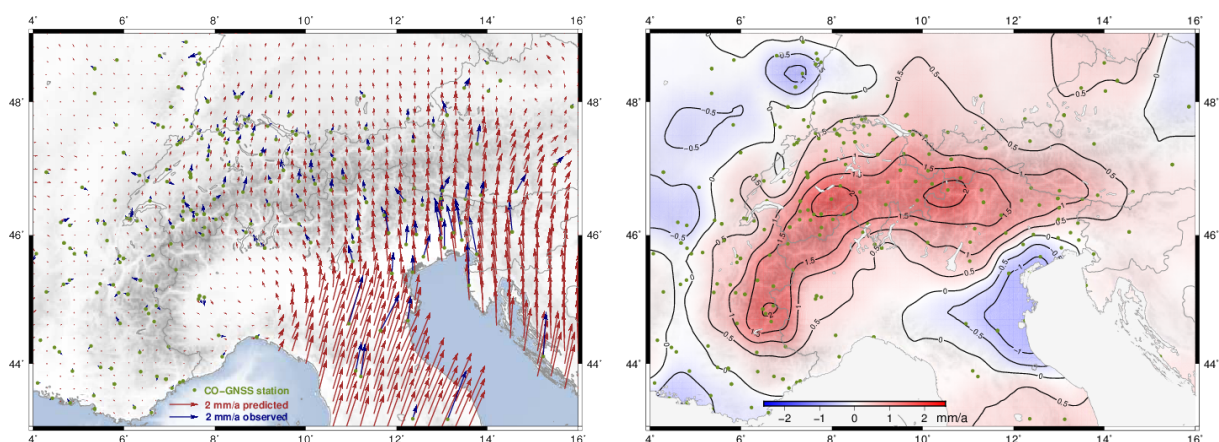


**Figure 1.2:** Present-day surface-kinematics of the Alpine region inferred from GNSS observations. Left: horizontal deformation with respect to the Eurasian plate; right: vertical deformation model.

## DORIS data analysis

In early 2018, DGFI-TUM took action to extend its SLR analysis software DOGS-OC to also analyse DORIS data in the IDS 2.2 format. In particular, the macromodels of the satellites Jason-1/-2/-3 and TOPEX/Poseidon were implemented according to analysis recommendations provided by the International DORIS Service (IDS). The implementation was done within a collaboration of DGFI-TUM with the NASA Goddard Space Flight Center (NASA GSFC), Greenbelt, USA. Moreover, the ability to estimate corrections to the wet part of the tropospheric zenith delay, the estimation of pass-wise frequency biases, and the modelling of station-dependent phase center offsets in the measurement direction were implemented in DOGS-OC.

The following DORIS-specific measurement corrections have been implemented:

- center of mass correction of the instrument at the satellite,
- phase center correction of the emitter (beacon),
- tropospheric refraction (different models available),
- relativistic correction (according to model of Moyer),
- frequency bias and frequency-drift,
- IDS phase law (at the beacon).

As it is realized for SLR, DOGS-OC allows also for DORIS to compute partial derivatives of the theoretical observation w.r.t. the included free parameter, i.e. dynamic parameter (e.g. initial state vector, gravity field coefficients, empirical accelerations), center of Mass correction, pole coordinates, time parameter UT1, station parameter (coordinates and velocities), station frequency biases, tropospheric (wet) scaling factors, etc.

## 1.2 Analysis of Satellite Laser Ranging Observations

### SLR data analysis

In the framework of the ILRS as an active analysis centre (AC) of the ILRS Analysis Standing Committee (ILRS-ASC) DGFI-TUM performs several routine analyses and contributes to different ILRS-ASC pilot projects. Table 1.4 summarizes the different contributions of DGFI-TUM. The “v170” and “v70” solutions are routinely processed on a daily and weekly basis and contain station coordinate (TRF) and Earth Orientation Parameter (EOP) solutions based on observations to the spherical near-Earth satellites LAGEOS-1 and -2 (LA-1/-2) and Etalon-1 and -2 (ET-1/-2). The weekly processing chain is also used to submit orbit solutions of the four prior mentioned satellites to the ILRS combination centers in the so called “SP3c” data format.

Fig. 1.3 shows the daily variance factors and analysed observations combined by the ILRS combination center. It is clearly visible that, after initial problems, the DGFI-TUM solution nowadays performs very stable and reasonable variance factors are obtained compared to the other ILRS ACs.

**Table 1.4:** DGFI-TUM routine solutions and pilot project contributions.

ILRS solution	Description
v170	Daily LA-1/-2 and ET-1/-2 TRF and EOP solutions
v70	Weekly LA-1/-2 and ET-1/-2 TRF and EOP solutions
v70-sp3c	Weekly LA-1/-2 and ET-1/-2 orbit solutions
v230	Contribution to the ILRS ASC pilot project on systematic error monitoring

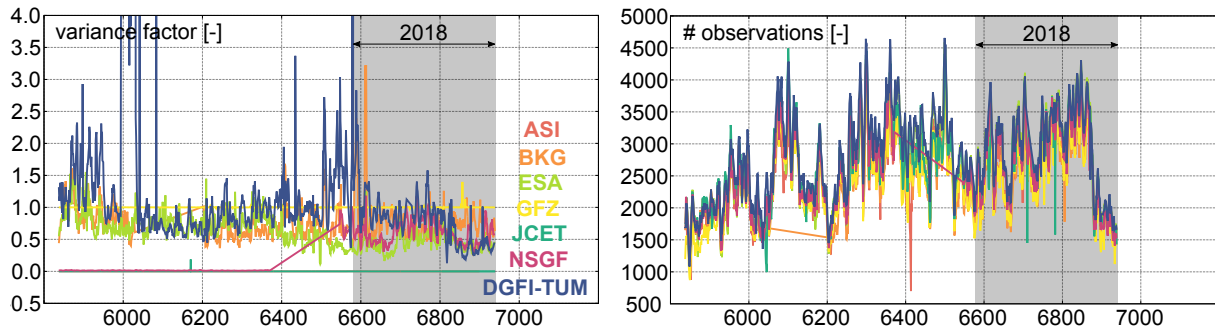


**Figure 1.3:** Daily variance factors and number of observations used for the analysis of the seven ILRS ACs. The numbers are computed by the ILRSB combination centre located at JCET, University of Maryland, USA.

DGFI-TUM also contributes to the pilot projects of the ILRS/ASC on the estimation of range biases for all stations (systematic error monitoring). Additionally, DGFI-TUM processes all spherical satellites and some non-spherical satellites on a regular basis for various applications. Results of this reprocessing are published in Bloßfeld et al. (2018). This work also contributed to the DFG project “Consistent dynamic satellite reference frames and terrestrial geodetic datum parameters” of the research unit FOR1503 “Space-time reference systems for monitoring global change and for precise navigation in space”.

Moreover, in 2018, the DOGS-OC/-CS environment (for details please see next subsection) was substantially revised including the pre- and post-processing environment for all ILRS contributions. The whole processing system was moved to a new server and all used pre- and post-processing routines were rewritten, updated or recompiled using modern FORTRAN standards and most recent compiler versions. Currently, a special focus is put on the post-processing evaluation programs in order to internally validate the computed solutions more efficiently.

In the future, DGFI-TUM will contribute to the ILRS-ASC pilot projects on the inclusion of LARES as a fifth satellite in the standard “pos+eop” solutions and the application of non-tidal loading corrections at the observation equation level.

## SLR data management

Since the foundation of the International Laser Ranging Service (ILRS) in 1998, the EUROLAS Data Centre (EDC) operated by DGFI-TUM acts as one of two global ILRS data centres (the second one is the Crustal Dynamics Data Information System, CDDIS, operated by NASA). The EDC, as an ILRS Operation Center (OC) and ILRS Data Center (DC), has to ensure the quality of submitted data sets by checking their format. Furthermore, a daily and hourly data exchange with the NASA OC and CDDIS is performed. All data sets and products are publicly available for the ILRS community via ftp (<ftp://edc.dgfi.tum.de>) and the dedicated website [edc.dgfi.tum.de](http://edc.dgfi.tum.de).

EDC is running several mailing lists for the exchange of information, data and results. In 2018, 53978 Consolidated Prediction Format (CPF) files of 116 satellites were sent automatically to SLR stations. Besides, EDC distributed SLR-Mails (71 messages in 2018), SLR-Reports (1322 in 2018) and Urgent and Rapid-Service-Mails (10 in 2018). In 2018, 40 SLR stations observed 128 different satellites. There were 28 new satellite missions tracked by SLR stations, namely BeiDou-3M1, BeiDou-3M2, BeiDou-3M3, BeiDou-3M9, BeiDou-3M10, CHEF-Sat, Galileo-215, Galileo-216, Galileo-217, Galileo-218, Galileo-219, Galileo-220, Galileo-221, Galileo-222, Glonass-138, Glonass-139, GRACE-FO-1, GRACE-FO-2, HY-2B, IceSAT-2, IRNSS-1I, PAZ, Tiangong-2, Sentinel-3B, SNET-1, SNET-2, SNET-3 and SNET-4.

In 2018, an updated specification of the format version 2 for Consolidated Laser Ranging Data (CRD), CPF was developed and released. The implementation phase is planned to be finished until 2020. Also new tools for managing site logs and site history logs were developed by the EDC and officially introduced in 2018.

## 1.3 Computation of Satellite Orbits

### Enhancement of the DGFI-TUM geodetic analysis software DOGS

In 2018, DGFI-TUM revised its software package DOGS-OC/-RI/-CS in order to implement modern FORTRAN standards, reduce redundant code, unify commonly used (e.g., by -OC and -RI) routines, implement a new and extended binary header format and to use up-to-date compilers within a totally new installed system architecture. Furthermore, steps towards a refined software versioning using Git has been realized. As a consequence of this significant software development step in 2018, several new DOGS version were released during the year ending with DOGS-OC version 5.5, DOGS-RI version 1.92 and DOGS-CS version 5.1.

The new DOGS-CS header format, which can be directly written by -OC and -RI contains all the information necessary to write a complete SINEX file without any external information needed. Therefore, also the interfaces from and towards SINEX format has been re-written.

### Impact of refined satellite attitude handling on the quality of Jason-2 orbits

For non-spherical satellites like Jason-2, the accurate knowledge of the actual satellite orientation is a prerequisite for precise computation of non-gravitational accelerations acting on the satellite. Moreover, it is used for the computation of the theoretical range and range rate between the tracking station and the satellite. The satellite orientation can be given in two forms: either in the so called “yaw-steering nominal attitude law” or in the quaternion-based form derived from, e.g., star camera measurements. In DOGS-OC, both forms of the attitude representation have been implemented and tested for Jason-2 orbits between 20 July 2008 and 28 February 2015 (see Fig. 1.4). Currently, the refined attitude handling is being implemented also for Jason-1 and Jason-3.

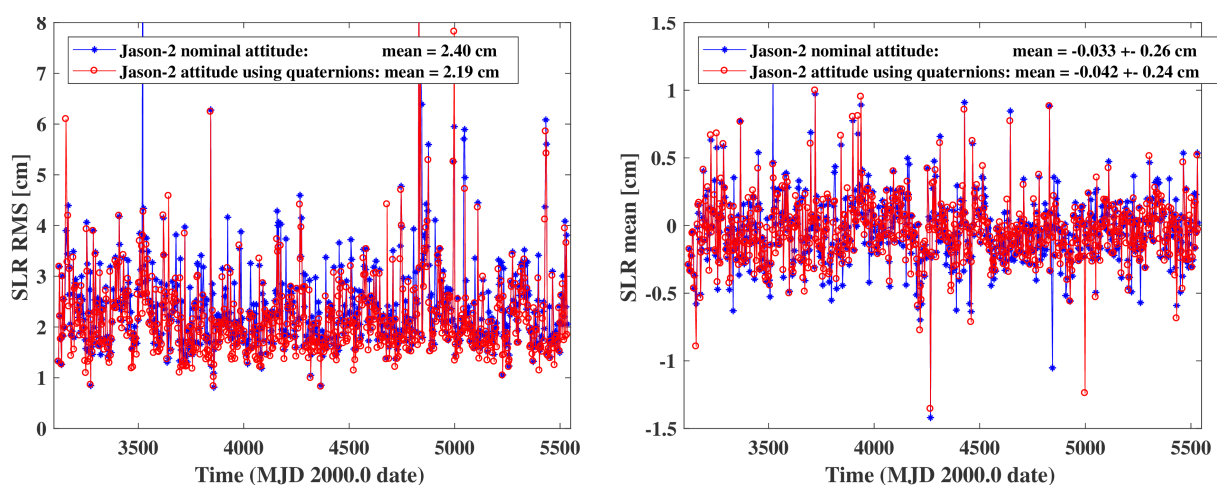


**Figure 1.4:** RMS (left) and mean (right) fits of SLR observations of Jason-2 computed using the nominal and measured satellite attitude in the quaternion form at the time interval from 20 July 2008 to 28 February 2015.

## Refined modelling of thermospheric drag (DFG project INSIGHT)

At DGFI-TUM, SLR observations to the spherical satellites ANDE-Pollux, ANDE-Castor and SpinSat are used to scale the thermospheric density provided by five empirical models CIRA86, NRLMSISE00, JB2008, DTM2013, and CH-Therm-2018 at the periods of low and high solar activity and, thus, to improve thermospheric drag acting to these satellites. More details are given in the cross-cutting research topic “Atmosphere”, see Section 3.1.

## Impact of T2L2 time bias corrections on geodetic parameters

SLR observations at some geodetic stations can be affected by range and time biases caused by instrumental problems. If not estimated or modelled, these biases can lead either to the exclusion of these observations due to high residuals, or to a degradation of the quality of the orbit computed using such observations. Range biases can be estimated within a precise orbit determination (POD). In contrast to this, time biases are highly correlated with the Earth’s rotation and, if not properly determined, may impact the Earth Rotation Parameters (ERP). To determine this effect, the Time Transfer by Laser Link (T2L2) experiment was performed on the Jason-2 satellite for the synchronization of remote ultra-stable clocks. Time bias corrections of the global network of SLR stations derived from this experiment have been made available in the ILRS handling file and reach values up to 3.4 ms. The corrections have been implemented in DOGS-OC and were used within a POD of some near-Earth geodetic satellites. Fig. 1.5 shows the impact of these time bias corrections on the pole coordinates (up to -0.2 mas) for LAGEOS-1/2. For Lares, an impact up to -1.0 mas was found.

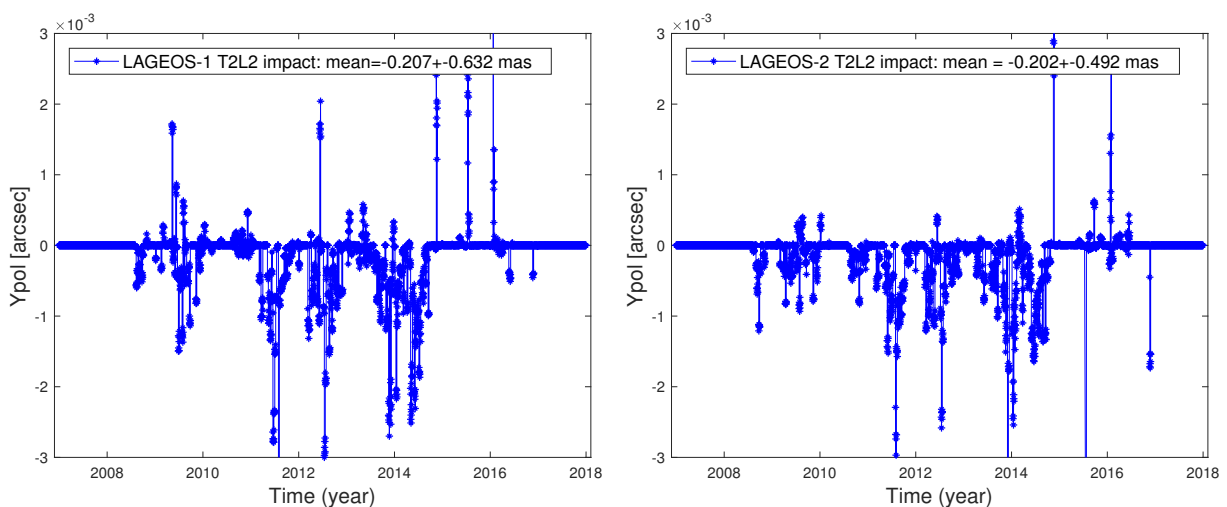


**Figure 1.5:** The impact of the T2L2 time corrections on the estimated  $Y_p$  pole coordinate for LAGEOS-1 (left) and LAGEOS-2 (right).

## Impact of TRF realizations on precise orbit determination (POD)

A Terrestrial Reference Frame (TRF) realization is a basis for precise orbit determination of satellites, since it defines the positions of crust-fixed tracking stations together with their temporal evolutions. DGFI-TUM investigates the impact of several most-recent ITRS realizations, namely DTRF2014, ITRF2014 and JTRF2014, on the RMS and mean fits of SLR observations of ten high and low Earth orbiting geodetic satellites. These three new TRFs were derived by adding additional six years of data (2009.0 to 2015.0), as compared to the previous ITRS

realizations DTRF2008 and ITRF2008. Fig. 1.6 exemplary shows the results obtained for the Jason-2 satellite between 20 July 2008 and 28 February 2015. It is clearly visible that all new ITRS realizations show an improvement in the RMS fits of SLR observations as compared to the previous ITRS realization for SLR stations only - the SLRF2008. More precisely, the smallest RMS fits were obtained when using JTRF2014 after editing for SLR stations Conception and Zimmerwald, as described in Rudenko et al. (2018), followed by DTRF2014 with non-tidal loading corrections. ITRF2014, on the contrary, indicates the largest absolute mean fits of SLR observations that are close to those obtained using SLRF2008. More results are given in Rudenko et al. (2018).

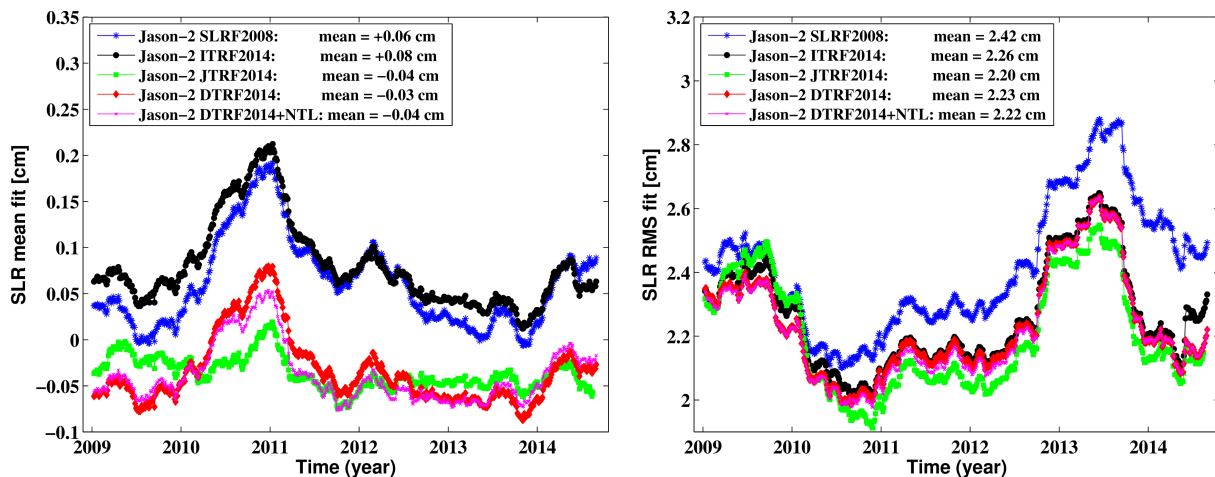


**Figure 1.6:** 50-week running averages of the RMS (left) and mean (right) fits of SLR observations for Jason-2 orbits derived using SLRF2008, ITRF2014, JTRF2014, DTRF2014 linear and DTRF2014 with non-tidal loading corrections.

## 1.4 Determination of Reference Frames

### Consistent realization of terrestrial and celestial reference systems

With the Resolution No. 3 of the International Union of Geodesy and Geophysics (IUGG) adopted by the General Assembly in 2011, the IUGG urged “that highest consistency between the ICRF, the ITRF, and the EOP as observed and realized by the IAG and its components such as the IERS should be a primary goal in all future realizations of the ICRS”. So far, the highest consistency could not be achieved, as three independent IERS product centers are in charge of computing the terrestrial and celestial reference frame as well as the EOP.

At DGFI-TUM, various studies and test combinations have been performed to estimate all three components (CRF, TRF and EOP) in a common adjustment. Within the project *Consistent celestial and terrestrial reference frames by improved modelling and combination*, part of the DFG Research Unit FOR1503 “Space-time reference systems for monitoring global change and for precise navigation in space”, the first simultaneous and consistent realization of TRF, CRF and EOP in accordance with the IUGG Resolution was obtained. The joint parameter estimation was based on homogeneously processed VLBI, GNSS, and SLR single-technique solutions over 11 years (2005.0–2016.0). Several types of combined solutions were computed following the selections of different local ties, EOP combination setups, and different weights of the techniques. The impacts of the different combination setups on CRF, TRF, and EOP were investigated.



The results of the combined estimation of the celestial and terrestrial reference frames were published by Kwak et al. (2018). Figure 1.7 demonstrates the benefits of the combination of VLBI, SLR and GNSS observations for the CRF in comparison with the usual VLBI-only solution. In particular, the declinations of the VLBA Calibrator Survey (VCS) sources and newly added sources which were not included in ICRF2 are improved significantly (smaller standard deviations) in the southern hemisphere. As the standard deviations of the non-VCS sources including defining sources are much smaller than those of the VCS sources, their changes are hardly recognizable in Fig. 1.7. However, they improve also in particular for the higher southern latitudes.

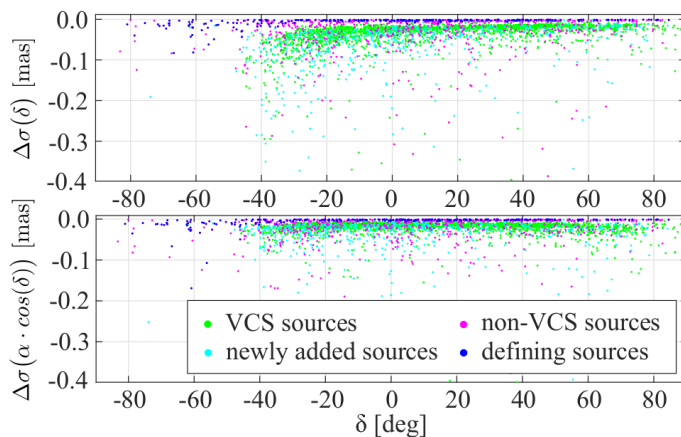


**Figure 1.7:** Differences of radio source declination and right ascension standard deviations of the combined VLBI, GNSS and SLR solution in comparison to the VLBI-only solution. The standard deviations of the VCS sources (green) and newly added sources (cyan), which were not included in ICRF2, are improved significantly, which is indicated by the negative differences displayed in the figure.

### DTRF2014: Validation of non-tidal loading corrections

In the DTRF2014 solution, for the first time, station coordinate time series were corrected at the normal equation level for non-tidal loading (NT-L) variations caused by the atmosphere and the hydrosphere. In order to validate the applied corrections and to verify if they improve the final TRF product, DGFI-TUM performed an analysis, where two different DTRF2014 versions (with and without NT-L corrections applied) are compared at co-locations sites. The left panel of Fig. 1.8 shows a global overview of the station observation time intervals of the DTRF2014 solution. The majority of stations contributed observations over more than 2000 days to the DTRF2014 whereas in some regions (e.g. Japan, right panel of Fig. 1.8) due to e.g., earthquakes, the DTRF2014 is based on rather short observation intervals.

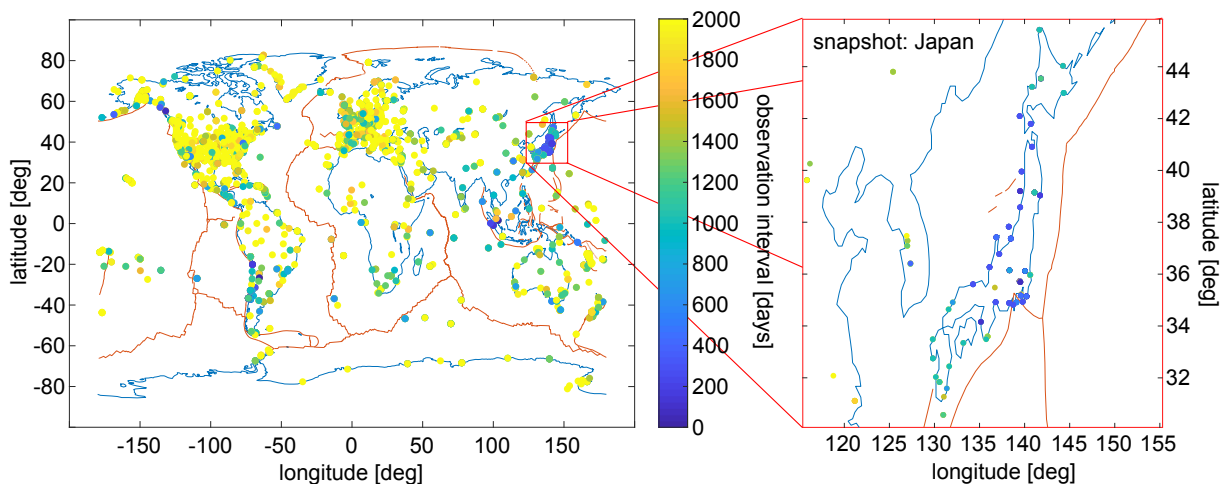


**Figure 1.8:** DTRF2014 station observation intervals (left panel: global plot, right panel: snapshot of Japan).

Fig. 1.9 shows the impact of the applied NT-L corrections on the DTRF2014 station coordinates and velocities. Those stations which contribute during a long time span to the DTRF2014 solution are not significantly affected by the NT-L corrections. On the other hand, stations with short observation time spans are significantly affected in station positions and station velocities. For very short observation time spans, changes in the positions and velocities of several mm and mm/yr can be found.

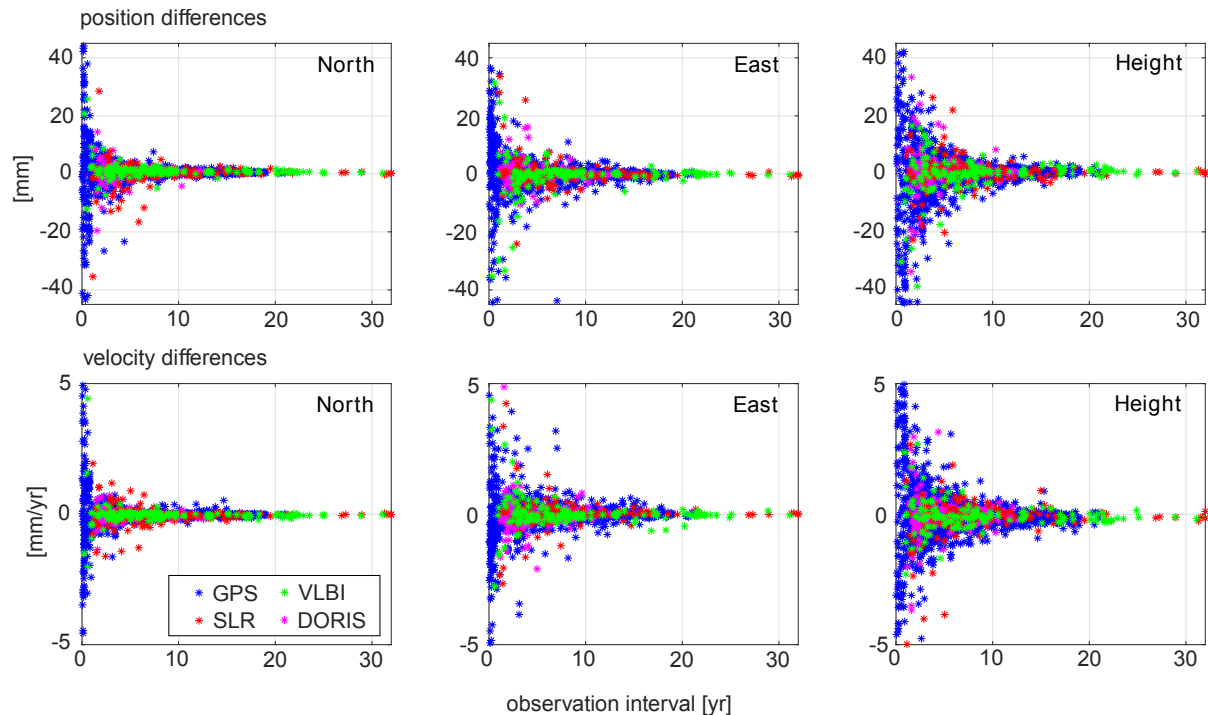


**Figure 1.9:** Impact of non-tidal loading corrections on DTRF2014 station coordinates and velocities.

The NT-L corrections are validated at selected co-location stations. Therefore, the positions given at the reference epoch of the DTRF2014 (0.0 UTC [JD2000]) are extrapolated to the local tie (LT) measurement epochs using their velocities. At the measurement epoch, the local ties are compared to the differences of the extrapolated station coordinates. It was found that if the NT-L corrections are applied, the discrepancies at the five fundamental stations (all techniques co-located) between the LTs and the coordinate differences get smaller. Moreover, the annual variations in the ILRS origin time series and the ILRS and IVS scale time series nearly totally vanish (see Fig. 1.10).

### Vertical reference systems

The Global Geodetic Observing System (GGOS) of the IAG, providing precise geodetic infrastructure and expertise for monitoring the System Earth, promotes the standardization of height systems worldwide. DGFI-TUM supports this initiative by coordinating the GGOS Focus Area Unified Height System, which main objective at present is the implementation of the International Height Reference System (IHRIS) as stated in the IAG Resolution No. 1 released in July 2015 (Sánchez 2018c). At present, the main challenges are the establishment of the International Height Reference Frame (IHRF), i.e., a global reference network with precise geopotential numbers referring to the IHRIS, and the preparation of required standards, conventions and procedures to ensure consistency between the definition (IHRIS) and the realization (IHRF).

Regarding the IHRF reference network, DGFI-TUM proposed a preliminary station selection, which was distributed to regional and national experts to get advice about the availability of

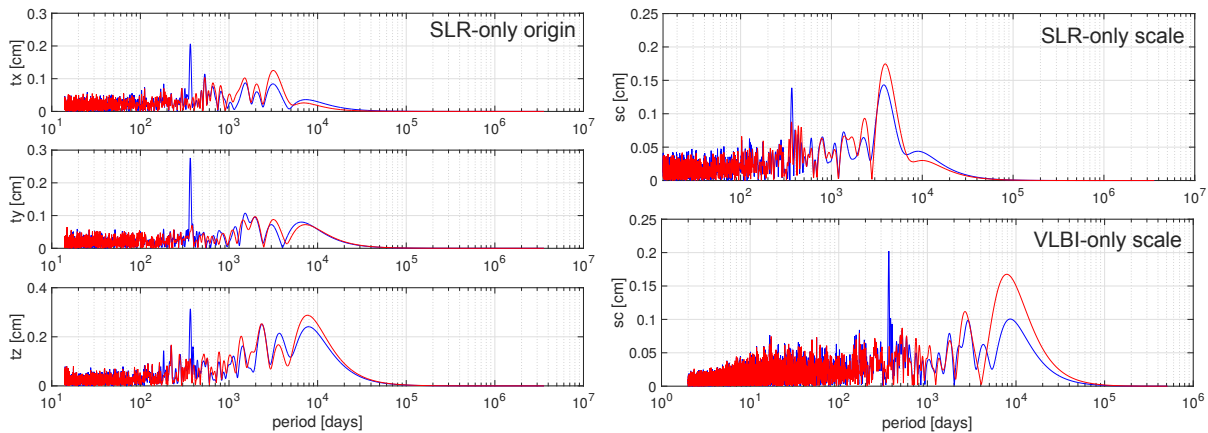


**Figure 1.10:** DTRF2014 SLR-only origin time series (left) and SLR-only/VLBI-only scale time series (right). Blue: DTRF2014, not corrected for NT-L variations, red: DTRF2014, corrected for NT-L variations.

gravity data, and the addition of further geodetic sites to improve the density and distribution of the IHRF stations in their regions/countries. In addition, in a joint effort with the IAG JWG 2.1.1 ‘Establishment of a global absolute gravity reference system’ (chair H. Wziontek, BKG, Germany), an optimal co-location between the IHRF and reference stations of the new International Gravity Reference Frame (IGRF) was evaluated. At present, 59 co-located sites have been identified, and the objective is to include additional IHRF or absolute gravity stations according to the necessities of IGRF or IHRF, respectively. As the IHRF/IHRF is understood as a main component of the UN Global Geodetic Reference Frame (GGRF), special care is given to the co-location of IHRF reference stations with the ITRF, the GGRF and the existing height systems (reference tide gauges and vertical reference networks). As an example, Figures 1.11 and 1.12 show the co-location sites between IHRF and VLBI, SLR, DORIS, and GGRF reference stations.

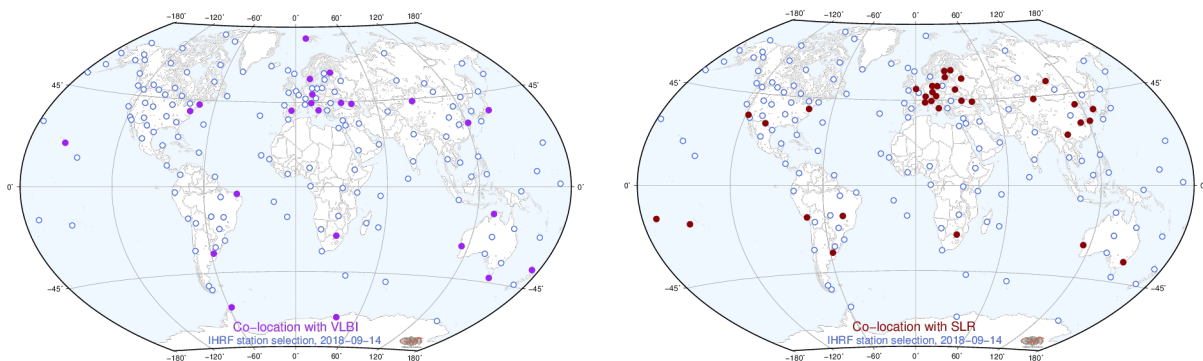


**Figure 1.11:** Co-location of IHRF reference network with VLBI (left), SLR stations (right).

Regarding the computation of geopotential numbers as primary IHRF coordinates, we started an experiment focused on the estimation and comparison of (quasi-)geoid heights and potential values using the same input data and the own methodologies/software of colleagues involved in the gravity field modelling of high resolution. The comparison of the results should highlight the differences caused by disparities in the computation methodologies. This experiment is based on (terrestrial and airborne) gravity data, terrain model and GNSS/levelling data made available by the US National Geodetic Survey (NGS) for an area of about 500 km x 800 km in Colorado, USA. The Colorado data were distributed in Feb. 2018, together with a document summarising a minimum set of basic requirements (standards) for the computations (Sánchez et al. 2018d). With these data, seven different groups working on the determination of IHRF coordinates

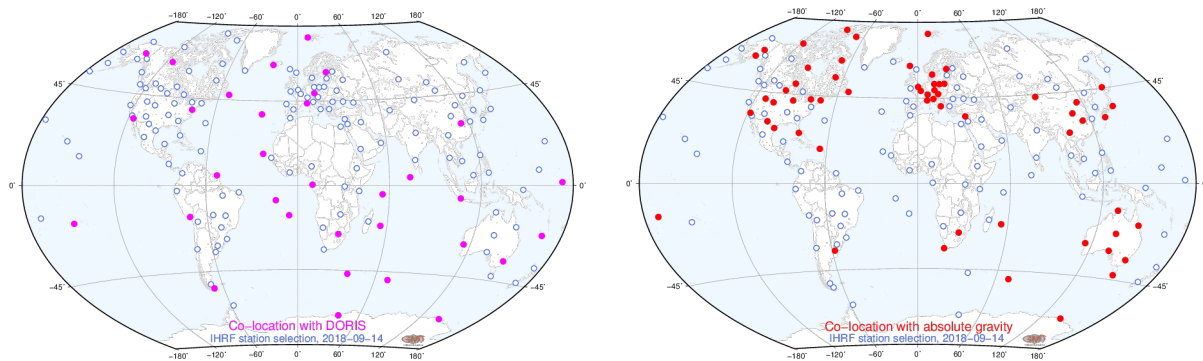


**Figure 1.12:** Co-location of IHRF reference network with DORIS (left) and absolute gravity reference stations (right).

computed potential values for some virtual geodetic stations located in that region. These first computations were presented during the Gravity, Geoid and Height Systems (GGHS2018) Symposium (Sep 17–21, 2018, Copenhagen). Four (of seven) solutions are consistent in the 1 dm level, with agreement within 1 cm to 2 cm in terms of standard deviation with respect to the mean value. The discrepancies between the individual solutions present a strong correlation with the topography, making evident that the modelling of terrain effects should be refined. However, since these are the first (preliminary) results, they are very promising. A convergence of the results at the 1 cm level may be reachable. The next steps are devoted to identify and remove sources of discrepancies between the solutions, to compute refined solutions (two or more iterations), and to compare potential differences with geopotential values derived from levelling and gravimetry.

These activities are developed under a strong international cooperation promoted by the GGOS-JWG: “Strategy for the IHRF realization” (chaired by DGFI-TUM), IAG-SC2.2: “Methodology for geoid and physical height systems”, IAG-JWG2.2.2: “The 1 cm geoid experiment”, ICCT-JSG0.15: “Regional geoid/quasi-geoid modelling – Theoretical framework for the sub-centimetre accuracy”, and the International Gravity Field Service (IGFS).

### Regional terrestrial reference frame in Latin America (SIRGAS)

A network of about 400 CO-GNSS stations distributed over Latin America gives the present realization of SIRGAS (Sistema de Referencia Geocéntrico para las Américas). This network is processed on a weekly basis to generate instantaneous weekly station positions aligned to the ITRF and multi-year (cumulative) reference frame solutions. The instantaneous weekly positions are especially useful when strong earthquakes cause co-seismic displacements or strong relaxation motions at the SIRGAS stations disabling the use of previous coordinates. The multi-year solutions provide the most accurate and up-to-date SIRGAS station positions and velocities. They are used for the realization and maintenance of the SIRGAS reference frame between two releases of the ITRF. Occasionally, the historical SIRGAS GNSS data are reprocessed to improve the reliability of the station position time series applying new analysis standards and models. DGFI-TUM, in its role as the IGS Regional Network Associate Analysis Centre for SIRGAS (IGS RNAAC SIRGAS), operationally provides the SIRGAS science data products via [www.sirgas.org](http://www.sirgas.org) and [ftp.sirgas.org](ftp://ftp.sirgas.org).

DGFI-TUM’s research in the context of SIRGAS is focused on designing the best strategy to ensure a high reliability of the regional reference frame as it is frequently affected by strong earthquakes. From one side, we are investigating the possibility of using SLR observations for the realization of the geocentric datum in the GNSS network (see DIGERATI). From the other

side, we are developing methodologies to incorporate seismic discontinuities in the computation of the GNSS-based reference frame realization to support the precise transformation of coordinates referring to pre-seismic and post-seismic frame solutions (see Sánchez 2018b).

As an example, Figure 1.13 presents a sequence of geodetic deformation models based on 24 years of high-level GNSS data analysis. Our results clearly show that the only stable areas in Latin America are the Guiana, Brazilian and Atlantic shields; the other tectonic entities, like the Caribbean plate and the North Andes, Panama and Altiplano blocks are deformable. The present surface deformation is highly influenced by the effects of seven major earthquakes ( $M_w > 7.4$ ) occurred since 2001. While earthquakes in Central America modified the aseismic deformation regime up to 12 mm/a, earthquakes in the Andes caused changes up to 35 mm/a. Before the earthquakes, the deformation vectors are roughly in the direction of plate subduction. After the earthquakes, the deformation vectors describe a rotation counter clockwise south of the epicentres and clockwise north of the epicentres. The strain fields reveal that this kinematic pattern slowly disappears by post-seismic relaxation. The DGFI-TUM research related to SIRGAS is accompanied under a strong international cooperation with Latin American organizations.

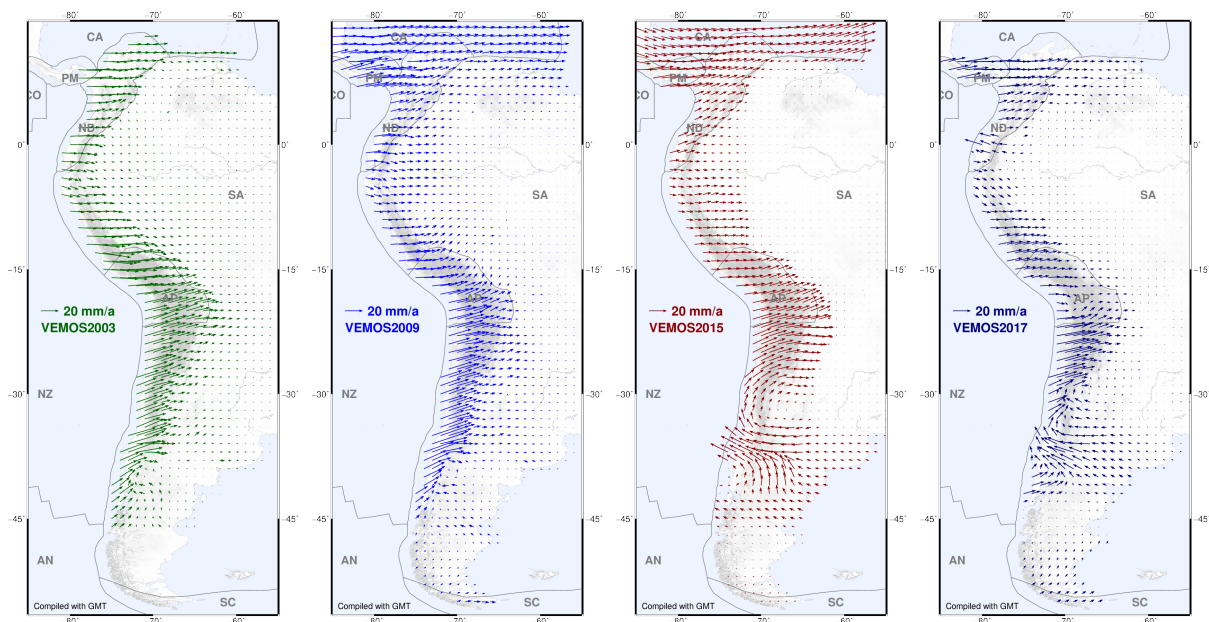


**Figure 1.13:** Surface deformation models for SIRGAS (VEMOS) relative to the South American plate: VEMOS2003 valid from 1995.4 to 2002.0, VEMOS2009 valid from 2000.0 to 2009.6, VEMOS2015 valid from 2012.2 to 2015.2, VEMOS2017 valid from 2014.0 to 2017.1.

## DFG project DIGERATI

Within the DFG-funded project DIGERATI (Direct Geocentric Realisation of the American Reference Frame by Combination of Geodetic Observation Techniques), investigations with respect to the optimum realization of an Epoch Reference Frame (ERF) for South and Central America are performed. In the first project phase, the work aimed at the influence of possible improvements of the global SLR network on SLR-derived reference frames.

Simulation studies have been performed to investigate the benefits of additional SLR stations for the estimation TRF parameters and EOPs. It could be demonstrated, that additional stations would be beneficial for the z-translation of the reference frame, the scale and the RMS of

the residuals of the Helmert transformation in Northern America, the Eastern Pacific, South America and the Indian Ocean region whereas the pole coordinates are improved mainly by additional stations in the East Asian region.

Another aspect of the SLR-related studies have been the performances of the existing stations. It could be shown that, taking into account limited funding, already the investment into a single station can bring a significant benefit (Figure 1.14).

$-\Delta WRMS$ [%]	$t_x$	$t_y$	$t_z$	<i>scale</i>	$x_{pole}$	$y_{pole}$	<i>LoD</i>
Arequipa 20 %	3	4	6	3	0	3	0
Haleakala 20 %	3	1	5	4	2	2	1
Badary 20 %	3	3	-1	3	2	2	0
all 20 % (Kehm et al., 2017)	10	27	14	49	10	10	4

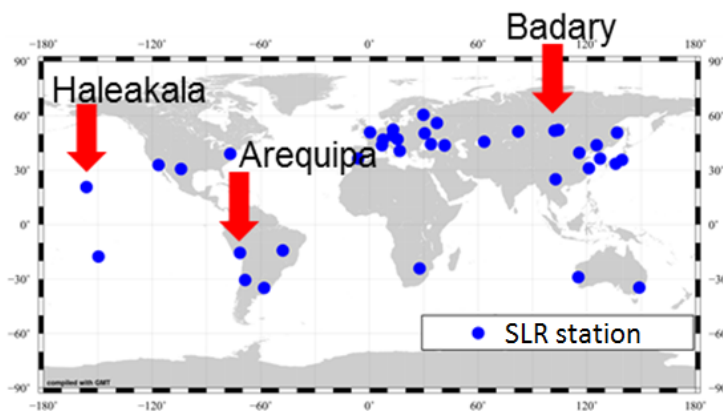


**Figure 1.14:** Impact of performance improvement of a single SLR station compared to a fully improved network as published by Kehm et al. (2017).

The numbers in the table indicate the percentage of improvement of the WRMS with respect to the reference solution.

## ESA project Independent Generation of Earth Orientation Parameters

Earth Orientation Parameters (EOPs) are the fundamental parameters for the description of the orientation between the terrestrial and the celestial reference frame as well as for the realization of precise time systems. The goal of the ESA project “Independent generation of Earth Orientation Parameters” is to find the optimum approach for the determination of consistent final, rapid and predicted EOP products from a combination of the space-geodetic techniques VLBI, SLR, GNSS and DORIS.

The project, which started in 2017, is lead by DGFI-TUM and includes partners from TUM (Chair of Satellite Geodesy), the Bundesamt für Kartographie und Geodäsie (BKG), the Deutsches Geoforschungszentrum Potsdam (GFZ), and the TU Wien (TUW). DGFI-TUM’s work within Phase 1 (Procedure Definition) of the project focused mainly on (1) existing state-of-the-art EOP products and potential areas for improvement, (2) the definition of the algorithms (combination method etc.), and (3) the implementation of the software branch for the final EOP products (all in close cooperation with the project partners responsible for the rapid combination and the prediction algorithms, respectively).

Following a comparison of the different combination approaches at observation equation, normal equation (NEQ) and parameter levels, it has been agreed to implement a combination at the NEQ level, enabling a consistent estimation with the benefit of being flexible in terms of technique-specific software packages for the pre-processing: while the technique-specific NEQs can be generated by independent softwares, only a common parametrization and consistent background models have to be guaranteed.

The combination software has been developed in a first working version, and investigations on the single-technique contributions as well as on the combination results have been performed (see Fig. 1.15). The chosen scenario has been evaluated with respect to ESA's accuracy requirements. Resulting from these investigations, recommendations for data processing at ESA have been defined and summarized. They contain a trade-off analysis with respect to their implementation effort and their potential benefits for the project as well as for ESA's current contribution to international service products.

Phase 1 of the project was completed, and Technical Notes on (1) ESA's current contribution to reference frames, time scales, and EOP, (2) state of the art of EOP determination, models and algorithms, and (3) combination scenarios recommended by the project team and the results from the preliminary software. Phase 2 of the project (Implementation and Validation) will cover the implementation, validation and documentation of the combination software.

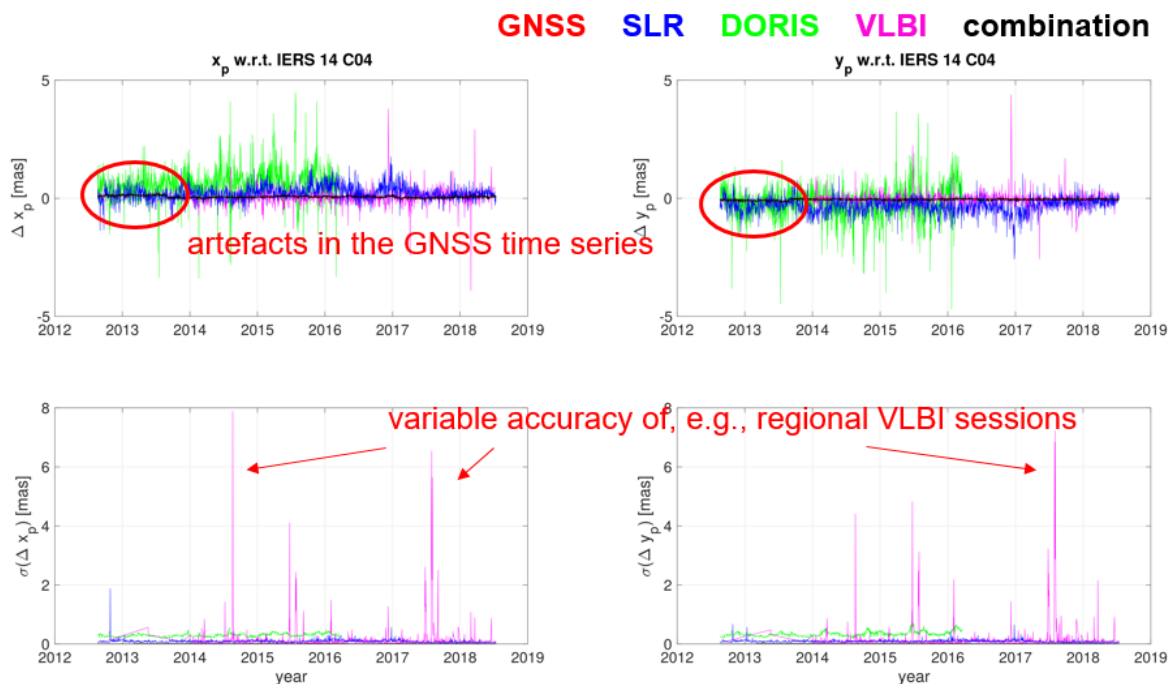


**Figure 1.15:** Terrestrial pole coordinate differences of the four single-technique solutions as well as of the combined solution w.r.t. the IERS 14 C04 time series. The lower panels show the respective standard deviations.

## DFG project CIEROT

The project CIEROT targets at the determination of cryospheric mass changes and their impact on Earth rotation. Polar motion excitation functions were derived from GRACE (Gravity Recovery and Climate Experiment) gravity field observations by transforming hydrological, oceanic and cryospheric mass changes into angular momentum variations. Since GRACE observations are contaminated by erroneous meridional stripes, filtering is essential in order to retrieve meaningful information about mass redistributions within the Earth's subsystems. However, filtering not only reduces the noise, but also smoothes the signal and induces leakage effects. Therefore, a new global grid point approach has been developed in order to reduce such filter effects. The method does not depend on geophysical model information and can be used to separate the signal of several subsystems in a uniform manner. The flowchart of this method is shown in Figure 1.16. Once and twice filtered equivalent water height information from GRACE

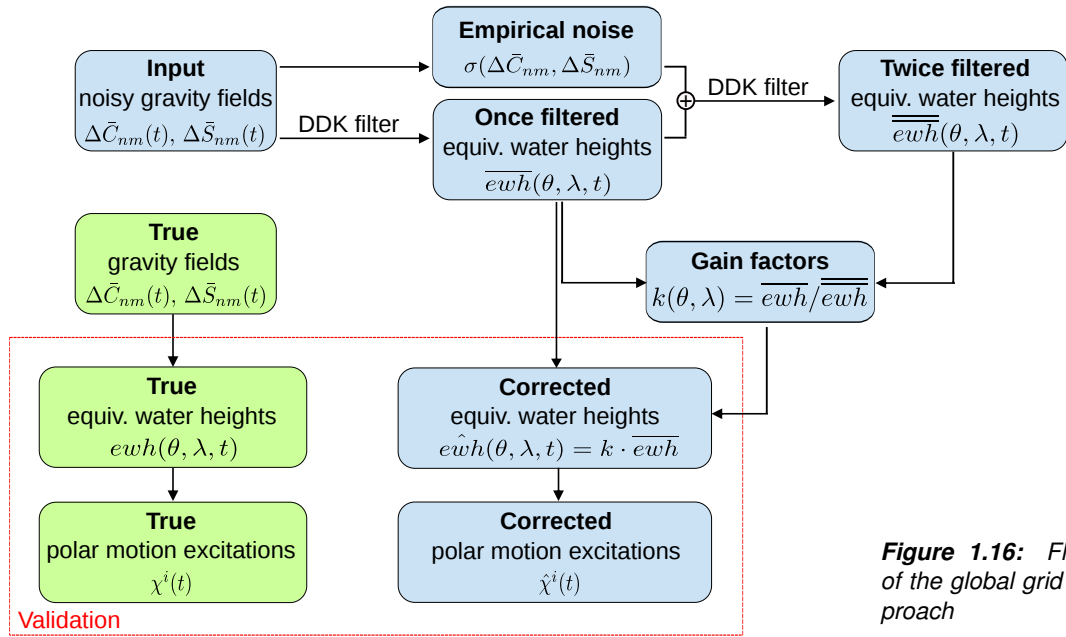


**Figure 1.16:** Flow chart of the global grid point approach

is used to determine gain factors for each grid point. Simulations have shown that the application of these gain factors can reduce erroneous filter effects in the GRACE-derived polar motion excitations up to 10 percent. Validations of real GRACE data with ocean model results reveal that the agreement can be significantly improved.

In 2018, the new Release-06 (RL06) GRACE gravity field solutions became available. Investigations showed that the results from different GRACE processing centers are more consistent among each other, and that the signal-to-noise ratio could be significantly reduced (Göttl et al., 2018). Especially the potential coefficients  $C_{21}$  and  $S_{21}$  show large modifications (up to 32%), mainly caused by the change of the mean pole model from cubic to linear. Concerning GRACE-derived polar motion excitation, the latest release update has a large impact on the oceanic (17%) and hydrological excitation (12%) but only a small impact on the contributions from ice loss in Antarctica (4%) and Greenland (1%). Due to the update from RL05 to RL06, the agreement with ocean model results could be improved by 4 to 15 percentage points, see Table 1.5.

**Table 1.5:** RMS differences (mas)/correlation coefficients between the GRACE-based equatorial effective angular momentum functions for the oceanic mass effect and ocean model results. Trends were removed prior to the determination of the RMS differences and correlation coefficients. The best values are marked in bold.

Gravity field solutions	$\chi_1^O$		$\chi_2^O$	
	ECCO (OAM)	ESMGFZ (OAM+SLAM)	ECCO (OAM)	ESMGFZ (OAM+SLAM)
CSR RL05	5.5/0.49	4.4/0.72	6.0/0.61	6.0/0.66
JPL RL05	8.3/0.35	6.8/0.64	7.7/0.41	6.8/0.60
GFZ RL05	5.7/0.51	4.9/0.69	6.8/0.50	6.7/0.58
ITSG-Grace2016	5.3/0.58	4.0/0.79	6.5/0.54	6.1/0.65
CSR RL06	4.6/0.60	3.9/0.76	5.7/0.66	5.2/0.75
JPL RL06	5.0/0.57	4.4/0.71	5.9/0.63	5.4/0.74
GFZ RL06	5.3/0.58	4.8/0.69	6.2/0.58	5.2/0.76
ITSG-Grace2018	<b>4.5/0.62</b>	<b>3.9/0.76</b>	<b>5.5/0.68</b>	<b>5.0/0.78</b>



## Related publications

- Angermann D., Bloßfeld M., Seitz M., Kwak Y., Rudenko S.: ITRS Combination Centres: Deutsches Geodätisches Forschungsinstitut der TU München (DGFI-TUM). In: Dick W.R., Thaller D. (Eds.), IERS Annual Report 2017, 2018
- Bloßfeld M., Rudenko S., Kehm A., Panafidina N., Müller H., Angermann D., Hugentobler U., Seitz M.: Consistent estimation of geodetic parameters from SLR satellite constellation measurements. *Journal of Geodesy*, 92(9), 1003–1021, doi:[10.1007/s00190-018-1166-7](https://doi.org/10.1007/s00190-018-1166-7), 2018
- Glomsda M., Kwak Y., Gerstl M., Angermann D., Seitz F.: New VLBI Solutions at Analysis Center DGFI-TUM. IVS 2018 General Meeting, Longyearbyen, Norway, 2018
- Göttl F., Schmidt M., Seitz F.: Mass-related excitation of polar motion: an assessment of the new RL06 GRACE gravity field models. *Earth, Planets and Space*, 70(1), doi:[10.1186/s40623-018-0968-4](https://doi.org/10.1186/s40623-018-0968-4), 2018
- Kehm A., Bloßfeld M., Pavlis E., Seitz F.: Future global SLR network evolution and its impact on the terrestrial reference Frame. *Journal of Geodesy*, doi:[10.1007/s00190-017-1083-1](https://doi.org/10.1007/s00190-017-1083-1), 2017
- Kwak Y., Bloßfeld M., Schmid R., Angermann D., Gerstl M., Seitz M.: Consistent realization of celestial and terrestrial reference frames. *Journal of Geodesy*, doi:[10.1007/s00190-018-1130-6](https://doi.org/10.1007/s00190-018-1130-6), 2018
- Rudenko S., Bloßfeld M., Müller H., Dettmering D., Angermann D., Seitz M.: Evaluation of DTRF2014, ITRF2014 and JTRF2014 by Precise Orbit Determination of SLR Satellites. *IEEE Transactions on Geoscience and Remote Sensing*, 56(6), 3148–3158, doi:[10.1109/TGRS.2018.2793358](https://doi.org/10.1109/TGRS.2018.2793358), 2018
- Sánchez L., Völksen Ch., Sokolov A., Arenz H., Seitz F.: Present-day surface deformation of the Alpine region inferred from geodetic techniques. *Earth System Science Data*, 10(3), 1503–1526, doi:[10.5194/essd-10-1503-2018](https://doi.org/10.5194/essd-10-1503-2018), 2018a
- Sánchez L.: SIRGAS Regional Network Associate Analysis Centre, Technical Report 2017. In: Villiger A., Dach R. (Eds.), International GNSS Service Technical Report 2017 (IGS Annual Report), 117–122, doi:[10.7892/boris.116377](https://doi.org/10.7892/boris.116377), 2018b
- Sánchez L.: Status report: GGOS Focus Area Unified Height System (FA-UHS), and JWG 0.1.2: Strategy for the Realization of the International Height Reference System (IHRM). Global Geodetic Observing System (GGOS), GGOS Days 2018, Tsukuba, Japan, 2018c
- Sánchez L., Ågren J., Huang J., Wang Y.M., Forsberg R.: Basic agreements for the computation of station potential values as IHRM coordinates, geoid undulations and height anomalies within the Colorado 1 cm geoid experiment. Global Geodetic Observing System (GGOS), 2018d

## 2 Research Area Satellite Altimetry

*About two thirds of the Earth's surface is covered by water. The exact determination of the geometrical shape of the water surface in space and time, and the investigation of its temporal changes in terms of underlying dynamic processes in the ocean and the continental hydro-sphere is one of DGFI-TUM's primary research goals. Our work targets at the determination of most accurate water levels from satellite altimetry using advanced analysis methods and improved orbit information in order to compute reliable water level trends on global, regional and local scales including uncertainty information. Meanwhile, more than 25 years of observation data are available from several generations of different missions.*

*This comprehensive data wealth forms the basis of DGFI-TUM's research to determine, monitor, and investigate the water stage of the open ocean, in coastal areas, in sea-ice regions, and of inland water bodies. In order to integrate contemporaneous and former altimetry missions to a consistent long-term multi-mission data set, their observations must continuously be updated, harmonized, and calibrated to eliminate systematic differences between the missions (Section 2.1). Over the oceans, the main focus is on the computation of reliable sea level trends, in particular in regions with difficult observation conditions, such as coasts and polar areas. In 2018, an additional focus was set on the determination and analysis of the sea state. The sea state, being related to patterns of waves and winds, is one of the so-called Essential Climate Variables (ECVs) and thus a key quantity to record and investigate the processes of climate change (Section 2.2). Over the continents, the observations are used to assess, monitor and predict water levels of inland water bodies and – by combining satellite altimetry data with remotely sensed horizontal water extents – to derive information on changes in water storage (Section 2.3).*

### 2.1 Multi-Mission Analysis

#### Calibration of Sentinel-3A

The inter-mission cross-calibration is a basic prerequisite for long-term sea level change studies on all spatial scales. Especially, for climate studies the consistent combination of successive missions is essential. DGFI-TUM is performing multi-mission altimeter crossover analysis (MMXO) on a regular basis in order to estimate relative radial errors between the different altimeter systems operating simultaneously. The cross-calibration is realized globally by minimizing a large set of single- and dual-satellite sea surface height (SSH) crossover differences computed between all contemporaneous altimeter systems. The total set of crossover differences creates a highly redundant network and enables a robust estimate of radial errors with a dense sampling for all altimeter systems analyzed. An iterative variance component estimation is applied to obtain an objective relative weighting between the different altimeter systems.

One of the most recent missions is Sentinel-3A launched in 2016. We use reprocessed data of the first 1.5 years of the mission for cross-calibration with other altimetry missions, especially with Jason-3. Sentinel-3A carries a Synthetic Aperture Radar (SAR) altimeter, however, in addition, Pseudo Low Resolution Mode (PLRM) data are provided, i.e. the SAR pulses are used to compute classical pulse-limited waveforms. The results show a range bias of 3.6 cm between Sentinel-3 SAR and Jason-3, which increases to 4.5 cm when PLRM data for Sentinel-3A are used. More importantly, a drift behavior between the two missions can be seen, originating from Sentinel-3A since it is not only detectable with respect to Jason-3 but also with respect

to Jason-2 and SARAL. As can be seen from Fig. 2.1 the drift is estimated yield 4.0 mm/year for SAR and only 2.0 mm/year for PLRM. However, it is important to keep in mind that the period under investigation is very short and a longer period is necessary to check the long-term behavior. Since model information are used for correcting atmospheric effects, the drifts cannot be caused by possible drifts in the radiometer on board of Sentinel-3A. Instead, a connection to the sea state bias (SSB) correction, which is not yet fully tuned for SAR measurements, is assumed. More information on the method of MMXO and detailed results are provided in Dettmering and Schwatke (in press).

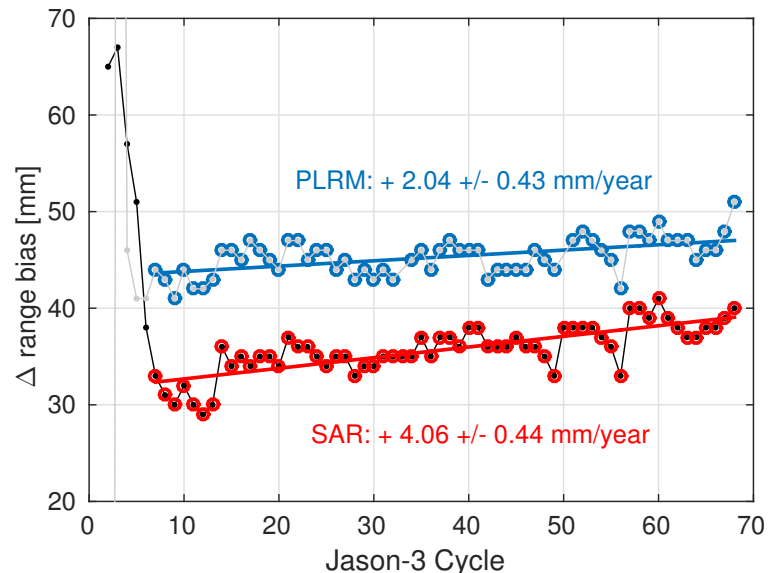


**Figure 2.1:** Relative range bias of Sentinel-3A SAR (red) and PLRM (blue) with respect to Jason-3 (from Dettmering and Schwatke, in press).

## 2.2 Sea Surface

### Performance of Sentinel-3A in the Baltic Sea

The European Earth Observation mission Sentinel-3 (S3) is one of the most recent satellite configurations in orbit, carrying among other sensors a Delay-Doppler altimeter (Synthetic Aperture Radar Altimeter, SRAL) for observing the sea level with an increased resolution. Furthermore, the Ocean and Land Color Instrument (OLCI), an imaging spectrometer with five cameras, is also mounted on the satellite. It provides multi-spectral optical images in parallel to the altimeter observation. The S3 mission, in its current state, consists of two identically constructed satellites (S3-A, S3-B), placed phaseshifted at the same orbit.

The Baltic Sea is a semi-enclosed peripheral sea of the Atlantic ocean with depths up to 200 meters. The Baltic Sea is characterized by complex bathymetry and coastlines. Moreover, northern parts of the Baltic Sea are seasonally covered by sea-ice. This region was used to test and evaluate the performance of S3-A. First investigations are performed in coastal areas with sea-ice coverage in the winter months. Figure 2.2 shows a comparison of data observed by the tide gauge station Kemi with altimetry-derived sea level anomalies obtained by applying different built-in retracker algorithms. Unexpectedly, the S3 ice-sheet retracker (i.e. a six parameter least-squares fit of a modified Gaussian form to the radar echo) shows the best agreement with a correlation of 0.86 and a standard deviation of  $\pm 0.18$  m. Other retracking strategies are failing or show stronger differences mainly caused by challenging coastal or sea-ice conditions.

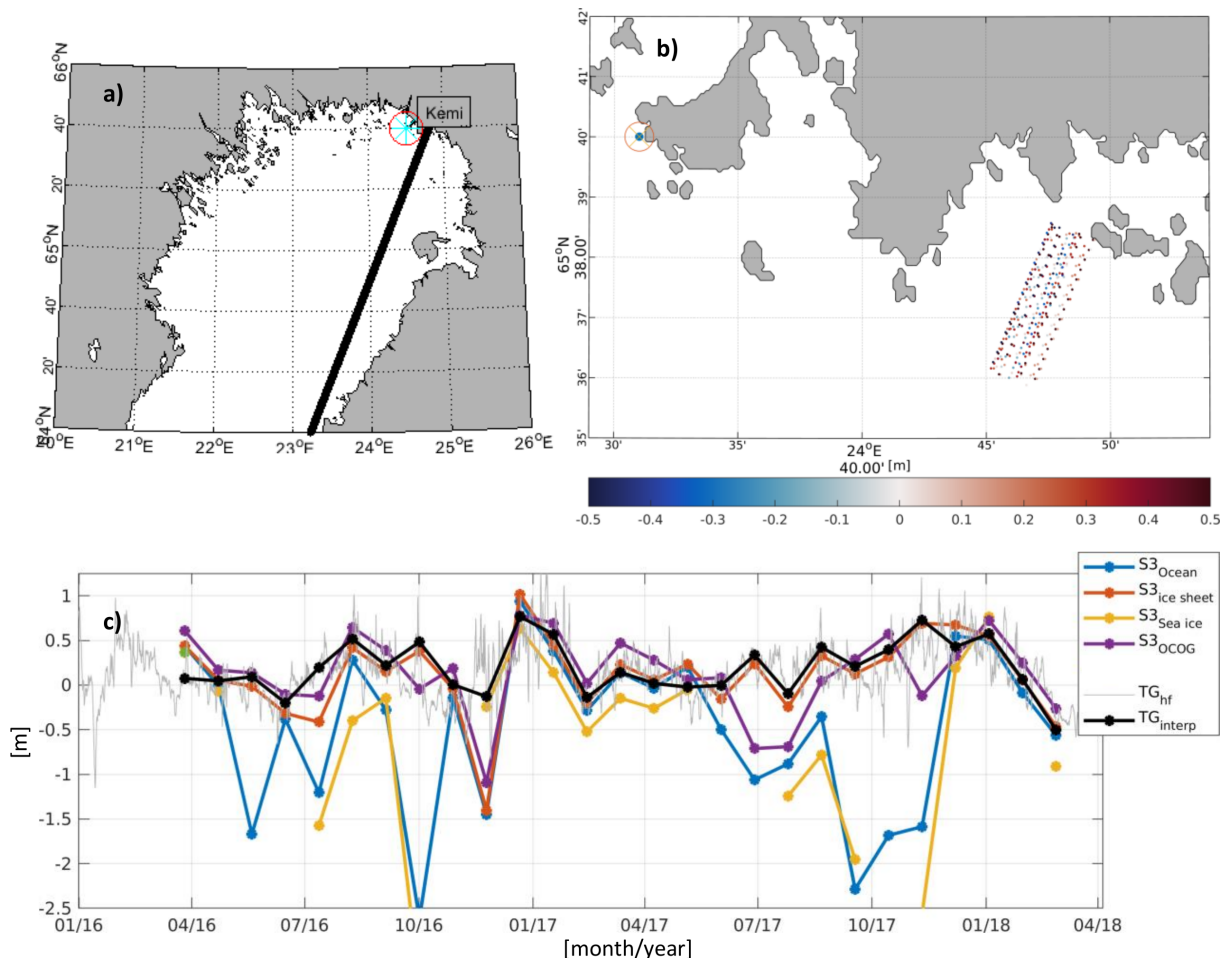


**Figure 2.2:** Overview (a) and detailed coastal conditions (b) of the tide gauge location Kemi. Comparison of sea level anomalies (c) obtained from different retracker algorithms with tide gauge records.

## Improving the Sea State Bias correction

The Sea State Bias (SSB) is among the time-variable corrections that are applied to sea surface height estimates from satellite altimetry. With a mean of 5 cm and a time-variable standard deviation of 2 to 5 cm in the open ocean, it is currently one of the largest sources of uncertainty linked with the altimetric signal. SSB is linked with both the signal processing of the radar echo and the physics of the measurement; its correct interpretation and the understanding of its coastal variability are essential to produce more accurate and more precise sea level estimations.

The determination of the SSB in coastal areas is even more challenging than in the open ocean. In these regions, since more than ten years, the altimetry community is trying to improve the sea level estimates that were previously discarded due to interferences in the signal and scarce reliability of the corrections, including SSB (see e.g. Restano et al., 2018). The physical effects related to the interaction of the radar echo with the crests and troughs of the waves and the numerical effects due to the way the altimeter tracks the echoes (both components of the SSB corrections) need to be reviewed for an altimetry product in the coastal ocean. Unlike in the open ocean, the shape of the waves is influenced by shoaling, refraction and bottom friction in the shelf seas and by depth-induced wave breaking and triad wave-wave interaction in waters shallower than 20-30 m. Moreover, the traditional open-ocean retracker algorithms are not able to estimate correctly in the coastal zone the SWH and wind speed, on which the parametric

relation that is used to compute SSB is not anymore valid. Finally, since the SSB models are empirically computed from altimetry observations, other components of the residual altimetric error might have a dependence on sea state that varies depending on the regions, such as tidal correction, which are also computed by means of altimetric data and are much less known in shelf seas than in open ocean. Therefore, correcting for the SSB using a model computed on a global scale might not be enough representative, in particular for shelf seas. For these reasons, we have developed a high-frequency and retracker-dependent SSB correction in order to improve the performances of HF altimetry data. Moreover, a specific regional SSB correction has been computed. The regions of study concerning the evaluation of the results are the Mediterranean Sea (Med) and the North Sea (NS). The dataset used are the Jason-2 altimetry data from the standard product (called SGDR) and from the reprocessed ALES product of DGFI-TUM.

Three different SSB corrections are applied to derive the sea level anomalies (SLA) in this study:

1. 1-Hz SSB is the SSB correction available at low frequency (LF) in the SGDR. The correction is derived using a non-parametric estimation: a statistical technique (kernel smoothing) is used to solve a large system of linear equations based on the observations and on a set of weights. The result is a 2D map of the SSB against wind speed and SWH.
2. 20-Hz SSB is the high-frequency (HF) SSB correction derived by using the same SGDR model and obtained courtesy of Ngan Tran from Collecte Localisation Satellites (CLS), but computed for each HF point using the HF wind speed and SWH estimations from SGDR and ALES. The computation of the current SSB model is based on an empirical relationship between three retracked parameters. While part of it is due to the physics of the waves and will manifest itself at LF, the model contains also a relation that is due to the correlated errors in the estimation, which is performed at HF. Applying the SSB model at LF therefore means assuming that the error component of the sea level estimation related to the sea state exists only at long wavelengths, reducing its impact on the short-wavelength components.
3. Reg SSB is the SSB correction derived using the regional parametric models computed using the Fu-Glazman (FG) model<sup>1</sup>, and then applied to each HF point using the HF wind speed and SWH estimations from SGDR and ALES.

The simple application of an SSB correction based on HF data improves the precision of HF sea level data by 14%. We notice, as shown in Fig. 2.3, that the improvement shown by the 20-Hz SSB indicates that this application is a method to reduce the retracker-related noise. Subsequently, the recomputation of a parametric regional SSB model improves it overall by 29%.

Therefore, as a first step, the SSB correction should be computed and applied using the high-rate measurements of SWH and backscatter coefficient. This is because a high-rate application of the SSB correction reduces the correlated errors between range and wave height estimations. Further advantages are also found using a recomputed regional model for each specific retracker. The future challenges will be therefore the development of different SSB regional solutions for LRM altimetry, including the interpretation of possible differences according to the selected regions, and the development of a SSB correction for the Delay-Doppler (DD) retracking.

---

<sup>1</sup>Fu, L.L. and Glazman, R., 1991. The effect of the degree of wave development on the sea state bias in radar altimetry measurement. *Journal of Geophysical Research: Oceans*, 96(C1), pp. 829–834

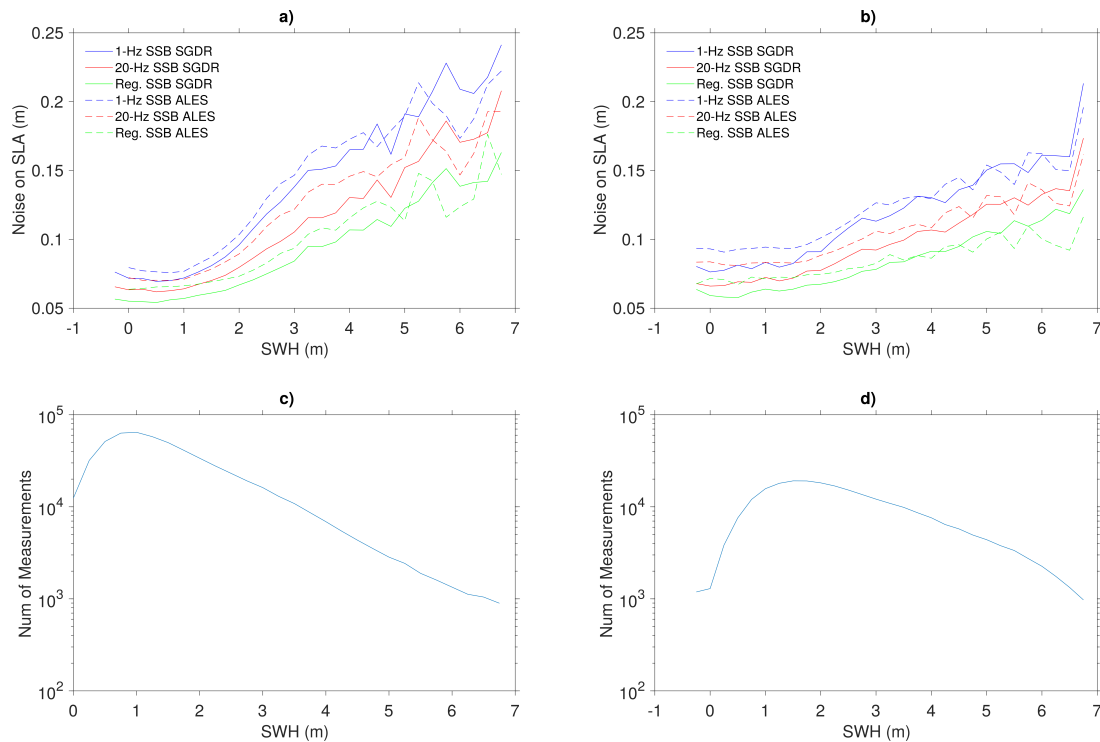


**Figure 2.3:** Noise of the sea level anomalies computed as difference between consecutive high-rate estimations using different SSB corrections analyzed in this study in Med (a) and NS (b). Continuous lines refer to SGDR data, while dashed lines refer to ALES data. The sea level anomalies were corrected with the original 1-Hz SSB correction (blue), with the 20-Hz SSB correction (red) and with the regional SSB correction (green). Number of measurements available with respect to the significant wave height in Med (c) and NS (d).

This work is a continuation of an initial assessment performed in 2016 and followed by a Master Thesis in 2017. Results and a wide validation were published this year by Passaro et al. (2018) where further details and analysis are provided. The research was partially funded by the *ESA Sea Level Climate Change Initiative*, in which DGFI-TUM is part of the Consortium.

### First Steps of the *ESA Sea State Climate Change Initiative*

The general condition of the ocean due to the action of wind waves and swell is defined as Sea State and constitute a very important parameter for ocean weather and climate. The Sea State has therefore been included in the list of *Essential Climate Variables* (ECVs) that the Climate Change Initiative of the European Space Agency studies - the same frame which allows for studying the sea level variations for several years (Legeais et al., 2018). The aim of this project is to develop a consistent multi-decadal global record on sea state parameters (principally Significant Wave Height, but potentially also mean square slope, wind speed, wave period and wave spectra). This will be achieved through careful retuning of altimeter algorithms and processing of SAR data, coupled with stringent quality control, independent assessment and climate evaluation.

DGFI-TUM is highly involved in the project, which involves a large number of European public and private institutions, and leads the Algorithm Development (AD) Team for the Satellite Altimetry part. The AD is responsible for the development of new estimation techniques that are able to improve the signal-to-noise ratio of the sea state parameters. Secondly, it has to guarantee that the strategy of choice is able to deliver estimations that are consistent during the 25 years of altimetry data in terms of biases and, as much as possible, in terms of performances. If on one side this means that the application of the same algorithm to all the missions

could be an advantage, on the other side we shall not ignore the wider possibilities and better performances that the Delay-Doppler processing in Cryosat-2 and the Sentinels provide. The team will start the work with several efforts in parallel: the ideas for a subwaveform retracker focused on the wave estimations will be presented, as well as the current status of an adaptive numerical retracker for sea state and advanced techniques to exploit the full information (from the so-called stack data) of SAR altimetry.

The other main duty is the planning and execution of an algorithm testing phase open to all external participants, in which the criteria for the evaluation of the algorithms and the final selection shall be established. Aside from typical criteria (bias with ground truth measured by buoys, comparison with model simulation of waves and wind), other priorities in the evaluation of the performances, aimed at maximizing the scientific exploitation of the future dataset will be discussed: for example, the accuracy for retrieving large wave heights and the performances in coastal zone.

The project started in 2018 and DGFI-TUM efforts were mainly on the definition of a set of rules and statistics to be used next year during the algorithm selection (called Round Robin Exercise). This was also the focus of the Master Thesis of E. Barbieri (2018). In Fig. 2.4 an example of these statistics is shown: wave height data from Jason-3 are evaluated against a wave model in the open ocean, showing very good correlation and a standard deviation of about 35 cm.

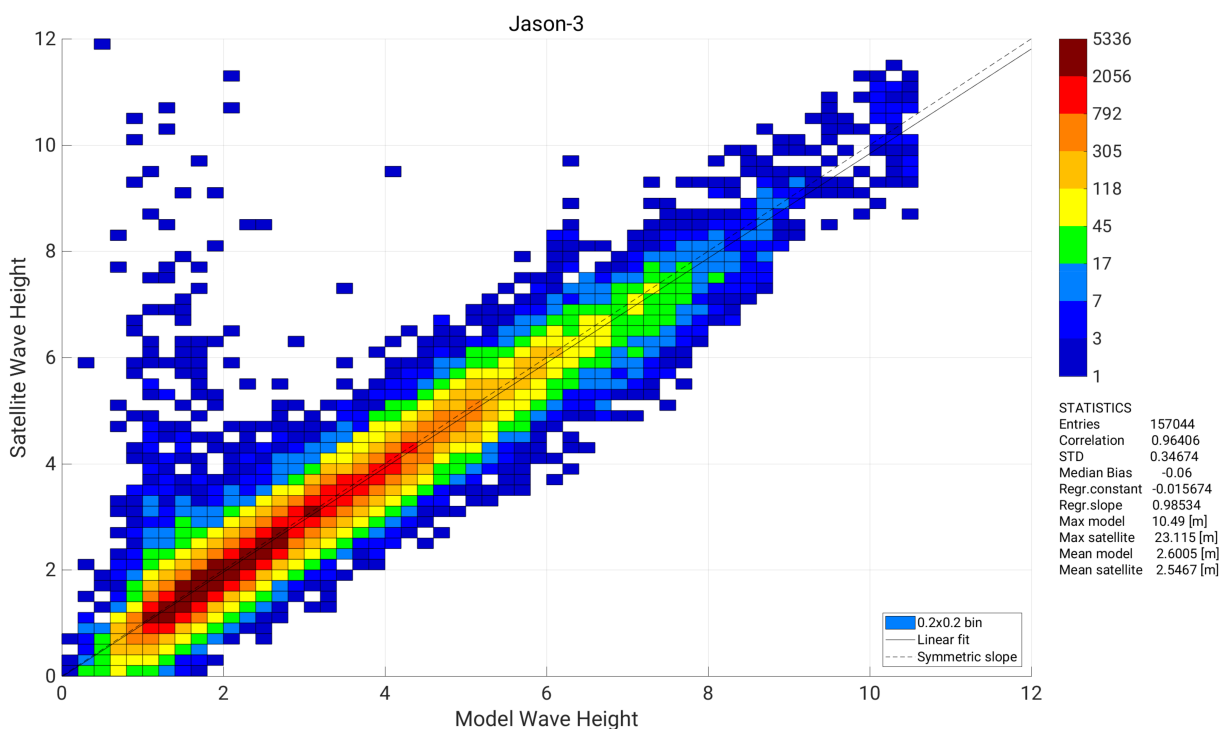


**Figure 2.4:** Density plot of Jason-3 Significant Wave Height retrievals against coincident values from the Mercator Wave Model available in Copernicus Marine Service. The chosen test area is the West Coast of the USA.

## Coastal Mean Sea Surface

The Strait of Gibraltar is the only gateway between the Mediterranean Sea and the Atlantic Ocean. Both seas have very different characteristics in terms of temperature, salinity and nutrients. Water exchange that takes place here may have consequences much farther away, for example contributing to the high salinity of the Nordic Seas, a key area for deep water

formation. Due to the prominent role of the ocean as a climate regulator, understanding the dynamics of this water exchange is essential to understand the climate in the Mediterranean as well as important features of the global ocean circulation.

Together with an international team of scientists satellite altimetry and model data was used to monitor the water level from the two sides of the strait (Gomez-Enri et al. 2018). Differences between the two sides are a way to monitor the surface water flow out and into the Mediterranean Sea. A mean sea level was recomputed using several years of dedicated reprocessed coastal data from the ALES algorithm<sup>2</sup>. This data allowed linking the sense of the surface currents in the strait to the wind regime. It is observed that specific wind events are able to reverse the mean circulation (which normally drives surface waters out of the Mediterranean) and therefore weaken the net Atlantic water inflow toward the Mediterranean Sea, as seen in the example of Fig. 2.5.

The study is a paramount example of the value of innovative coastal sea level data from satellites to improve the knowledge of ocean dynamics in areas where previously only sparse in-situ data could offer a localized view. It is also an example of the need of coastal oceanography to evolve as a synergy of different remote sensing, model and in-situ data.

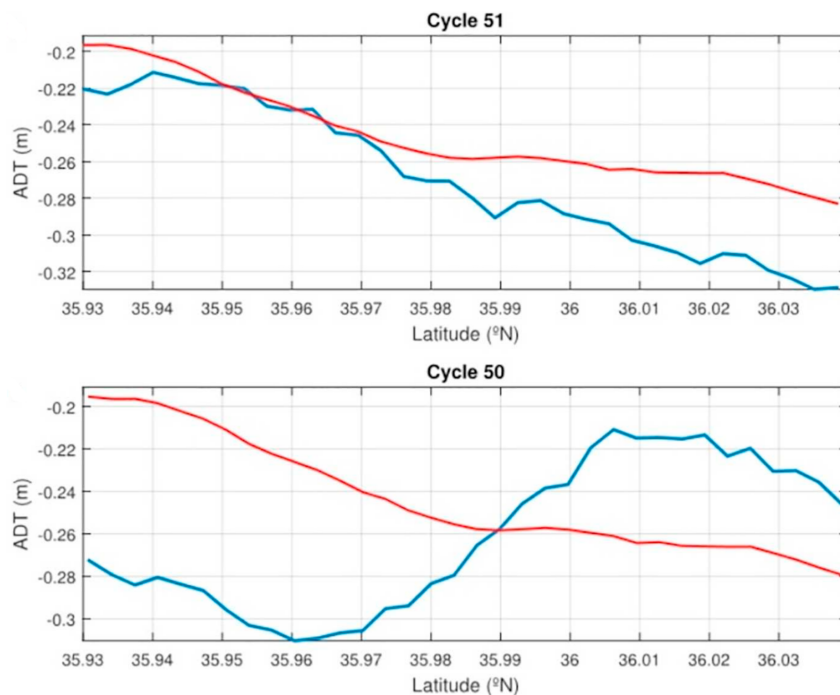


**Figure 2.5:** Two examples of Absolute Dynamic Topography (ADT, in blue) measured by reprocessing the Envisat altimetry data across the Strait of Gibraltar, against the coastal mean sea level in red. All data were computed using the ALES algorithm. Above, the mean situation in which the sea level on the North is higher than in the South. Below, the reversal of the situation, due to Ekman transport generated by strong easterlies winds.

## Ocean topography in the northern Nordic Seas from ocean modeling and satellite altimetry

Satellite altimetry observations in the northern Nordic Sea have been used to monitor the dynamic ocean topography (DOT) for more than two decades and provide information about

<sup>2</sup>Passaro M., Cipollini P., Vignudelli S., Quartly G., Snaith H.: ALES: A multi-mission subwaveform retracker for coastal and open ocean altimetry. Remote Sensing of Environment 145, 173-189, doi:10.1016/j.rse.2014.02.008, 2014



changes in the ocean circulation, the major current pathways and water mass transformation. The region spans the area from north of Iceland to the Fram Strait between the East Greenland Coast, Spitsbergen and the Barents Sea. It embodies the major ocean current pathways of the in- and outflowing water masses of the Arctic Ocean. Moreover, the region is directly affected by sea-ice coverage, melting glaciers with enhanced fresh water inflow and rapid sea state changes.

The observations are characterized by an irregular sampling due to the along-track profiling instrument geometry and fixed orbit characteristics. One of the main work packages of the DFG project NEG-OCEAN considers the bridging of periods, where altimetry data is missing (e.g. due to ice-coverage) and to fill observation gaps using the ocean model FESOM (Finite Sea-Ice Ocean Model, developed by the Alfred-Wegener Institute). The model, based on an unstructured mesh with local refinements better than 1 km, provides daily outputs of differential water heights and includes a sea-ice drift parameter considering the major drift ways of sea-ice floes.

In order to evaluate the potential of a possible combination of the altimetry-derived along-track DOT elevations – carefully preprocessed by waveform classification (Dettmering et al., 2018) and retracking (Passaro et al., 2018) – and the FESOM differential water heights, a comparison of both quantities has been performed. The comparison is based on the analysis of the temporal variability, the frequency content and regional signal patterns. It indicates systematic discrepancies and consistencies.

The FESOM water level estimates are interpolated to the altimetry tracks before both datasets are averaged daily. A harmonic frequency analysis (Fourier Analysis) is performed in order to analyze the phase and amplitude spectrum as well as constant offsets. Figure 2.6 displays the temporal evolution of daily DOT means from altimetry and FESOM, the amplitude spectrum and the estimated dominating annual signal. The clear offset between the model and the observations can be explained by different height references. Both datasets show consistent dominant frequencies, but the magnitudes differ due to a smoother model output. The stronger smoothing of the model and the phase difference in the annual signal can be assigned to an insufficient consideration of the freshwater inflow (e.g. glacier runoff) and coarse atmospheric forcing models.

In a second step, a spatial differential analysis (Fig. 2.7) indicates regional deflections of > 40 cm due to errors and artifacts in the underlying geoid model in higher latitudes. Further discrepancies can be found in the Greenland Shelf region due to very high ocean and sea-ice dynamics that cause uncertainties in the altimetry range estimations. Regionally determined correlations are high, especially in the central Greenland Sea; more results can be found in (Müller et al. 2019).

### **Updated Empirical Ocean Tide model: first impressions from the North Sea**

A preliminary version of the EOT model – namely the EOT18t – was recently implemented, and takes advantage of the latest progresses in altimetry, e.g. by coastal retracking (Piccioni et al., 2018). The method used to derive the single tidal constituents is a least-squares based harmonic analysis, performed on Sea Level Anomalies corrected for the FES2014 tide model. Fifteen tidal constituents are computed on a regular grid with a resolution of 1/8 degree. For each grid node, altimetric observations are selected within a radius of 330 km, and weighted with a Gaussian function dependent on the distance to the node. The data used for this purpose are 1-Hz sea level observations available on the DGFI-TUM's open Altimetry Database (openADB). Observations from the following missions were included in the computation, reaching a temporal coverage of ca. 25 years: Topex, Jason-1, Jason-2, Envisat, ERS-2, ERS-1.

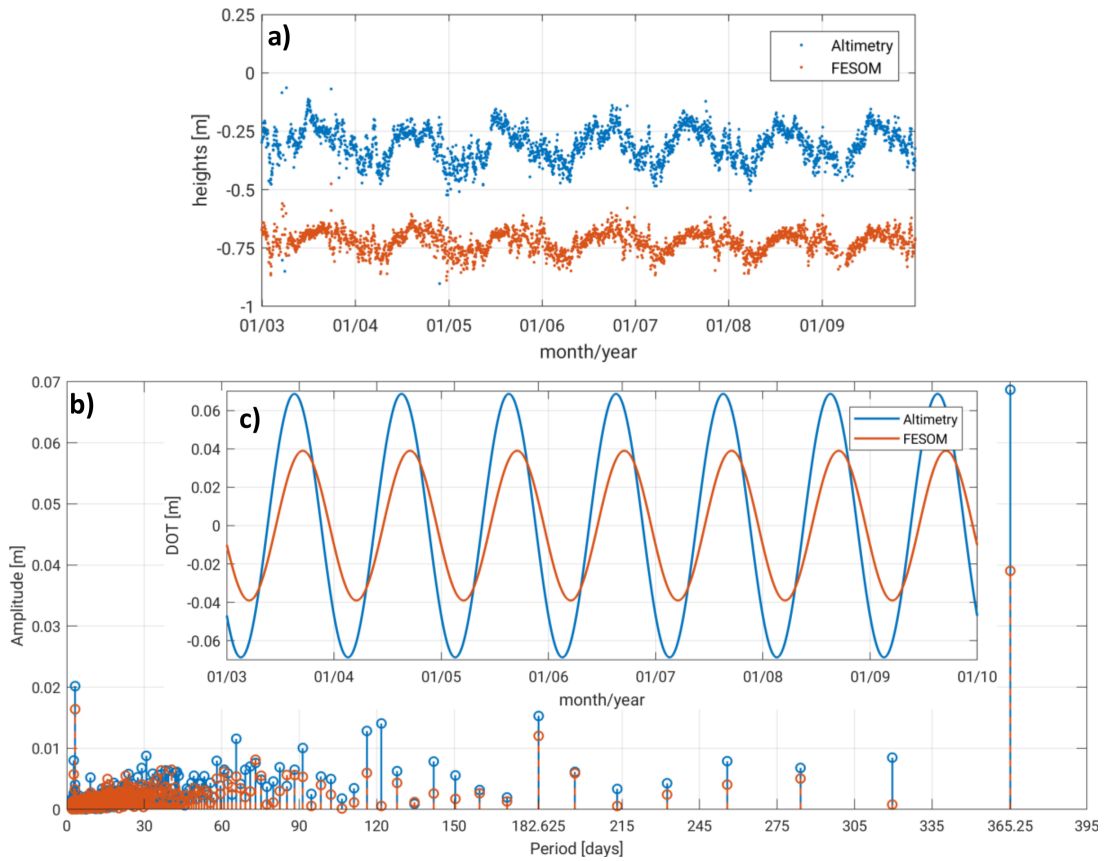


**Figure 2.6:** Temporal evolution of daily means (a), amplitude spectrum (b) and estimated annual signal (c) based on along-track data between 2003–2009 (Müller et al. 2019).

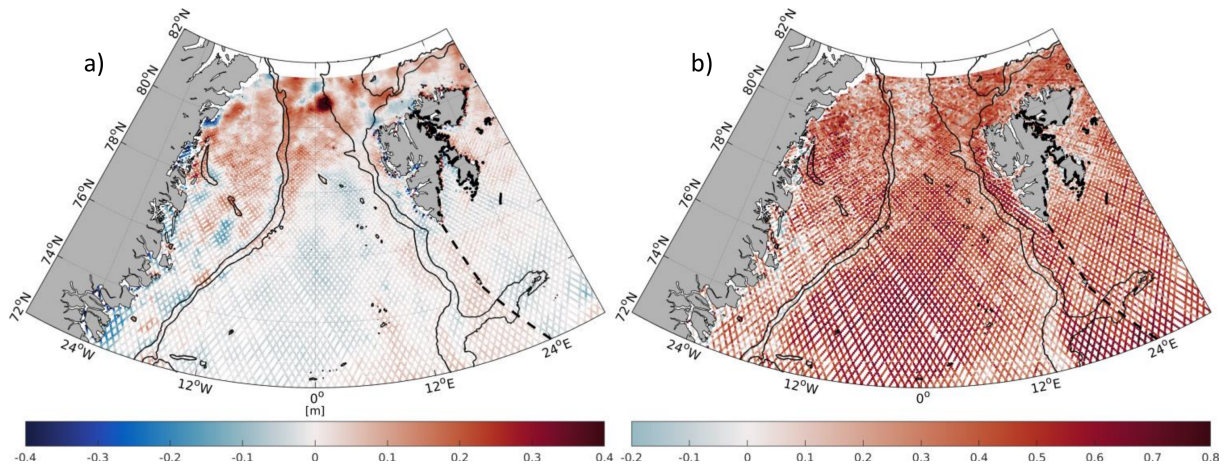


**Figure 2.7:** Differences (a) and correlations (b) between altimetry and FESOM residual DOT between 2003–2009, sorted in along-track bins (Müller et al. 2019).

A regional assessment of the EOT18t model was carried out in the North Sea, which is an area characterized by a large number of in-situ observations that allow an analysis of the model performance over shallow and coastal seas.

The evaluation of the model was performed with comparing the root-mean-square (RMS) and root-sum-squared (RSS) errors of the derived EOT18t tidal constants with the errors of already existing models. The errors are computed against the in-situ harmonic constants available in the TICON dataset, and integrated with additional data located in shelf seas and provided by external sources. In a first comparison with the previous DGFI-TUM model, the EOT11a,

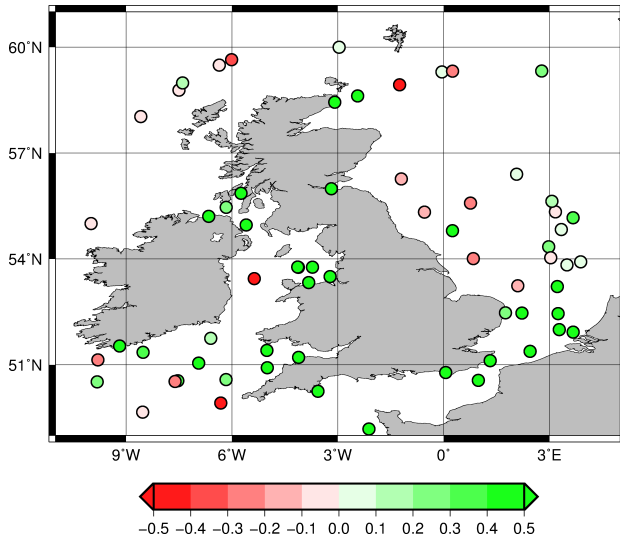


**Figure 2.8:** RSS difference (in cm) between EOT11a and EOT18t against in-situ data. Improvements for EOT18t are in green.

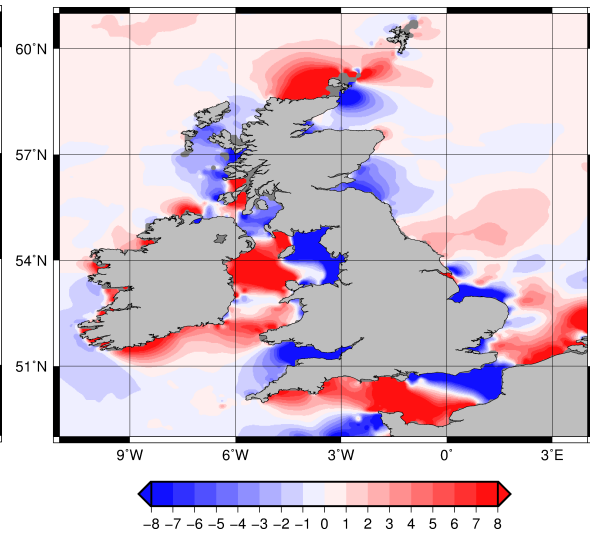


**Figure 2.9:** Difference of in-phase component of M2 tide between EOT18t and EOT11a. Scale in cm.

EOT18t shows improvements in most of the sites considered: In Fig. 2.8 a general performance enhancement with EOT18t can be measured in terms of RSS values (the green markers represent the improvements for the single in-situ locations). This result is primarily due to the use of updated altimetry data and the exploitation of FES2014, which is characterized by a high-resolution bathymetry and a refined mesh at the coast. This is also the reason why the largest differences between the models can be observed at coastal areas. Figure 2.9 shows the discrepancies seen in the in-phase M2 constituent, that mainly occur in proximity of narrow seas with complex coastal areas, such as the Irish Sea and the English Channel.

A summary of the performance of the most recent models against in-situ data is shown in Table 2.1, in terms of RMS and RSS errors. The results are displayed for all the major constituents available from the in-situ measurements. Each value represents the average computed over all the locations. A performance enhancement in EOT18t with respect to its former version is observed for all constituents, reaching an overall improvement of ca. 1 cm. In particular, M2, S2, and M4 are improved by more than 1 cm. EOT18t is also in line with the displayed tide models, and reflects the general behavior of its background model. Further updates will be applied to EOT18t. A new grid with latitude-independence and finer coastline fit is currently tested, and the use of coast-tailored altimetric products, together with alternative processing techniques are being evaluated and eventually integrated in order to improve tidal estimates in coastal areas, where most of the models still show poor performance.

Constituents	EOT18t	EOT11a	FES2014	TPX08	DTU10	GOT4.8
M2	3.42	5.69	3.47	6.37	4.59	16.14
N2	1.12	1.85	1.17	1.72	1.93	2.37
S2	1.46	2.86	1.49	2.18	2.27	5.90
K1	1.12	1.17	1.04	1.20	1.17	1.87
O1	0.64	0.76	0.66	0.80	0.73	0.95
Q1	0.72	0.75	0.70	0.78	0.72	0.79
M4	0.59	2.75	0.62	0.99	2.19	2.28
RSS	4.11	5.01	4.12	4.90	4.77	6.70

**Table 2.1:** Comparison of the averaged RMS and RSS errors (cm) of the existing tide models computed for the major tidal constituents.

## The TICON dataset

For the validation of empirically derived ocean tides models, such as the EOT, a validation by in-situ observations from tide gauges is indispensable. To allow for an easy comparison, DGFI-TUM generated a validation dataset, which has been made available for public use. The TICON (Tidal CONstants) dataset contains harmonic constants of 40 tidal constituents computed for 1145 tide gauges located on a quasi-global scale. The tidal estimations are based on publicly available sea level records of the second version of the Global Extreme Sea Level Analysis (GESLA) project and were derived performing a least-squares harmonic analysis on the sea level time series. The geographical distribution of TICON can be seen in Fig. 2.10.

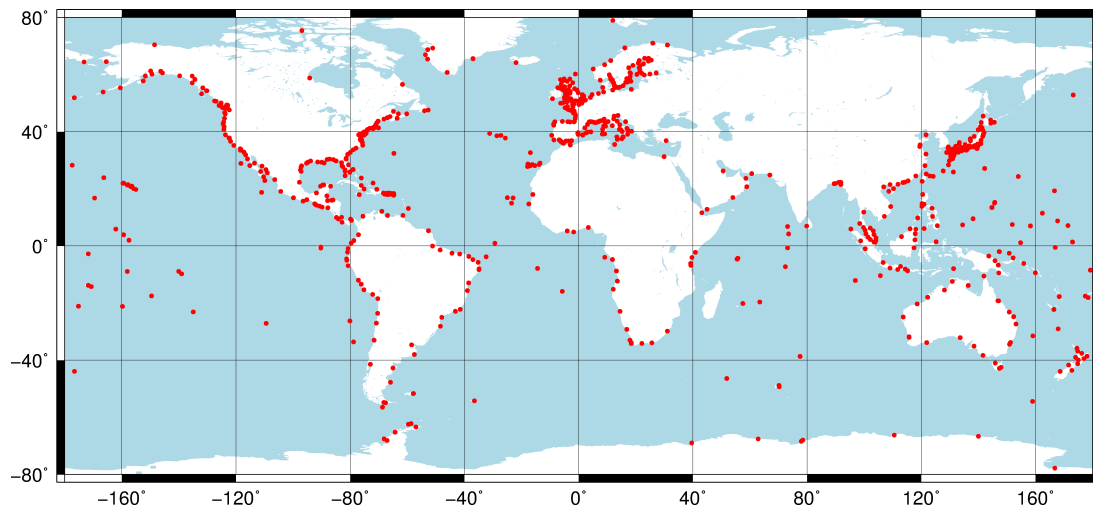


**Figure 2.10:** Geographical distribution of TICON data.

The dataset was built using an automatic program that computes the harmonic constants for the 40 tidal constituents. The script performs a preliminary selection of records suitable for the analysis, according to the period of the data acquisition. The minimum record length allowed is one year, in order to overcome problems related to the tidal signal separation. With a second screening observations with no quality control or flagged as incorrect or doubtful are excluded. In some cases the records show a severe shortening of the observation period because the flagging occurs at the extremes of the time series. After removing the flagged values at the extremes of the records, the amount of missing data for more than 500 records is below 3%.

Finally, in order to perform the least squares for the longest time series possible, a threshold of 30% of missing observations was set, below which the records are processed for their full length. This criterion is used to compute the tidal harmonic on the full time series, reducing the risk of processing records with highly scattered observations. With these criteria, 1145 records were processed, that correspond to the 89.7% of the total 1276 original public GESLA records. The results are stored in a text file, and include additional information on the position of the stations, the starting and ending years of the analyzed record, the estimated error of the fit, a code that corresponds to the source of the record, and additional information on the single time series.

TICON finds applications in the sea level and ocean tide community, and it represents a validation dataset that has a direct access and is easy to handle, and allows the users to select the records according to their needs. TICON has been published via the the PANGAEA data repository from where it is freely available ([doi:10.1594/PANGAEA.896587](https://doi.org/10.1594/PANGAEA.896587)).

## 2.3 Inland Altimetry

### Enhancement of the *Database for Hydrological Time Series of Inland Waters (DAHITI)*

The DGFI-TUM has been developing the Database for Hydrological Time Series of Inland Waters (DAHITI) since 2013. It can be accessed via [dahiti.dgfi.tum.de](http://dahiti.dgfi.tum.de). DAHITI provides water level time series of globally distributed inland water bodies, such as lakes, rivers and reservoirs. Currently, about 1600 targets are available (for comparison: ~700 in 2017). More than 500 users are registered in DAHITI, and the international community makes use of the data for a wide variety of applications and studies.



**Figure 2.11:** Map of inland water targets available via the DAHITI website

The algorithm for estimating water level time series combines an extended outlier detection and a Kalman filter approach (described in detail in (Schwatke et al. 2015)<sup>3</sup>). Also 200 targets have been created or updated until now whose water levels are based on data from the new Sentinel-3A and Sentinel-3B altimeters launched in 2016 and 2018, respectively.

A major step in 2018 was the extension of the data holding of DAHITI by a new data type, namely by time series of surface areas for lakes and reservoirs. Currently, about 50 surface area time series are available in DAHITI. The applied approach for the computation of surface areas is described in the next section; see also (Schwatke et al. 2019) for more details.

### Automated extraction of time-variable water surfaces of lakes and reservoirs (AWAX)

In many hydrological applications and for the calibration of hydrological models, information on water storage changes of lakes and reservoirs are required. These can be derived from remote sensing data, i.e. four dimensional information based on water levels and surface areas.

<sup>3</sup>Schwatke C., Dettmering D., Bosch W., Seitz F.: DAHITI – an innovative approach for estimating water level time series over inland waters using multi-mission satellite altimetry. *Hydrology and Earth System Sciences* 19(10): 4345–4364, 2015, doi:[10.5194/hess-19-4345-2015](https://doi.org/10.5194/hess-19-4345-2015)

Satellite altimetry has been proven to be a valuable tool for monitoring water level changes of inland water bodies. Since 2017, DGFI-TUM has been working to develop the AWAX approach for the computation of monthly surface area time series of lakes and reservoirs for the time span between 1984 and 2018 using optical images from Landsat and Sentinel-2 (Schwatke et al., 2019).

In the first step of this approach, monthly land-water masks are computed from Landsat and Sentinel-2 observations. Therefore, the five water indexes, *Modified Normalized Difference Water Index (MNDWI)*, *New Water Index (NWI)*, *Automated Water Extraction Index for Non-Shadow Areas ( $AWEI_{nsh}$ )*, *Automated Water Extraction Index for Shadow Areas ( $AWEI_{sh}$ )* and *Tasseled Cap for Wetness ( $TC_{wet}$ )* are used and combined, and an automated threshold computation is applied. The resulting water masks still contain data gaps caused by, e.g., clouds, cloud shadows, snow and data voids.

In the second step, all monthly land-water masks for a respective lake or reservoir are accumulated in order to estimate a long-term water probability mask between 1984 and 2018. Then, this mask is used in an iterative approach for filling the data gaps of all monthly masks. Finally, a surface area time series is computed.

Figure 2.12 shows the initial (gray) and final (orange) surface area time series of the Toledo Bend Reservoir. Furthermore, the filled area (green) and the used Landsat and Sentinel-2 data are presented.

For comparison, also water levels from in-situ stations (light red) and satellite altimetry (blue)

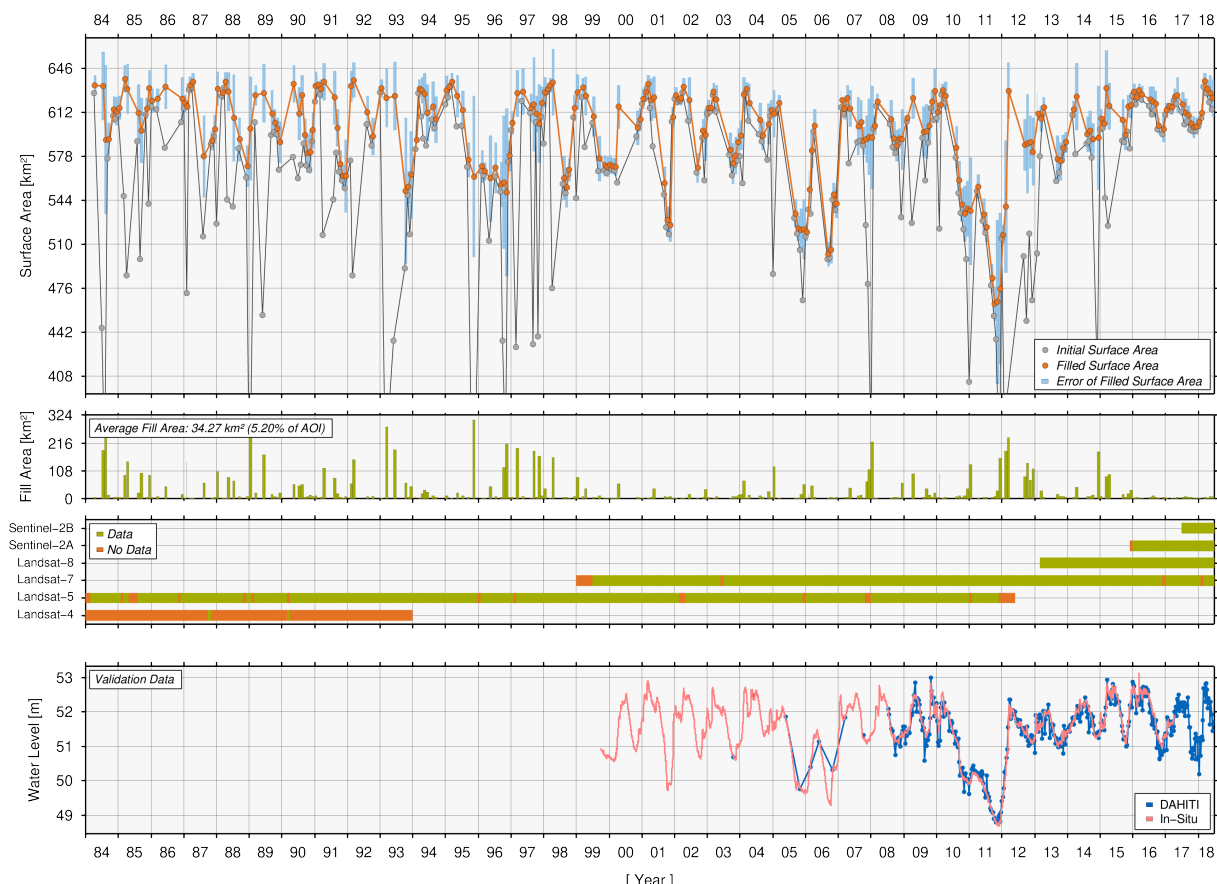


**Figure 2.12:** Initial and final surface area (with errors) time series of Toledo Bend Reservoir (USA) with additional information on filled areas and used optical data. For comparison, the bottom plot shows water level time series from in-situ data and DAHITI.

are displayed. As expected, a high correlation between water stage and area is obvious. For the displayed example, the correlation  $R^2$  between the surface area from AWAX and in-situ measurements of the water level is 0.52 for the initial surface areas (with data gaps). This value increases to 0.88 for the final gap-filled surface areas, which is an improvement of about 68%. When using water levels derived from satellite altimetry instead of in-situ observations, the correlation  $R^2$  is 0.80.

### DFG project WALES

In 2018, the DFG funded Research Unit *GlobalCDA* (Understanding the global freshwater system by combining geodetic and remote sensing information with modelling using a calibration/data assimilation approach) was started. It aims at improving the understanding of the global continental hydrosphere by combining observational data and hydrological modelling.

The global freshwater system as an integral part of the global water cycle has a huge impact on human societies. Nevertheless, it is far from being comprehensively understood, as shown by the fact that contemporary global hydrological models differ significantly in their results. At the same time, realistic estimates of water fluxes and storage changes are crucial for determining water availability and the assessment of hydrological hazards like floods or droughts. Furthermore, efforts towards sustainable development rely on accurate projections on a quantitative basis. This is especially relevant in the light of massive anthropogenic interference with natural waters, accompanied by changing climate conditions and limited water resources.

Within GlobalCDA multiple new geodetic and remote sensing data are exploited in an ensemble-based calibration (C) and data assimilation (DA) approach allowing a flexible parameter (calibration) and state (data assimilation) adjustment of the hydrological model in use. Since June 2018, nine international project groups are working on the implementation of the C/DA setup, improvements of the global hydrological model and enhanced data processing strategies. DGFI-TUM is part of the Research Unit with the project WALES (Refined estimates of absolute water levels for inland waters from multi-mission satellite altimetry). With WALES, DGFI-TUM is in charge of providing water level time series for globally distributed inland water bodies that are overflowed by at least one satellite altimetry mission. Moreover, particular emphasis is placed on the development of automatic processing schemes and reliable uncertainty estimations.

In the context of monitoring land waters remote sensing techniques have become more and more relevant in the recent past. This is attributed to the fact that the amount of in-situ stations worldwide is steadily declining, and many lakes, rivers and glaciers especially in remote areas are not monitored at all. Accordingly, the GlobalCDA research unit focuses on data sets inferred from various satellite missions for calibration and assimilation into the hydrological model. This includes the use of time-dependent components of the gravitational field, measured by GRACE, to estimate regional changes of the total water storage. Water level time series for inland water bodies, derived from satellite altimetry (SA), are combined with information on the water extent as determined by satellite images to calculate lake and river discharges. Furthermore, global glacier mass changes are computed by analyzing digital elevation models.

In the frame of WALES, an automated target detection algorithm has been developed. Individual water bodies are identified on the basis of water occurrence maps that are inferred from satellite images. Several image processing techniques are applied to the input mask in order to remove small scale structures (below 600 m size) and to close gaps that occur for example in case of bridges or islands (below 400 m extent). The former is performed by an operation called Erosion that reduces the size of structures along their margins. Subsequently, original shapes of remaining water bodies are reconstructed by the inverse process (called Dilation).

The resulting mask is subjected to a closing step that, for instance, merges two parts of a lake that are separated by a bridge. Via this approach, a list of well-defined SA targets with information on their spatial extent, size and the number of altimeter observations per target can be derived. This procedure was applied to the Mississippi River Basin (MRB) that serves as a test region for the GlobalCDA research unit.

About 600 lakes and reservoirs, each with a surface area of more than 10 km<sup>2</sup>, were found, half of them overflowed by at least one of the three SA missions Envisat, Jason-2, or Sentinel-3A. For each of these 300 SA targets a virtual station and a water level time series can be determined, e.g. in DAHITI. In Fig. 2.13 the results for the MRB are shown. Identified water bodies are plotted in light (SA data are available) and dark (not monitored by SA) blue. The map on the lower left side shows the representation of Lake Texoma in the final land-water mask together with available altimeter data points.

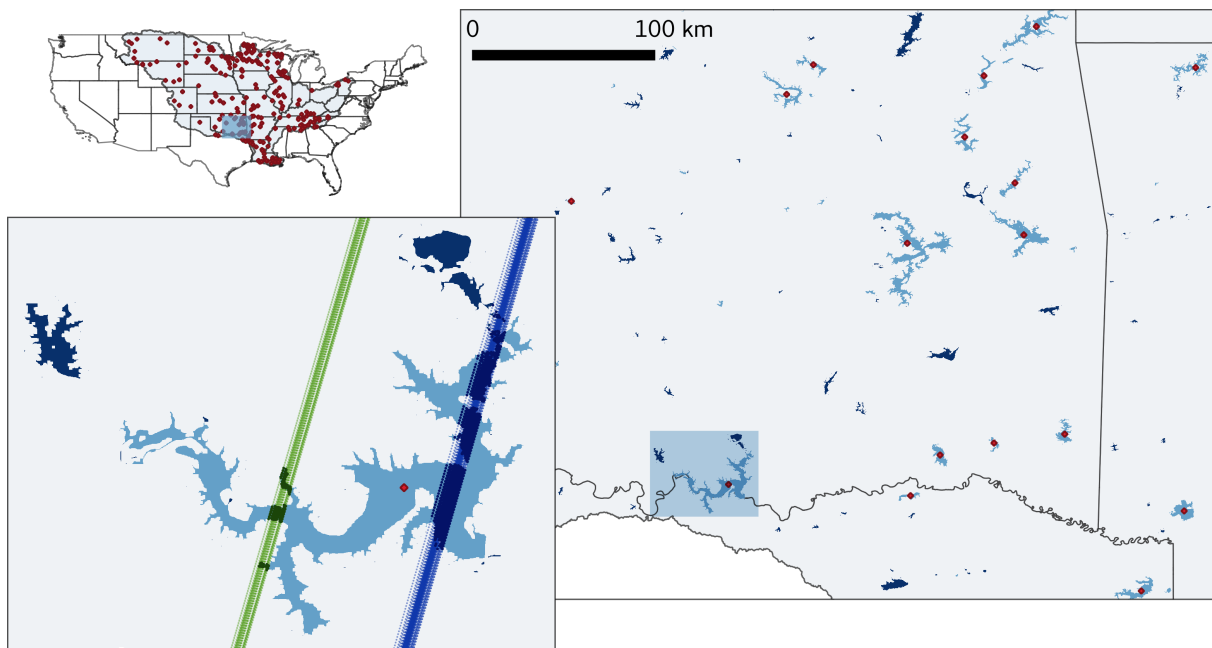


**Figure 2.13:** Results of the automated target detection applied to the Mississippi River Basin: All water bodies that are overflowed by at least one altimetry mission are marked in light blue. For targets with a surface area of more than 10 km<sup>2</sup> corresponding virtual stations shown as red dots. In contrast, detected water bodies that are not monitored by SA are plotted in dark blue. In the detail view of Lake Texoma on the lower left side altimeter data points are shown as blue (Envisat) and green (Sentinel) trace of dots.

## Related publications

Dettmering D., Schwatke C.: Multi-Mission Cross-Calibration of Satellite Altimeters: Systematic differences between Sentinel-3A and Jason-3. International Review Workshop On Satellite Altimetry Cal/Val Activities and Applications, Chania, Greece, April 2018. International Association of Geodesy Symposia, in press

Dettmering D., Wynne A., Müller F.L., Passaro M., Seitz F.: Lead Detection in Polar Oceans—A Comparison of Different Classification Methods for Cryosat-2 SAR Data. Remote Sensing, 10(8), 1190, doi:10.3390/rs10081190, 2018



- Gómez-Enri J., González C.J., Passaro M., Vignudelli S., Álvarez O., Cipollini P., Mañanes R., Bruno M., López-Carmona M.P., Izquierdo A.: Wind-induced cross-strait sea level variability in the Strait of Gibraltar from coastal altimetry and in-situ measurements. *Remote Sensing of Environment*, 221, doi:[10.1016/j.rse.2018.11.042](https://doi.org/10.1016/j.rse.2018.11.042), 2018
- Legeais J.-F., Ablain M., Zawadzki L., Zuo H., Johannessen J.A., Scharffenberg M.G., Fenoglio-Marc L., Fernandes M.J., Andersen O.B., Rudenko S., Cipollini P., Quartly G.D., Passaro M., Cazenave A., Benveniste, J.: An improved and homogeneous altimeter sea level record from the ESA Climate Change Initiative. *Earth System Science Data*, 10(1), 281–301, doi:[10.5194/essd-10-281-2018](https://doi.org/10.5194/essd-10-281-2018), 2018
- Müller F. L., Wekerle C., Dettmering D., Passaro M., Bosch W., Seitz F.: Dynamic ocean topography of the northern Nordic seas: a comparison between satellite altimetry and ocean modeling. *The Cryosphere*, 13(2), doi:[10.5194/tc-13-611-2019](https://doi.org/10.5194/tc-13-611-2019), 2019
- Passaro M., Rose S.K., Andersen O.B., Boergens E., Calafat F.M., Dettmering D., Benveniste J.: ALES+: Adapting a homogenous ocean retracker for satellite altimetry to sea ice leads, coastal and inland waters. *Remote Sensing of Environment*, 211, 456–471, doi:[10.1016/j.rse.2018.02.074](https://doi.org/10.1016/j.rse.2018.02.074), 2018
- Passaro M., Zufikar Adlan N., Quartly G.D.: Improving the precision of sea level data from satellite altimetry with high-frequency and regional sea state bias corrections. *Remote Sensing of Environment*, 245–254, doi:[10.1016/j.rse.2018.09.007](https://doi.org/10.1016/j.rse.2018.09.007), 2018
- Piccioni G., Dettmering D., Passaro M., Schwatke C., Bosch W., Seitz F.: Coastal Improvements for Tide Models: The Impact of ALES Retracker. *Remote Sensing*, 10(5), doi:[10.3390/rs10050700](https://doi.org/10.3390/rs10050700), 2018
- Piccioni G., Dettmering D., Bosch W., Seitz F.: TICON: Tidal CONstants based on GESLA sea-level records from globally-located tide gauges. *Geoscience Data Journal*, in review
- Restano M., Passaro M., Benveniste J.: New Achievements in Coastal Altimetry. *EOS*, 99, doi:[10.1029/2018eo106087](https://doi.org/10.1029/2018eo106087), 2018
- Schwatke C., Scherer D., Dettmering D.: Automated Extraction of Consistent Time-Variable Water Surfaces of Lakes and Reservoirs based on Landsat and Sentinel-2. *Remote Sensing*, 11(9), 1010, doi:[10.3390/rs11091010](https://doi.org/10.3390/rs11091010), 2019

## 3 Cross-Cutting Research Topics

Three overarching research topics *Atmosphere, Regional Gravity Field, and Standards and Conventions* are closely interlinked with the research areas *Reference Systems and Satellite Altimetry*.

The atmosphere (Section 3.1) is of crucial importance for the analysis of all space-geodetic observations. Satellite orbits are disturbed by atmospheric drag, and the measurement signals are affected by refraction and signal delay. Such effects must be properly handled in precise orbit determination and geodetic data analysis, and the optimisation of respective correction models means a significant research challenge. But vice versa, the disturbances of the different signals carry valuable information on the state and dynamics of the atmosphere. This information can be used to investigate atmospheric processes and space weather impacts, and it is of great interest for other disciplines. Space weather, in particular, is given more and more attention by politics and sciences as it can cause severe damage to modern infrastructure, such as navigation systems or power supply and communications facilities. Over the past years, DGFI-TUM has built up a strong expertise in modelling and predicting global and regional structures of the electron and the neutral density within the Earth's ionosphere and thermosphere, respectively, from the joint evaluation of space geodetic observations. The institute participated in the preparation of a position paper on space weather research in Germany, and in the frame of the project OPTIMAP it closely cooperates with the German Space Situational Awareness Center (Weltraumlagezentrum) since many years. Furthermore, DGFI-TUM chairs the Global Geodetic Observing System (GGOS) Focus Area on Geodetic Space Weather Research.

For various applications in geodesy, the precise knowledge of the Earth's gravity field (Section 3.2) is of high relevance. Among these applications are the realization and unification of height systems and the determination of high-precision satellite orbits. The latter are a prerequisite for the computation of accurate reference frames or for reliable estimates of water heights from satellite altimetry. Furthermore, the geoid provides the reference surface for the ocean circulation. Temporal changes of the gravity field contain information about mass transports in the Earth system and are of great interest, for example, for the investigation of dynamic processes in the Earth's interior or within the hydrosphere. DGFI-TUM primarily focuses on theoretical and practical aspects of regional gravity field determination. The goal is the creation of high-resolution and high-precision potential fields for delimited areas through a combination of various data types, such as space- and airborne gravity measurements, satellite altimetry, and terrestrial and ship gravimetry.

In order to assure highest consistency of parameters and products, the definition and application of common standards and conventions (Section 3.3) is indispensable. On the international level, DGFI-TUM is deeply involved in the activities of the competent bodies for defining standards in geodesy and monitoring their implementation. DGFI-TUM chairs the GGOS Bureau of Products and Standards (BPS) and operates it jointly with several partners. In the frame of the United Nations Global Spatial Information Management (UN-GGIM), DGFI-TUM provides the IAG representative for the Key Area "Data Sharing and Development of Standards" to the UN-GGIM Subcommittee "Geodesy".

### 3.1 Atmosphere

The Earth's atmosphere can be structured into various layers depending on different physical parameters such as temperature or charge state. In the latter case we distinguish mainly

between the neutral atmosphere up to roughly 50 km altitude and the ionosphere approximately between 50 km and 1000 km altitude.

The Earth's ionosphere plays a key role in monitoring space weather, because it responds to solar storms with an increase of the electron density. Space-geodetic observation techniques, such as terrestrial GNSS, satellite altimetry, space-borne GPS (e.g. as radio occultation) and DORIS provide valuable global information about the state of the ionosphere. In precise orbit determination (POD) of low-Earth-orbiting (LEO) satellites a major problem is modelling the non-gravitational perturbations. Among them, the atmospheric drag acceleration – mainly depending on the thermospheric density – is the largest for LEOs with altitudes lower than 1000 km. Consequently, the knowledge of the thermospheric density is of crucial importance for the POD of LEOs. Figure 3.1 gives an overview on the current work of DGFI-TUM in the frame of ionosphere-thermosphere modelling. The left-hand part shows the ionosphere modelling chain, starting from the measurements of space-geodetic observation techniques and leading to the setup of models for the electron density or the vertical total electron content (VTEC); the right-hand part depicts the thermosphere modelling approaches related to a POD of LEO satellites based, in particular, on SLR and DORIS measurements and providing models of the neutral density. The bridging components between the two tracks – the ionosphere and the thermosphere modelling chain – are (1) a physical thermosphere-ionosphere coupling model and (2) Sun observations reflecting space weather events such as solar flares and coronal mass ejections (CME). The final products of DGFI-TUM's modelling strategy for the neutral and the electron density as well as VTEC may be disseminated to users as GGOS products via the GGOS Bureau of Standards and Products (BPS); see Section 3.3. The flowchart in Fig. 3.1 fits rather well to the structure of the IAG GGOS Focus Area on Geodetic Space Weather Research which was introduced in detail in DGFI-TUM's Annual Report 2017.

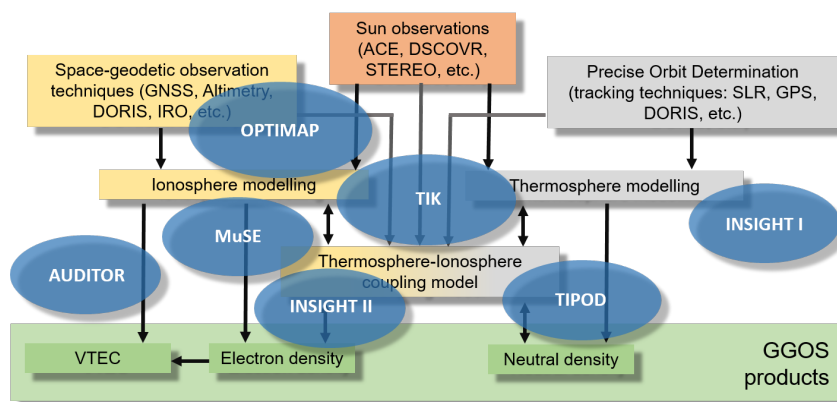


**Figure 3.1:** Current work structure of the research topic 'Atmosphere': the blue coloured oval areas indicate the third-party funded projects running at DGFI-TUM in 2018 (project acronyms written in white letters). The location of the oval areas point to their scientific content and their role in the structure of the research topic.

The blue coloured oval areas in Fig. 3.1 indicate the altogether seven third-party funded projects running at DGFI-TUM during 2018. The EU Horizon 2020 funded project AUDITOR (Advanced Multi-Constellation EGNSS Augmentation and Monitoring Network and its Application in Precision Agriculture) and the project DFG funded project INSIGHT-I (Interactions of Low-orbiting Satellites with the Surrounding Ionosphere and Thermosphere) of the first phase of the SPP 1788 Dynamic Earth have been finalized mid of 2018, the running phase of the project OPTIMAP (Operational Tool for Ionospheric Mapping And Prediction), funded by Bundeswehr GeoInformation Centre (BGIC) and performed in collaboration with the German Space Situational Awareness Center (Weltraumlagezentrum), was extended by additional three years in autumn 2018; the project TIK (Operational prototype for the determination of the thermospheric density on the basis of a coupled thermosphere-ionosphere model) funded by German

Ministry for Economic Affairs and Energy (BMWi) via German Aerospace Center (DLR) and running since March 2017, was already introduced in the last year's Annual Report. Besides the aforementioned projects AUDITOR, INSIGHT-I, OPTIMAP and TIK the three DFG projects MUSE (Multi-Satellite ionosphere-plasmasphere Electron density reconstruction), INSIGHT-II and TIPOD (Development of High-precision Thermosphere Models for Improving Precise Orbit Determination of Low-Earth-Orbiting Satellites) complete the 2018 project collection. Whereas MUSE, as a project of the first phase of the DFG-SPP 1788 was originally started at DLR in Neustrelitz and since October 2018 continued at DGFI-TUM, the two other projects belong to the second phase of the DFG-SPP 1788. The DGFI-TUM part of INSIGHT-II deals with an extension of the electron density modelling, in particular, in the absence of radio occultation measurements. TIPOD focuses on the estimation of selected key parameters of the physical coupled thermosphere-ionosphere model TIE-GCM from a suite of different observation techniques providing thermospheric density data.

According to the work plan shown in Fig. 3.1 we will present in the following results of our latest investigations on VTEC and neutral density modelling, namely (1) the computation of high-resolution global VTEC maps, (2) the construction of a Multi Kalman filtering approach for (near) real-time modelling based on data with different latencies and (3) the improvement of thermospheric density models by using SLR observations.

### High Resolution VTEC Maps Based on Multi-Scale B-spline Representations

For more than two decades the IGS (International GNSS Service) Ionosphere Associated Analysis Centers (IAAC) provide Global Ionosphere Maps (GIM) of VTEC, mostly based on spherical harmonic (SH) expansions up to spectral degree  $n_{\max} = 15$ , provided with a spatial resolution of  $2.5^\circ \times 5^\circ$  with respect to latitude  $\varphi$  and longitude  $\lambda$ , and a temporal sampling of two hours. Unlike this procedure, DGFI-TUM's VTEC modelling approach

$$\begin{aligned} VTEC(\varphi, \lambda, t) &= f_{J_1, J_2}(\varphi, \lambda, t) = \sum_{k_1=0}^{K_{J_1}-1} \sum_{k_2=0}^{K_{J_2}-1} d_{k_1, k_2}^{J_1, J_2}(t) \phi_{k_1}^{J_1}(\varphi) \tilde{\phi}_{k_2}^{J_2}(\lambda) \\ &= \boldsymbol{\phi}_{J_1}^T(\varphi) \mathbf{D}_{J_1, J_2}(t) \tilde{\boldsymbol{\phi}}_{J_2}(\lambda). \end{aligned} \quad (3.1)$$

uses localizing basis functions, namely tensor products of polynomial and trigonometric B-splines. To be more specific, in Eq. (3.1) the vectors  $\boldsymbol{\phi}_{J_1}(\varphi) = (\phi_{k_1}^{J_1}(\varphi))$  and  $\tilde{\boldsymbol{\phi}}_{J_2}(\lambda) = (\tilde{\phi}_{k_2}^{J_2}(\lambda))$  contain the  $K_{J_1} = 2^{J_1} + 2$  polynomial B-splines  $\phi_{k_1}^{J_1}(\varphi)$  of resolution level  $J_1$  and shift  $k_1$  as basis functions with respect to latitude  $\varphi$  and the  $K_{J_2} = 3 \cdot 2^{J_2}$  trigonometric B-splines  $\tilde{\phi}_{k_2}^{J_2}(\lambda)$  of resolution level  $J_2$  and shift  $k_2$  as basis functions with respect to longitude  $\lambda$ ; furthermore, the  $K_{J_1} \times K_{J_2}$  matrix  $\mathbf{D}_{J_1, J_2}(t) = (d_{k_1, k_2}^{J_1, J_2}(t))$  collects the unknown time-dependent scaling coefficients  $d_{k_1, k_2}^{J_1, J_2}(t)$ .

In opposite to SH models the approach (3.1) allows (1) for handling data gaps appropriately, (2) for establishing sparse normal equation systems within the parameter estimation procedure, and (3) for setting up a multi-scale-representation (MSR) to determine GIMs of different spectral content directly by applying the so-called pyramid algorithm and to perform highly effective data compression techniques. The estimation of the MSR model parameters, i.e. the scaling coefficients, is finally performed by a Kalman-Filter driven by near real-time (NRT) GNSS data.

Within the project OPTIMAP we deduced the two inequality chains

$$\begin{aligned} J_1 &\leq \log_2 \left( \frac{180^\circ}{\Delta\varphi} - 1 \right) \leq \log_2 (n_{\max} - 1), \\ J_2 &\leq \log_2 \left( \frac{120^\circ}{\Delta\lambda} \right) \leq \log_2 \left( \frac{2 \cdot n_{\max}}{3} \right). \end{aligned} \quad (3.2)$$

They relate the levels  $J_1$  and  $J_2$  in the left term, the maximum SH degree  $n_{\max}$  in the right term, and, in the mid term, the mean global sampling intervals  $\Delta\varphi$  and  $\Delta\lambda$  of the input data, i.e. the GNSS measurements with respect to latitude  $\varphi$  and longitude  $\lambda$ . Given the numerical values 1 to 6 for the B-spline levels  $J_1$  and  $J_2$ , Table 3.1 presents the corresponding largest numerical values for  $n_{\max}$  as well as  $\Delta\varphi$  and  $\Delta\lambda$  by evaluating the inequalities (3.2).

**Table 3.1:** Values for the B-spline levels  $J_1$  and  $J_2$ , the maximum SH degree  $n_{\max}$  and the input data sampling intervals  $\Delta\varphi$  and  $\Delta\lambda$ ; the left part presents the numbers along a meridian (upper inequalities in Eq. (3.2)), the right part the corresponding numbers along the equator and its parallels (lower inequalities in Eq. (3.2)).

	Latitude						Longitude						
$J_1$	1	2	3	4	5	6	$J_2$	1	2	3	4	5	6
$n_{\max}$	3	5	9	17	33	63	$n_{\max}$	3	6	12	24	48	96
$\Delta\varphi$ [°]	60	36	20	10.5	5.45	2.85	$\Delta\lambda$ [°]	60	30	15	7.5	3.75	1.875

From the spectral point of view the inequalities (3.2) comprise the following three scenarios:

1. Given the global sampling intervals  $\Delta\varphi$  and  $\Delta\lambda$ , the mid terms of (3.2) are determined. The maximum degree  $n_{\max}$  is calculable from the right-hand side inequalities and may be inserted into the SH expansion of VTEC. The left-hand side inequalities yield the level values  $J_1$  and  $J_2$  which are required in the B-spline expansion (3.1).
2. A given numerical value for  $n_{\max}$  fixes the right terms of (3.2). The data input sampling intervals  $\Delta\varphi$  and  $\Delta\lambda$  can be deduced from the right-hand side inequalities. Next, the level values  $J_1$  and  $J_2$  are calculable from the left-hand side inequalities and used in the B-spline expansion (3.1).
3. If the processing time of VTEC maps must be observed, the level values  $J_1$  and  $J_2$  are limited, since the number of numerical operations exponentially increases with the level values. In this case, the left-hand side inequalities make it possible to estimate the data sampling intervals  $\Delta\varphi$  and  $\Delta\lambda$ . Finally, the right-hand side inequalities yield the maximum SH degree  $n_{\max}$ .

As already mentioned, most of the GIMs produced by the IAACs are based on series expansions in SHs up to a maximum degree of  $n_{\max} = 15$ . Following the above listed second strategy and Table 3.1 we obtain for this example the approximations  $J_1 = 4$  (for  $n_{\max} = 17$ ) and  $J_2 = 3$  (for  $n_{\max} = 12$ ) for the two B-spline levels  $J_1$  and  $J_2$ . Inserting these numbers into the B-spline expansion (3.1) yields the spectrally closest representation to the current IGS solutions.

For the evaluation of GNSS data we have to define an appropriate coordinate system. Here we follow the standard procedure and use the Sun-fixed Geocentric Solar Magnetic (GSM) coordinate system. Figure 3.2 shows the global distribution of the Ionospheric Pierce Points (IPP), i.e. the intersection points of the raypaths between the signal transmitting GNSS satellites and the terrestrial receivers at IGS stations with the sphere of the so-called Single-Layer-Model (SLM), related to GNSS VTEC observations for September 6, 2017 at 13:00 UT. Since our B-spline model (3.1) is set up in the GSM coordinate system and the scaling coefficients  $d_{k_1, k_2}^{J_1, J_2}(t)$  are restricted to the state equation of the Kalman Filter (Erdogan et al., 2017), we select  $\Delta\varphi = 5^\circ$  and  $\Delta\lambda = 10^\circ$  as appropriate values for the global mean sampling intervals of the input data as introduced in the inequality equations (3.2). Consequently, the B-spline level values  $J_1 = 5$  and  $J_2 = 3$  are taken from Table 3.1.

The MSR means a successive low-pass filtering of the target function  $f(\varphi, \lambda, t)$  into two directions, namely latitude  $\varphi$  and longitude  $\lambda$ , in the same manner. If a signal  $f(\varphi, \lambda, t)$  is represented

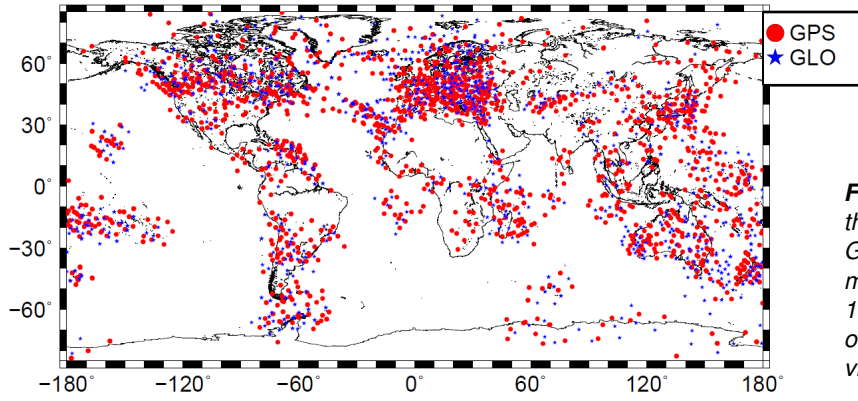


**Figure 3.2:** Global distribution of the IPPs from GPS (red dots) and GLONASS (blue stars) measurements for September 6, 2017, at 13:00 UT. Besides dense clusters over continents large data gaps are visible over the oceans.

up to the level values  $J_1$  with respect to latitude and  $J_2$  with respect to longitude, i.e.  $f(\varphi, \lambda, t) \approx f_{J_1, J_2}(\varphi, \lambda, t)$  the application of the two-dimensional (2-D) MSR allows for the computation of low-pass filtered signal approximations down to the level pairs  $(J_1-1, J_2-1), (J_1-2, J_2-2), \dots$ ; for details see (Goss et al. 2019). The principal structures of the ionospheric key parameters such as VTEC, however, are usually parallel to the geomagnetic equator. Consequently, we also deal with a 1-D MSR of the signal  $f(\varphi, \lambda, t) \approx f_{J_1, J_2}(\varphi, \lambda, t)$  with respect to the latitude only. In this case the MSR reads

$$f_{J_1, J_2}(\varphi, \lambda, t) = f_{J_1-J, J_2}(\varphi, \lambda, t) + \sum_{j=1}^J g_{J_1-j, J_2}(\varphi, \lambda, t) \quad (3.3)$$

consisting of the low-pass filtered version  $f_{J_1-J, J_2}(\varphi, \lambda, t)$  and the band-pass filtered detail signals  $g_{J_1-j, J_2}(\varphi, \lambda, t)$  for  $j = 1, \dots, J$ . Thus, signal approximations down to the level pairs  $(J_1-1, J_2), (J_1-2, J_2), \dots, (J_1-J, J_2)$  are obtained. The 1-D pyramid algorithm is visualized in Fig. 3.3 with  $J'_1 = J_1 - J$  (see Goss et al. 2019).

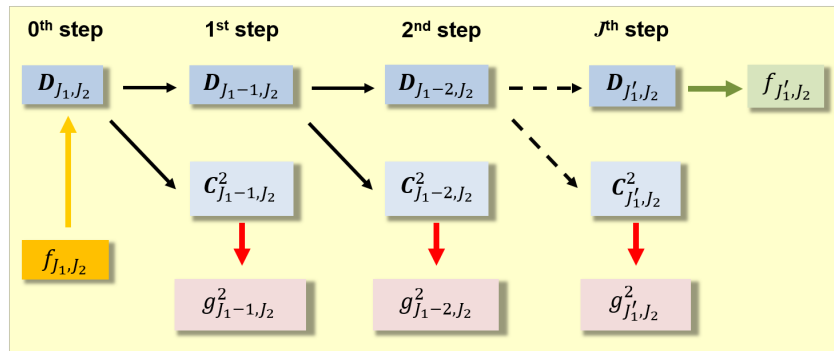


**Figure 3.3:** 1-D MSR of the signal  $f_{J_1, J_2}(\varphi, \lambda, t)$  with respect to the latitude  $\varphi$ . The 0<sup>th</sup> step on the left-hand side conforms with Eq. (3.1).

In the given case we start with the levels  $J_1=5$  and  $J_2=3$  and apply the MSR according to Fig. 3.3 to compute the low-pass filtered version of VTEC with levels  $J_1-1=4$  and  $J_2=3$ . Consequently, Eq. (3.3) reads  $f_{5,3}(\varphi, \lambda, t) = f_{4,3}(\varphi, \lambda, t) + g_{4,3}(\varphi, \lambda, t)$ . The developed approach allows for the construction of various products which differ both in their spectral and their temporal resolution. Following the official 4-digit identification coding of the GIMs from the IAACs we denote the high-resolution NRT product  $f_{5,3}(\varphi, \lambda, t)$  as 'ophg' and the NRT product  $f_{4,3}(\varphi, \lambda, t)$  of lower resolution as 'oplg'. To be more specific, the first digit 'o' refers to the processing software OPTIMAP. The second digit 'p' is chosen according to the temporal resolution  $\Delta T$  of the created VTEC maps, i.e. according to Table 3.2 we use 't' for  $\Delta T = 10$  minutes, '1' for  $\Delta T = 1$  hour and '2' for  $\Delta T = 2$  hours. The third digit describes the spectral resolution and is selected as 'l' for 'low'

**Table 3.2:** List of the NRT products ‘ophg’ and ‘oplg’ from DGFI-TUM as well as the two best-known products of the IAACs CODE and UPC, namely the final product ‘codg’ and the rapid product ‘uqrg’.

Institution	DGFI-TUM		CODE	UPC
Product Type	NRT ophg $J_1=5, J_2=3$	NRT oplg $J_1=4, J_2=3$	final	rapid
$\Delta T = 2$ h	o2hg	o2lg	—	—
$\Delta T = 1$ h	o1hg	o1lg	codg	—
$\Delta T = 15$ min	—	—	—	uqrg
$\Delta T = 10$ min	othg	otlg	—	—

and ‘h’ for ‘high’. Finally, the last digit indicates the model domain and is set to ‘g’ for ‘global’. An overview of the DGFI-TUM products and the two best-known maps from CODE and UPC is given in Table 3.2.

Figure 3.4 shows an example of the high resolution VTEC map ‘ophg’ ( $f_{5,3}(\varphi, \lambda, t)$ ) and the low resolution VTEC map ‘oplg’ ( $f_{4,3}(\varphi, \lambda, t)$ ) as well as the detail signal  $g_{4,3}(\varphi, \lambda, t)$ . It is clearly visible that the latter means a band-pass filtered version of ‘ophg’.

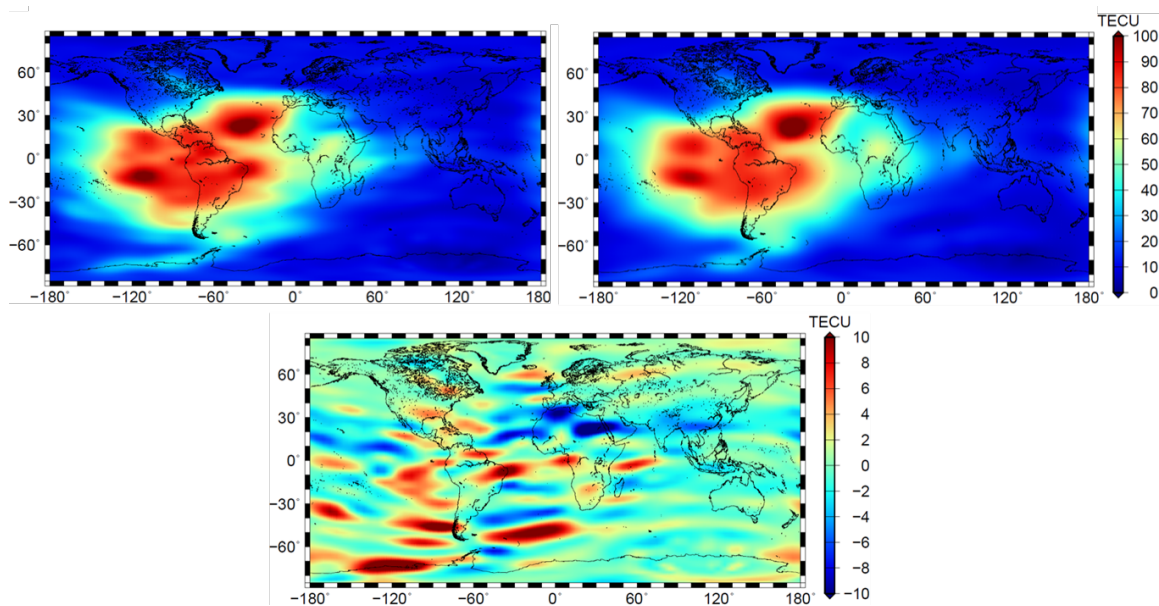


**Figure 3.4:** High resolution VTEC map ‘ophg’ (top left panel) and low resolution VTEC map ‘oplg’ (top right panel) during the St. Patrick storm event on March 17, 2015 at 19:00 UT; the bottom panel shows the detail signal representing the differences between the two top VTEC maps.

To assess the quality we compare the VTEC products listed in Table 3.2 among each other. In DGFI-TUM’s Annual Report 2016, two validation methods were considered, namely (1) the dSTEC analysis and (2) the comparison with altimetry VTEC data. Since the dSTEC analysis is the most frequently used validation method, we refrain from a comparison with satellite altimetry observations.

In the following assessment, we focus on the solar storm time during September 2017. Altogether we consider six products of DGFI-TUM with different spectral content (‘ophg’:  $J_1 = 5, J_2 = 3$ ) and (‘oplg’:  $J_1 = 4, J_2 = 3$ ) and different temporal sampling resolution ( $\Delta T = 2$  hours,  $\Delta T = 1$  hour,  $\Delta T = 10$  minutes) as well as the IAAC products ‘codg’ and ‘uqrg’. The performance of the

dSTEC analysis is based on the values

$$dSTEC(t_k) = dSTEC_{obs}(t_k) - dSTEC_{map}(t_k) \quad (3.4)$$

where  $dSTEC_{obs}(t_k)$  is the difference of the GPS geometry-free linear combination  $L_4(t_k)$  observed at time moment  $t_k$  with another geometry-free linear combination  $L_4(t_{ref})$  computed along the same continuous arc but at a reference time moment  $t_{ref}$  characterized by the highest elevation angle. The computed dSTEC values from the VTEC maps denoted as  $dSTEC_{map}(t_k)$  at the same time moments  $(t_k, t_{ref})$  and the same IPP locations are obtained by multiplying the estimated VTEC values with an elevation-dependent mapping function. All products are given with a spatial resolution of  $2.5^\circ \times 5^\circ$  and the aforementioned temporal resolution of  $\Delta T$ . Since GNSS measurements are taken along the satellite arcs, the corresponding IPPs are located spatially within a grid cell and temporally between the discrete time moments of the products. In order to calculate the VTEC values for  $dSTEC_{map}(t_k)$ , spatial and temporal interpolation techniques are applied (Goss et al., 2019). The RMS values of the daily  $dSTEC(t_k)$  variations obtained during September 2017 are presented in Fig. 3.6 for selected observation sites shown in Fig. 3.5.

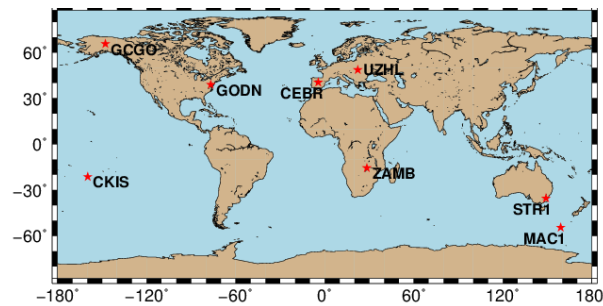


**Figure 3.5:** The geographical locations and identifiers of the receiver sites used in the dSTEC analysis

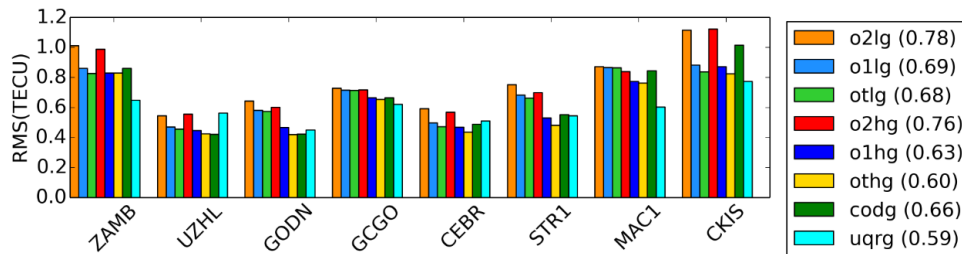


**Figure 3.6:** Results of the statistical evaluations presenting the average RMS values (in parentheses in the legend) of the differences between the observed and the computed dSTEC values according to Eq. (3.4) with respect to the receiver sites shown in Fig. 3.5.

Before evaluating the results of the comparison of the six DGFI-TUM products it can be expected that the average RMS values of ‘o2hg’ and ‘o2lg’ are larger than the corresponding values for shorter sampling intervals and that the average RMS values for a product of higher B-spline levels, e.g. ‘othg’, are smaller than the corresponding values for products of lower B-spline levels such as ‘otlg’. By comparing the corresponding colour bars in Fig. 3.6, i.e. orange (‘o2lg’) vs. red (‘o2hg’), blue (‘o1lg’) vs. dark blue (‘o1hg’) and green (‘otlg’) vs. yellow (‘othg’), the aforementioned expectations are all confirmed.

As mentioned in the context of Table 3.1 the B-spline levels  $J_1 = 4$  and  $J_2 = 3$  fit the best to the highest degree  $n_{max} = 15$  of a SH expansion. To be more specific, we compare the product ‘o1lg’ with CODE’s product ‘codg’ characterized by a SH expansion up to degree  $n_{max} = 15$  and a time resolution of  $\Delta T = 1$  hour. By comparing the average RMS values of ‘o1lg’ (0.80



TECU) and ‘codg’ (0.77 TECU) we can state that the overall quality of the NRT product ‘o1lg’ is comparable with that of the final product ‘codg’.

Finally, we interpret the comparison of DGFI-TUM’s high resolution models ‘ophg’ with UPC’s product ‘uqrg’ which is at the time known as the most precise product of the IAACs. It is characterized by a temporal resolution of  $\Delta T = 15$  minutes and thus, temporally comparable with ‘othg’. Summarizing these investigations, we can state that the overall quality of the two products ‘othg’ and ‘uqrg’ is very close to each other. It is worth to be mentioned again that ‘othg’ is a NRT product with a latency of less than 3 hours whereas ‘uqrg’ is a rapid product with a latency of around 1 day. Thus, in NRT applications the DGFI-TUM product ‘othg’ outperforms all other products used in the comparisons presented above.

### Multi-Kalman-Filtering

As shown in Fig. 3.2 GNSS observations cover continental regions and are due to their high spatio-temporal resolution the main source for the construction of VTEC maps. However, large data gaps exist due to the inhomogeneous distribution, especially over the oceans. Therefore, other techniques such as DORIS, satellite altimetry and radio occultations can mitigate the data gap problem and improve the accuracy and reliability of ionospheric maps. However, data derived from these complementary measurement systems are currently provided with latencies of a few hours up to a few days; latencies of one or more days are for sure too large for allowing an inclusion in NRT ionosphere models. Figure 3.7 shows the concept of the Multi-Kalman-Filter (MKF) as developed within the project OPTIMAP. Here we follow the motto to use the data as soon as they are available. The MKF consists of four filters related to the aforementioned observation techniques. The GNSS filter as the main filter is labelled as ‘ $I = 0$ ’, the altimetry filter labelled as ‘ $I = 1$ ’ combines GNSS and satellite altimetry data, the IRO filter labelled as ‘ $I = 2$ ’ combines GNSS, satellite altimetry and IRO data and, finally, the DORIS filter labelled as ‘ $I = 3$ ’ combines GNSS, satellite altimetry, IRO and DORIS data. Combinations of GNSS, altimetry and DORIS data can be realized, too, as well as GNSS and DORIS and other combinations. The only requirement for the application of the MKF is the inclusion of the main filter ‘ $I = 0$ ’ as the basis.

Due to the large latencies of IRO and DORIS data, we reduce our first investigations to the main filter ‘ $I = 0$ ’ and the delayed filter ‘ $I = 1$ ’ as shown in the upper part of Fig. 3.8. At the present time moment  $t_k$  both an hourly block of GNSS data between  $t_k - 2h$  and  $t_k - 1h$  as well as an hourly block of altimetry data from the Jason-2/3 mission between  $t_k - 4h$  and  $t_k - 3h$  are downloaded from the corresponding data centres.

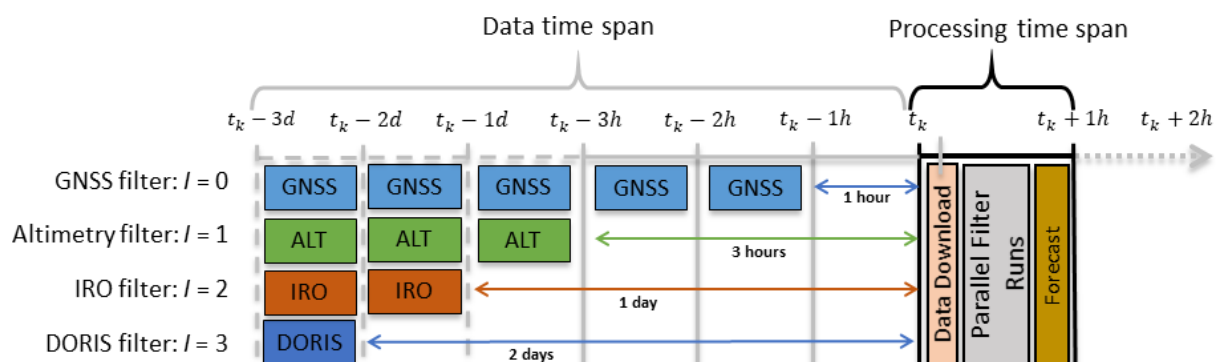


**Figure 3.7:** Multi-Kalman-Filter (MKF) concept based on data with (very) different latencies; whereas GNSS (1 hour) and satellite altimetry (3 hours) can be used for generating NRT maps, the two other techniques (IRO and DORIS) are characterized by latencies of one or even more days;  $t_k$  means the present time moment

The main filter ' $I = 0$ ' starts at  $t_k + \Delta t'$  after the data download and the pre-processing step for the GNSS data as shown in Fig. 3.7. The filter estimates the unknown ionospheric parameters sequentially by incorporating the GNSS data collected between at  $t_k - 2$  h and  $t_k - 1$  h.

The altimetry filter ' $I = 1$ ' starts at  $t_k + \Delta t''$  with a delay for data download and pre-processing and combines the latest available altimetry data between  $t_k - 4$  h and  $t_k - 3$  h with the already estimated B-spline coefficients from the main GNSS filter. Considering the idea that the ionosphere has a memory and changes slowly, improvements on the B-spline coefficients due to the altimetry data can be propagated further to the next time epochs. To achieve this goal, the altimetry filter runs between  $t_k - 3$  h and  $t_k - 1$  h without altimetry data but using the B-spline coefficients from the GNSS filter.

Figure 3.8 shows snapshot maps created from the estimated ionospheric parameters of the GNSS and the altimetry filter with a 10 minute time resolution. The top left maps in the two boxes show the results from the GNSS filter ' $I = 0$ '. The bottom left maps show the results of the Altimetry filter ' $I = 1$ '. The overall data distribution derived from GNSS and altimetry data is depicted in the top panel of the mid column in the boxes. The bottom panels in the mid column of the two boxes show the difference maps clearly revealing the improvements of the altimetry filter; the corresponding standard deviation maps in the right column of the two boxes display significant improvements along the altimetry tracks, too, and visualize the impact of the MKF.

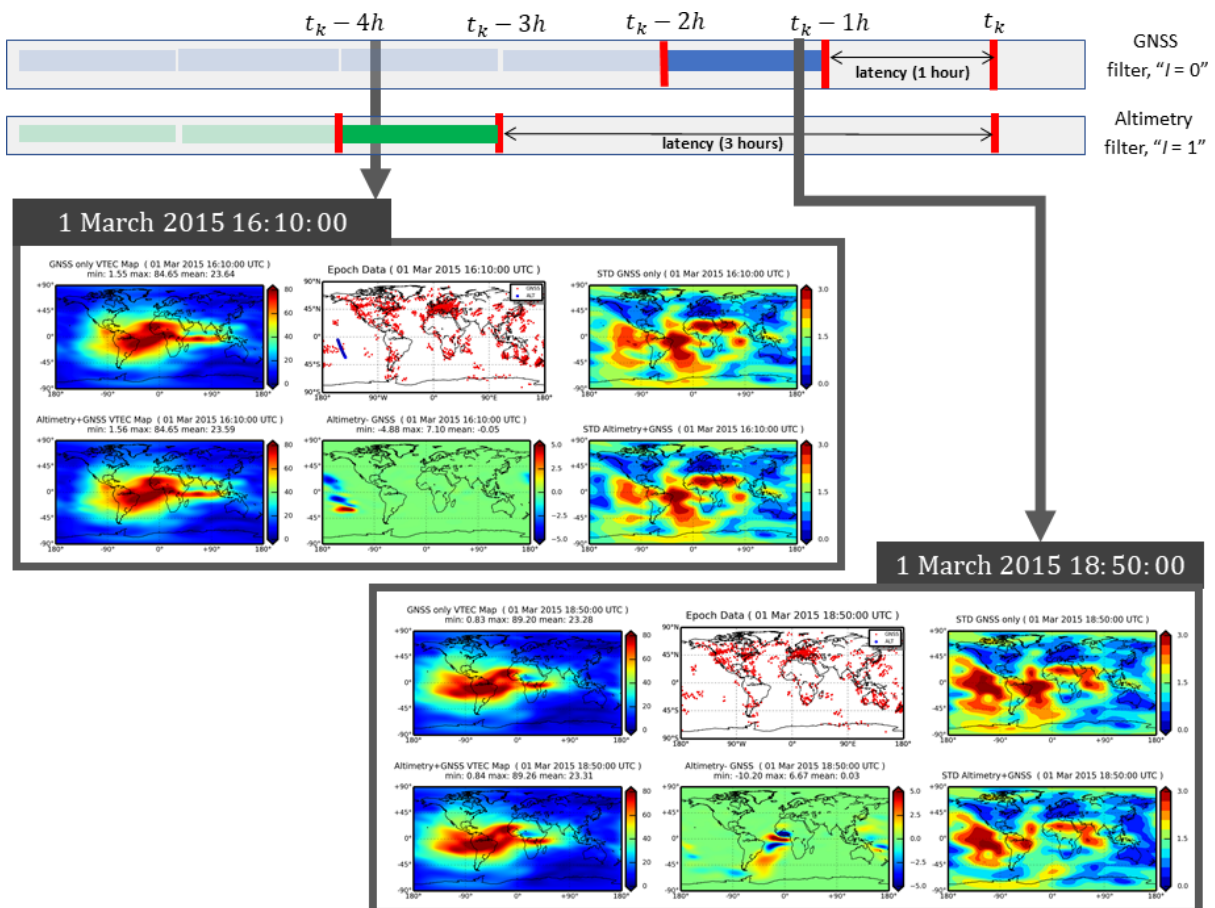


**Figure 3.8:** Example for the application of the MKF: the configuration consists of the GNSS filter ' $I = 0$ ' and the Altimetry filter ' $I = 1$ '. The two boxes are related to different time moments: the first (upper) one shows results for a time moment within the hour altimetry data is provided, the second (lower) one shows the corresponding results for a later time moment. The panels in the left column in each of the boxes show the VTEC results from the GNSS filter (top) and the Altimetry filter (bottom), the right column displays the corresponding standard deviation maps. The upper panel in the mid column of the boxes show the data distribution, the lower panel the difference between the two VTEC maps, i.e. the improvement of the altimetry data along the satellite track.

Besides GNSS and satellite altimetry, DORIS can contribute to a data densification around continental regions. The data acquired from satellites equipped with the DORIS system are currently provided with a latency of 2 days. In a case study we simulate the existence of low-latency DORIS data and investigate their impact on the quality of NRT VTEC products. To be more specific, we generate DORIS data with a 1 hour and a 3 hour latency and include them into the MKF approach as shown in Fig. 3.9. The DORIS filters with latencies of 1 hour and 3 hours are labelled as ' $I = 3a$ ' and ' $I = 3b$ ', respectively. The DORIS filters make use of data collected from the Jason-2, Jason-3, Saral and HY-2A mission.

The VTEC maps obtained by the altimetry filter combining GNSS and Jason-2/3 data were used for the validation of the VTEC maps derived from the two DORIS filters. In the first study case, the latency of the DORIS data is set to 1 hour, i.e. identical to the latency of the GNSS data. The results show that DORIS significantly improves the VTEC maps, at least in regions which are less or not supported by GNSS. The top panel of the left box depicts the GNSS (red), satellite altimetry (black) and DORIS (light blue) data distribution for a specific time moment. The bottom panel shows the differences of the ' $I = 0$ ' (red) and ' $I = 3a$ ' (light blue) filters with respect to the altimetry filter ' $I = 1$ ' along the altimetry track.

In the second case study, the latency is set to 3 hours. As shown in Fig. 3.9, the filter combines the DORIS observations with the estimated B-spline coefficients from the GNSS filter within the time interval  $t_k - 4h$  to  $t_k - 3h$ . After a running time of 1 hour the filter makes use only of the output of the GNSS filter, which follows the same filtering procedures performed for the Altimetry filter. The right box shows the differences of the ' $I = 0$ ' (red) and the ' $I = 3b$ ' (light blue) filter with respect to the results of the altimetry filter  $I = 1$  calculated at the same epoch.

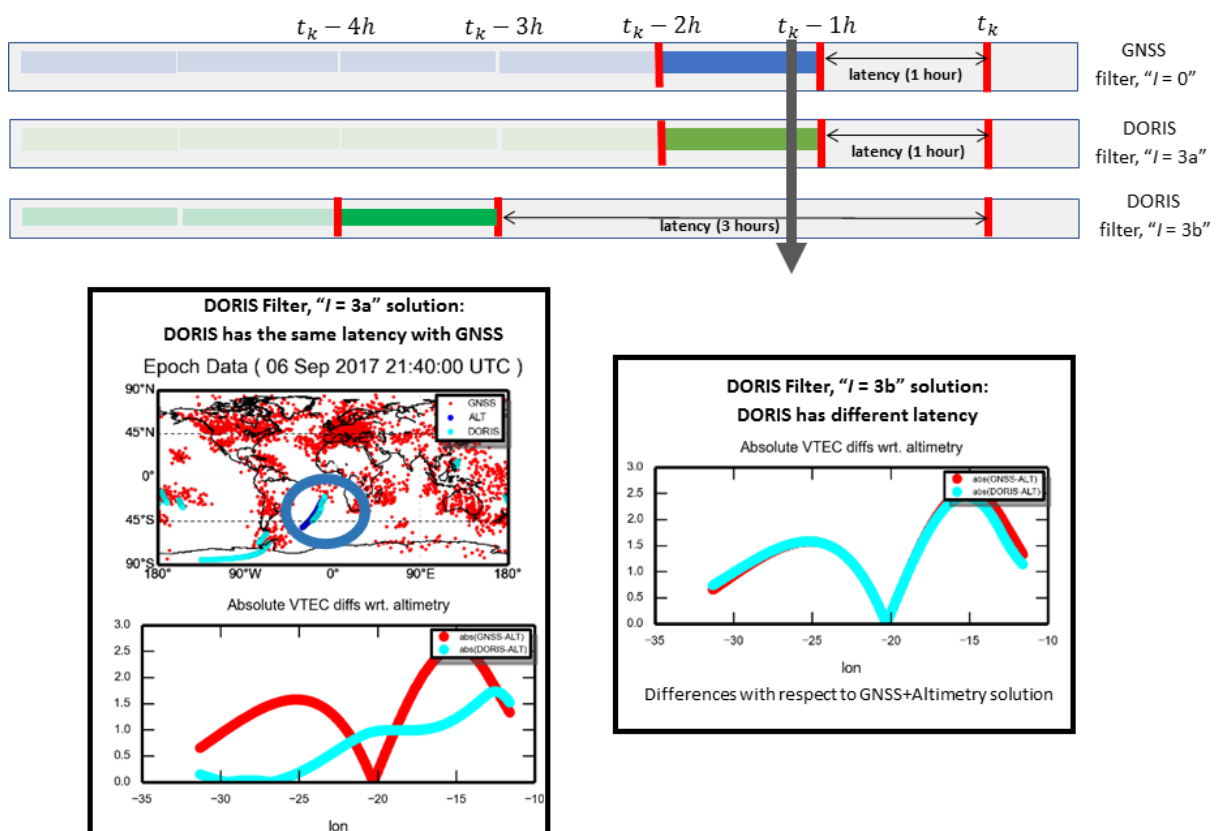


**Figure 3.9:** Example for the application of the MKF: the configuration consists of the GNSS filter labelled as ' $I = 0$ ' and the two DORIS filters labelled as ' $I = 3a$ ' as well as ' $I = 3b$ ' and based on simulated DORIS data with latencies of 1 hour and 3 hours, respectively. The illustrations in the boxes are related to the same time moment: the bottom panel in the left box shows the comparison results of the filter ' $I = 3a$ ' and the right box illustrates the corresponding comparison based on the filter ' $I = 3a$ '.

Improvements of the DORIS filter compared to the GNSS-only solutions are less pronounced but still visible.

### **Calibration of thermospheric density provided by empirical models using SLR observations to LEO satellites**

The precise knowledge of the density of the Earth's thermosphere is important for satellite mission planning, precise orbit determination (POD), re-entry predictions and collision avoidance of LEO satellites. Empirical thermosphere models have been derived since the beginning of the space era from observations, e.g., from mass spectrometers, incoherent scatter radar and later from accelerometer data of CHAMP and GRACE.

A new approach (Panzetta et al., 2018) has been developed at DGFI-TUM to estimate scale factors of the integrated thermospheric density using Satellite Laser Ranging (SLR) observations to spherical Earth orbiting satellites in combination with a full POD of these satellites. In this approach, the impact of all known gravitational and non-gravitational forces acting on a satellite is computed. A benefit of this method consists in a possibility to monitor the correlations between all estimated parameters in order to have a deep understanding of the system behavior. Due to the correlation between the atmospheric drag and the aerodynamic total drag coefficient, the latter is computed analytically using the Sentman model as a gas-surface interaction model which studies how gas particles exchange energy and momentum with the surface of an object by averaging over all thermospheric species. A priori values of thermospheric density are computed using an empirical model. This method allows us to calibrate the thermospheric density provided by various models.

Using this approach scale factors with respect to thermospheric density provided by the empirical models CIRA86, NRLMSISE00, JB2008, DTM2013 and the recently developed CH-Therm-2018 (Xiong et al., 2018) have been estimated using SLR observations to the ANDE-P satellite from 16 August 2009 to 3 October 2009, the ANDE-C satellite from 16 August 2009 to 26 March 2010 and SpinSat from 29 December 2014 to 21 June 2015, i.e. at periods of low and high solar activity and an altitude range from 248 to 425 km (Rudenko et al., 2018). This analysis indicates that CIRA86, NRLMSISE00, JB2008, and DTM2013 overestimate the thermospheric density during the period of low solar activity (the scale factors are below 1 for these models) and slightly underestimate the thermospheric density during the period of high solar activity (the scale factors are above 1). These scaled thermospheric density values, shown in the right panel of Fig. 3.10, agree much better than the thermospheric density values directly provided by the empirical models; see Fig. 3.10, left panel.

The initial version of the CH-Therm-2018 model obtained from the analysis of CHAMP observations from August 2000 to July 2009 was, on the contrary, underestimating the thermospheric density. Therefore, in the final version of this model, the thermospheric density was scaled by the median value (1.267) of the scale factors obtained from the analysis of SLR observations to the ANDE-P satellite from 16 August 2009 to 3 October 2009.

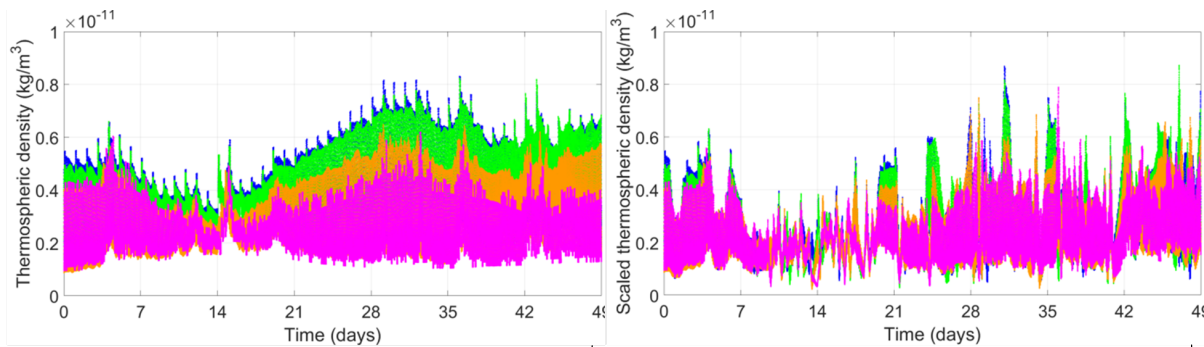


**Figure 3.10:** Left: thermospheric density values computed from the empirical models NRLMSISE00 (blue), CIRA86 (green), DTM2013 (orange) and JB2008 (magenta); right: scaled thermospheric density values calculated by multiplying the empirical model values with 6-hour scale factors estimated from the SLR observations to ANDE-P during the time span between 16 August 2009 and 3 October 2009 (Panzetta et al., 2018).

### Related publications

- Erdogan E., Schmidt M., Seitz F., Durmaz M.: Near real-time estimation of ionosphere vertical total electron content from GNSS satellites using B-splines in a Kalman filter. *Annales Geophysicae* 35(2), 263–277, doi:[10.5194/angeo-35-263-2017](https://doi.org/10.5194/angeo-35-263-2017), 2017
- Goss A., Schmidt M., Erdogan E., Görres B., Seitz F.: High Resolution Vertical Total Electron Content Maps Based on Multi-Scale B-spline Representations. *Annales Geophysicae Discussions*, doi:[10.5194/angeo-2019-32](https://doi.org/10.5194/angeo-2019-32), in review, 2019
- Panzetta F., Bloßfeld M., Erdogan E., Rudenko S., Schmidt M., Müller H.: Absolute thermospheric density estimation from SLR observations of LEO satellites – A case study with ANDE-Pollux satellite. *Journal of Geodesy*, 93(3), 353–368, doi:[10.1007/s00190-018-1165-8](https://doi.org/10.1007/s00190-018-1165-8), 2018
- Rudenko S., Schmidt M., Bloßfeld M., Xiong C., Lühr H.: Calibration of empirical models of thermospheric density using satellite laser ranging observations to near-Earth orbiting spherical satellites. In: Freymueller J., Sánchez L. (Eds.), *International Association of Geodesy Symposia*, doi:[10.1007/1345\\_2018\\_40](https://doi.org/10.1007/1345_2018_40), 2018
- Schmidt M., Erdogan E., Goss A., Hernández-Pajares M., García Rigo A., Lyu H.: Development and validation of sequential UBS and NABS models, , 2017
- Xiong C., Lühr, Schmidt M., Bloßfeld M., Rudenko S.: An empirical model (CH-Therm-2018) of the thermospheric mass density derived from CHAMP satellite. *Annales Geophysicae*, 36(4), 1141–1152, doi:[10.5194/angeo-36-1141-2018](https://doi.org/10.5194/angeo-36-1141-2018), 2018

## 3.2 Regional Gravity Field

The DFG project "Optimally combined regional geoid models for the realization of height systems in developing countries" (ORG4Heights) has been running jointly at DGFI-TUM and the Chair of Astronomical and Physical Geodesy of TUM since March 2016. In developing countries where observations, if at all, are only available with heterogeneous density and quality, the optimal combination of different gravity data sets is of great importance for regional gravity refinement. Various types of heterogeneous observations can be combined within a parameter estimation process to benefit from their individual strengths and favorable features.

Since regional gravity field problems are usually ill-posed (1) due to the downward continuation of the signal to the surface of the Earth, (2) due to given data gaps and (3) due to the number of chosen basis functions, e.g. in case of spherical radial basis functions (SRBFs), a regularization is in most cases inevitable for parameter estimation.

### Regularization method

Choosing an appropriate numerical value for the regularization parameter is a crucial issue for accurate regional gravity field modeling. Generalized cross validation (GCV), the L-curve criterion and variance component estimation (VCE) are three of the most commonly used methods for estimating the regularization parameter. The L-curve is a graphical procedure: plotting the norm of the regularized solution vector against the norm of the residuals by changing the numerical value for the regularization parameter  $\lambda$  shows a typical 'L-curve' behaviour, i.e. the resulting graph looks like the capital letter 'L'. The corner point of the 'L' means a compromise of the minimization of the solution norm and the residual norm and thus, can be interpreted as the 'best fit' that corresponds to the desired regularization parameter. VCE is a useful method if several data sets need to be combined in a parameter estimation procedure. The variance components are estimated by an iterative process, starting from initial values for the unknown variance factors of the observations as well as the prior information and ending in the convergence point; for details see e.g. Liang (2017). Based on these two methods, we propose two new approaches for the determination of the regularization parameter, which combine the L-curve method and VCE. The first approach, denoted as 'VCE + L-curve method', starts with the calculation of the relative weights between the observation techniques by means of VCE. Based on these weights the L-curve method is applied to determine the regularization parameter. In the second approach, denoted as 'L-curve method + VCE', the L-curve method determines first the regularization parameter and then the relative weights between the observation techniques obtained from VCE.

### Comparison of different regularization methods

Two methods, denoted as CM (combination model) 1 and CM 2 (Schmidt et al., 2015) are investigated for combining different observation techniques. CM 2 takes the relative weights between the observation techniques into consideration while CM 1 relies on an equally weighted scenario. Furthermore, five methods for choosing the regularization parameter are applied: (1) the 'L-curve method based on CM 1', (2) 'VCE based on CM 1', (3) 'VCE based on CM 2', (4) 'VCE + L-curve method', (5) 'L-curve method + VCE' are applied to combine four different types of data sets in Europe respectively. All observation as well as validation data are obtained from the ICCT (Inter-Commission Committee on Theory) Joint Study Group 0.3, part of the IAG (International Association of Geodesy) programme running from 2011 to 2015 ([jsg03.dgfi.tum.de](http://jsg03.dgfi.tum.de)). The comparison of the five methods is visualized in Fig. 3.11 (where

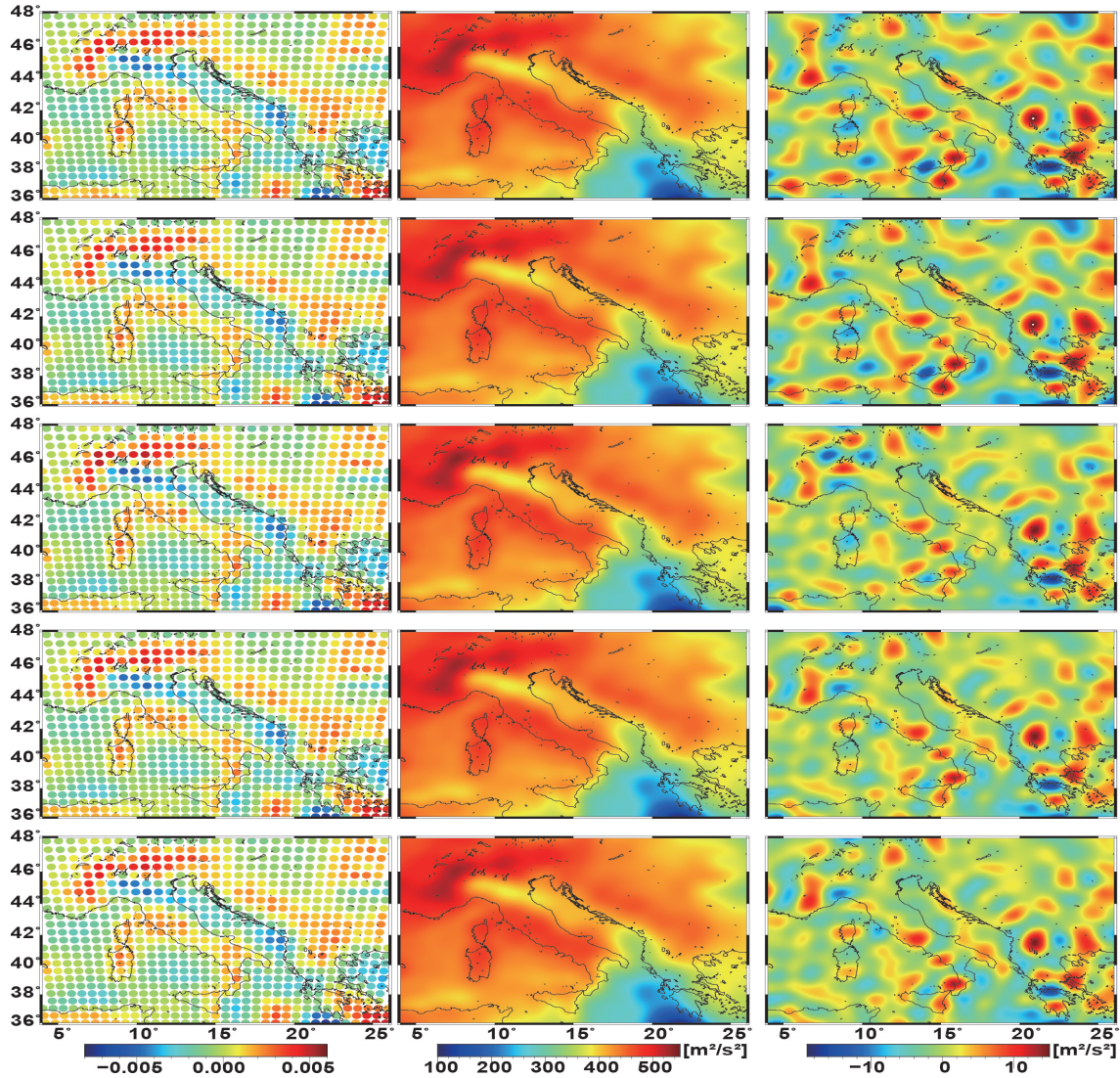


**Figure 3.11:** Left column: estimated scaling coefficients  $d_k$ , mid column: recovered disturbing potential and right column: differences w.r.t the validation data. The results are obtained using the regularization methods ‘L-curve method based on CM 1’ (first row), ‘VCE based on CM 1’ (second row), ‘VCE based on CM 2’ (third row), ‘VCE + L-curve method’ (fourth row) and ‘L-curve method + VCE’ (fifth row); see also Table 3.3 for numerical results.

GRACE data and terrestrial data are combined) and Fig. 3.12 (where GRACE, GOCE, airborne and terrestrial data are combined). The terrestrial and airborne data are measured in terms of gravity disturbance  $\delta g$ , which can be represented by the observation equation

$$\delta g(\mathbf{x}) + e(\mathbf{x}) = \sum_{k=1}^K d_k B_r(\mathbf{x}, \mathbf{x}_k) \quad (3.5)$$

where  $\mathbf{x} = r \cdot \mathbf{r}$  is the position vector of the observation  $\delta g$  with radial distance  $r$  from the geocentre,  $\mathbf{x}_k = R \cdot \mathbf{r}_k$  is the position vector of the SRBF

$$B_r(\mathbf{x}, \mathbf{x}_k) = \sum_{n=0}^{N_{\max}} \frac{2n+1}{4\pi} \left( \frac{n+1}{r} \right) \left( \frac{R}{r} \right)^{n+1} B_n P_n(\mathbf{r}^T \mathbf{r}_k) \quad (3.6)$$

located on the spherical Earth of radius  $R$ . Furthermore, in Eq. (3.5)  $e(\mathbf{x})$  means the observation error and  $d_k$  for  $k = 1, 2, \dots, K$  are the unknown scaling coefficients which need to be determined within a parameter estimation. In Eq. (3.6) the functions  $P_n$  for  $n = 1, 2, \dots, N_{\max}$  are the Legendre polynomials of degree  $n$  and  $B_n$  the corresponding Legendre coefficients specifying the shape

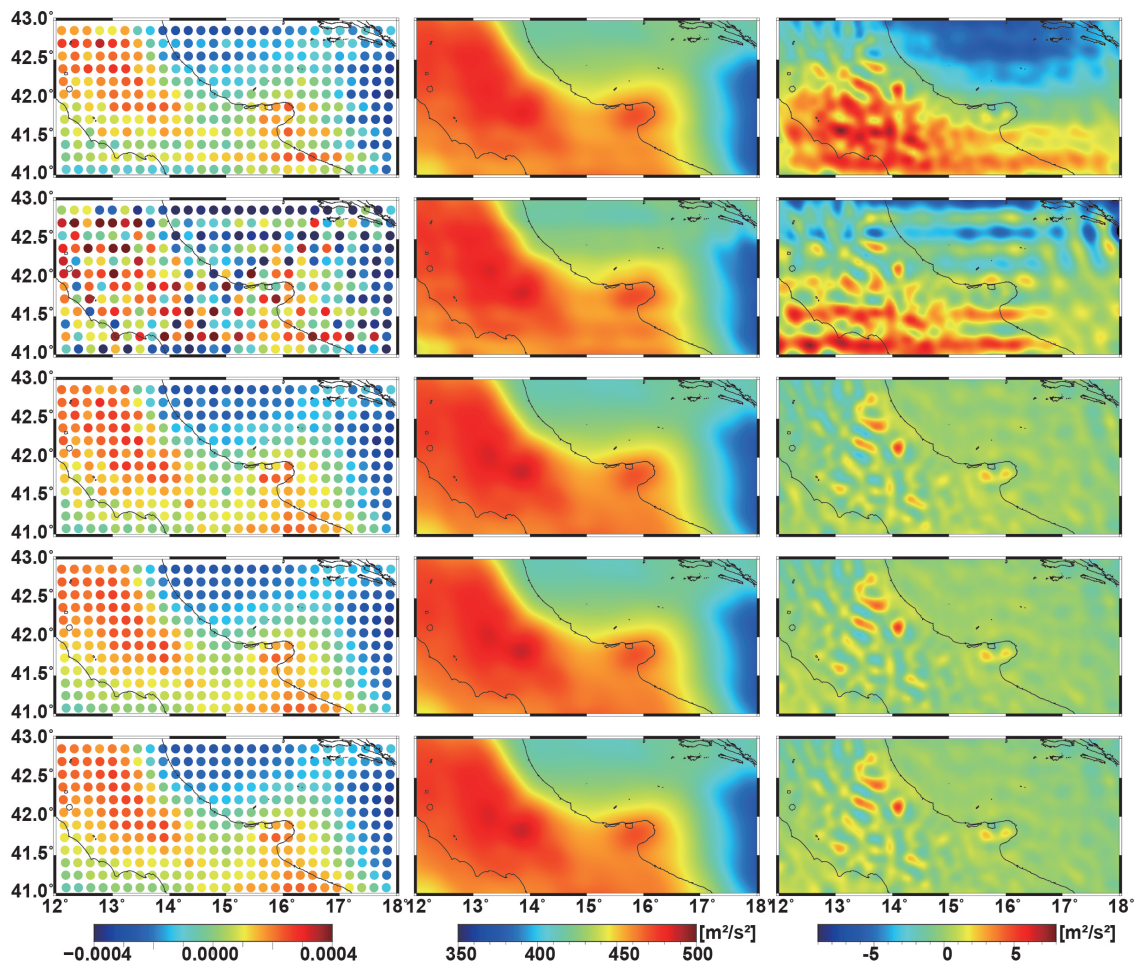


**Figure 3.12:** Left column: estimated scaling coefficients  $d_k$ , mid column: recovered disturbing potential and right column: differences w.r.t the validation data. The results are obtained using the regularization methods 'L-curve method based on CM 1' (first row), 'VCE based on CM 1' (second row), 'VCE based on CM 2' (third row), 'VCE + L-curve method' (fourth row) and 'L-curve method + VCE' (fifth row); see also Table 3.3 for numerical results.

**Table 3.3:** The assessments of the results: the RMS values and the correlations between the estimated coefficients and the validation data for each regularization parameter choice method when different types of observations are combined.

	GRACE + Terrestrial		GRACE + GOCE + Airborne + Terrestrial	
	RMS ( $\text{m}^2/\text{s}^2$ )	Correlation	RMS ( $\text{m}^2/\text{s}^2$ )	Correlation
The L-curve method based on CM 1	4.4317	0.5578	3.2876	0.8746
VCE based on CM 1	4.4421	0.5590	2.5510	0.6022
VCE based on CM 2	3.7648	0.5598	0.8282	0.9050
VCE + L-curve method	3.6107	0.5687	0.7837	0.9199
L-curve method + VCE	3.6422	0.5676	0.7983	0.9187



of the SRBF. In our numerical investigations we use the Shannon kernel in the analysis step and the Blackman kernel in the synthesis step (Liu et al., 2019). For the other observation types – GRACE and GOCE – the corresponding SRBFs have to be set up. A full list of basis functions adapted to different gravitational functionals can be found in (Liu et al., 2019). From the estimated scaling coefficients the disturbing potential can be computed, compared with the validation data and assessed by the criteria:

1. root mean square (RMS) error with respect to the validation data over the area of investigation,
2. correlation factor between the estimated coefficients and the validation data.

In Table 3.3 the results of the assessment are listed.

Based on these results, the following conclusions can be drawn:

1. From the five methods considered here, ‘VCE + L-curve method’ performs the best, and always gives the smallest RMS value as well as the largest correlation.
2. ‘L-curve method + VCE’ and ‘VCE based on CM 2’ also show a good and stable performance; ‘L-curve method + VCE’ outperforms ‘VCE based on CM 2’ regarding both the RMS value and correlations.
3. Generally, results provided by the CM 1 based methods (the first two) are not as good as the others. The larger the spectral resolution between each observation technique is, the worse these methods perform.

### Related publications

Liang W.: A regional physics-motivated electron density model of the ionosphere. PhD thesis, Technical University of Munich, 2017

Liu Q., Schmidt M., Pail R., Willberg M.: Regularization methods for the combination of heterogeneous observations using spherical radial basis functions. *Solid Earth Discuss.*, doi: [10.5194/se-2019-60](https://doi.org/10.5194/se-2019-60), in review, 2019.

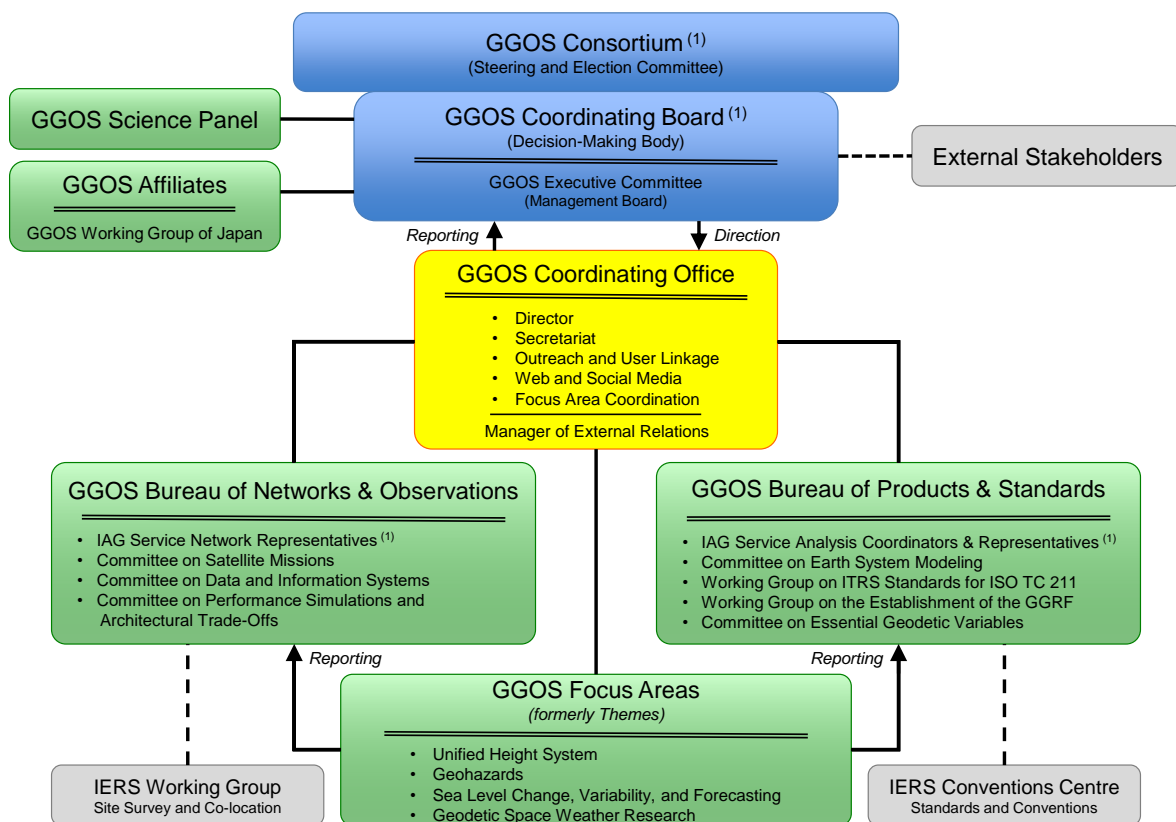
Schmidt M., Göttl F., Heinkelmann R.: Towards the combination of data sets from various observation techniques. In: Kutterer H., Seitz F., Alkhatib H., Schmidt M. (Eds.), *The 1st International Workshop on the Quality of Geodetic Observation and Monitoring Systems (QuGOMS’11)*, IAG Symposia 140: 35–43, Springer, doi:[10.1007/978-3-31910828-5\\_6](https://doi.org/10.1007/978-3-31910828-5_6), 2015.

### 3.3 Standards and Conventions

Unified standards and conventions are a fundamental requirement for the integration of the different geometric and gravimetric observations and for the generation of consistent geodetic products. Towards this aim, the Bureau of Products (BPS) has been established as a component of IAG's Global Geodetic Observing System (GGOS). The new organizational structure of GGOS is given in Fig. 3.13. In 2018, the GGOS Affiliates and the Manager of External Relations have been added as new components. GGOS Affiliates are national or regional organizations that coordinate geodetic activities in that country or region. GGOS Affiliates allow increased participation in GGOS, especially by organizations in under-represented areas of Africa, Asia-Pacific, and South and Central America. In the new GGOS structure, the Manager of External Relations has been included in the GGOS Coordinating Office. Three of the GGOS components are chaired by DGFI-TUM: The Bureau of Products and Standards (see below), the Focus Area "Unified Height System" (see Section 1.4), and the Focus Area "Geodetic Space Weather Research" (see Section 3.1).

#### GGOS Bureau of Products and Standards

The BPS is operated by DGFI-TUM and IAPG of the Technische Universität München within the Forschungsgruppe Satellitengeodäsie (FGS). The main objectives of the BPS are (1) to serve as contact and coordinating point for the homogenization of IAG standards and products, (2) to



(1) GGOS is built upon the foundation provided by the IAG Services, Commissions, and Inter-Commission Committees

Figure 3.13: Organizational structure of IAG's Global Geodetic Observing System (GGOS).

keep track of the adopted geodetic standards and conventions across all IAG components, and to initiate steps to close gaps and deficiencies, and (3) to focus on the integration of geometric and gravimetric parameters and to develop new geodetic products, needed for Earth sciences and society.

The present BPS staff members are D. Angermann (director), T. Gruber (deputy director), M. Gerstl, R. Heinkelmann (GFZ), U. Hugentobler, L. Sánchez and P. Steigenberger (DLR). In its current structure the following GGOS entities are associated with the BPS:

- Committee “Contributions to Earth System Modelling”, Chair: M. Thomas (Germany),
- Committee “Essential Geodetic Variables (EGVs)”, Chair: R. Gross (USA),
- Joint Working Group “Establishment of the Global Geodetic Reference Frame (GGRF)”, Chair: U. Marti (Switzerland),
- Working Group “ITRS Standards for ISO TC211”, Chair: C. Boucher (France).

The Bureau comprises the staff members, the chairs of the associated GGOS components as well as representatives of the IAG Services and other entities. The present status of the associated members as BPS representatives is summarized in Table 3.4.

As regards the development of standards, there is a link with the IERS Conventions Center, the Commission A3 “*Fundamental Standards*” of the International Astronomical Union (IAU), the IAU Working Group “*Numerical Standards for Fundamental Astronomy*”, the Bureau International de Poids et Mesures (BIPM), the Committee on Data for Science and Technology (CODATA), and the International Organization for Standardization (ISO) with its Technical Committee ISO/TC211.

**Table 3.4:** Representatives of IAG Services and other entities (status: December 2018).

IERS Conventions Center	G. Petit (until 2016) N. Stamatakos (since 2017)	BIPM (France) USNO (USA)
IERS Analysis Coordinator	T. Herring	MIT (USA)
IGS Representative	U. Hugentobler (BPS staff)	TUM (Germany)
ILRS Analysis Coordinator	E. Pavlis	UMBC/NASA (USA)
IVS Analysis Coordinator	J. Gipson	GSFC/NASA (USA)
IDS Analysis Coordinators	J.-M. Lemoine, H. Capdeville	CNES/GRGS (France)
IDS Representatives	F. Lemoine, J. Ries	GSFC, CSR (USA)
IGFS Chair	R. Barzaghi	Politecnico Milano (Italy)
BGI Chair	S. Bonvalot	IRD (France)
ISG President	M. Reguzzoni	Politecnico Milano (Italy)
ICGEM Chair	F. Barthelmes (until 2017) E. Sinem Ince (since 2018)	GFZ (Germany) GFZ (Germany)
IDEMS Director	K. Kelly	ESRI (USA)
IGETS Director	H. Wziontek	BKG (Germany)
Gravity Community (corresp. member)	J. Kusche	Univ. Bonn (Germany)
IAG Representative to ISO	J. Ihde (until 2017) D. Angermann (since 2018)	BKG, now GFZ (Germany) DGFI-TUM (Germany)
IAG Communication and Outreach	J. Adam	Univ. Budapest (Hungary)
IAU Commission A3 Representative	C. Hohenkerk	United Kingdom
IAU Representative	R. Heinkelmann (BPS staff)	GFZ (Germany)
Control Body for ISO Geodetic Registry	M. Craymer (Chair), L. Hothem (Vice Chair)	NRCan (Canada) USA

### *Summary of BPS activities in 2018*

- A key activity of the BPS was the compilation of an inventory of standards and conventions used for the generation of IAG products, which has been published in the IAG Geodest's Handbook 2016. In 2018, the BPS team has started to update this inventory. The changes include updates on the organization structure of GGOS and the BPS, as well as the replacement of the previous realizations (i.e., ICRF2, ITRF2008, EOP 08 C04) by the latest versions ICRF3, ITRF2014 and EOP 14 C04. The 2nd version of this document will be published online on the GGOS website. Concerning the recommendations given in the BPS inventory a lot of progress has already been achieved and several activities have been initiated by the responsible IAG components (see Angermann et al., 2018).
- In the field of standards and conventions the BPS closely interacts with the IERS Conventions Centers and IAU Commission A3 "Fundamental Standards". A topic of discussion during the GGOS Days 2018 in Tsukuba (Japan) was the interaction of the BPS and the IERS Conventions Center regarding the re-writing/revising of the IERS Conventions. As a result, the director of the BPS has been nominated as the Chapter Expert for the "General Definitions and Numerical Standards".
- The BPS also supports the development of new products derived from a combination of geometric and gravimetric observations. Towards this aim various activities have been initiated and dedicated GGOS entities have been established to focus on the development of integrated products, such as the Focus Area "Unified Height System", the Focus Area "Geodetic Space Weather Research" and the Joint IAG Working Group "Establishment of the Global Geodetic Reference Frame (GGRF)".
- The director of the BPS has been nominated by the IAG Executive Committee as the IAG Representative to the UN Global Geospatial Information Management (UN-GGIM) Subcommittee "Geodesy" (the former GGRF Working Group) for the Focus Group "Data Sharing and Development of Geodetic Standards". The chair of this Focus Group is Michael Craymer (Canada). In 2018, the BPS contributed to the GGRF Roadmap Implementation Plan to the UN-GGIM Committee of Experts for the 8th session in New York (August, 2018). As a main result, this Focus Group formulated three main recommendations on data sharing and common standards along with a number of actions to be accomplished in these two fields.
- In 2018, the Committee on the definition of Essential Geodetic Variables (EGVs) has been established as a new GGOS component associated with the BPS. The members of the Committee on EGVs comprise the GGOS Science Panel, representing the IAG Commissions, the Inter-Commission Committee on Theory, and the four GGOS Focus Areas, as well as representatives of the IAG Services. The Committee on EGVs is chaired by R. Gross. It consists of 34 members in total. Examples of EGVs might be the position of reference objects (ground stations, radio sources), EOPs, ground- and space-based gravity measurements, etc. Such EGVs could then serve as a basis for a gap analysis to identify requirements concerning observational properties and networks, accuracy, spatial and temporal resolution and latency.

### **Related publication**

Angermann D., Gruber T., Gerstl M., Heinkelmann R., Hugentobler U., Sánchez L., Steigenberger P.: GGOS Bureau of Products and Standards: Recent Activities and Future Plans. International Association of Geodesy Symposia, 10.1007/1345\_2018\_28, 2018

## 4 Information Services and Scientific Transfer

Through its involvement in the international scientific organizations IUGG, IAU and IAG, as well as through the collaboration in various national and international projects, the DGFI-TUM is strongly networked with other institutions worldwide.

In particular in the context of its engagement in the IAG Services that form the backbone for the national and international spatial data infrastructure by coordinating and supporting geodetic research on the international level, the the institute operates - mostly by long-term commitments - data centers, analysis centers, and research centers (cf. Section 1) as well as different internet portals (Section 4.1). In various national and international Commissions, Services, Projects, Working and Study Groups, and in the Global Geodetic Observing System (GGOS), the DGFI-TUM takes leading positions and several functions in management and support (Section 4.2). Section 4.3 lists the articles printed or published online in 2018, and Section 4.4 provides the list of posters and talks presented by DGFI-TUM staff at numerous national and international conferences, symposia and workshops that are listed in Section 4.5. Guests who visited DGFI-TUM in the frame of research co-operations during 2018 are listed in Section 4.6.

### 4.1 Internet representation

The DGFI-TUM operates several independent internet sites and mailing lists in order to meet the growing demand for scientific information and to exchange scientific results and data

In 2018, DGFI-TUM maintained the following web sites:

#### Deutsches Geodätisches Forschungsinstitut der Technischen Universität München (DGFI-TUM)

The web site of DGFI-TUM at [www.dgfi.tum.de](http://www.dgfi.tum.de) highlights current research results and informs about the institute's structure and current research programme. It presents the national and international projects of DGFI-TUM as well as its contributions to various international scientific organizations. The web site (see Fig. 4.1) also provides a complete list of publications, reports and presentations since 1994. Annual Reports and DGFI Reports are available in electronic form.

The screenshot shows the DGFI-TUM website interface. The main content area features a news article titled "River levels tracked from space" with a sub-headline "The 4,300 kilometer Mekong River is a lifeline for South-East Asia. If this mighty river system bursts its banks, flooding can affect the lives and livelihoods of millions of people. Permanent monitoring of the river's water stage is thus essential. Using the example of the Mekong river with its pronounced changes in water level, an innovative method to monitor complex river basins solely based on satellite data has been developed in collaboration between TUM scientists from geodesy and mathematics. The approach allows for modeling how water levels are impacted on various sections of the river by extreme weather events such as heavy rainfall or drought over extended periods. The approach uses measurement data collected from various altimetry satellite missions. In a first step, their raw observations are analysed applying specially developed retracking algorithms in order to create precise time series of water levels for the crossing points of the satellites' tracks with the river. Altimetry satellites on repetitive orbits usually pass over the same points on a repeating cycle of 10 to 35 days. As a result, water level data are captured for each of these points at regular intervals. But the study also integrates observations collected by Cryosat-2, a SAR altimetry satellite on a long-repeat orbit. The SAR altimetry method is superior to conventional systems in terms of accuracy, and the long-repeat orbit results in a very dense spatial resolution of the observations. But at the same time, the temporal resolution of Cryosat-2 data is very low. Thus, the points observed by Cryosat-2 are

The article is accompanied by a map of the Mekong river system in Southeast Asia, showing the distribution and number of altimetry observations. The map includes labels for major cities like Vientiane, Luang Prabang, and Phnom Penh, and rivers like the Mekong, Chao Phraya, and Salween. A legend indicates "Cryosat-2 SAR altimetry" and "non-long-repeat missions along rivers". A scale bar at the bottom of the map shows distances from 0 to 300 km.

The website sidebar on the left contains navigation links: Home, About DGFI-TUM, DGFI-TUM in the media, Research, Projects, Science Data Products, International Services, Staff, Publications, Posters/Presentations, Teaching, Opportunities for Master's Theses / Masterarbeiten, and Location. The right sidebar features the TUM logo, the institute's name, contact information for Prof. Dr.-Ing. habil. Florian Seitz, and a "See also" section with links to various data centers and services.

Figure 4.1: Web site of DGFI-TUM at [www.dgfi.tum.de](http://www.dgfi.tum.de)

## Geocentric Reference System for the Americas (SIRGAS)

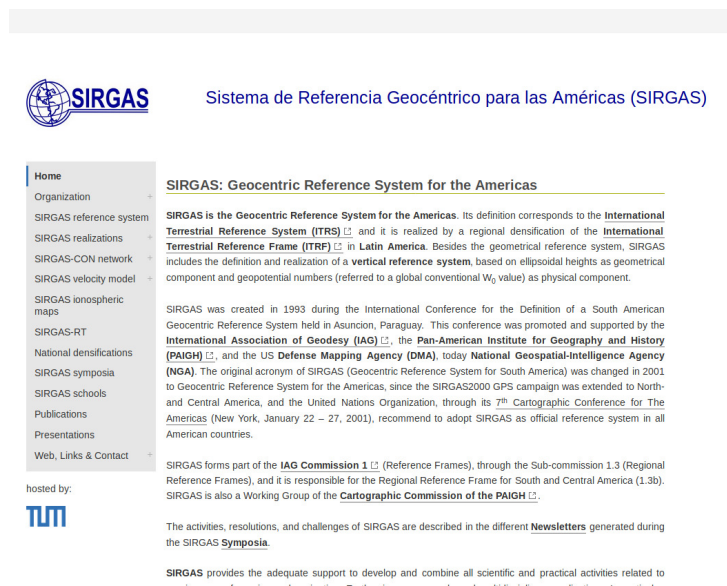


Figure 4.2: Web site of SIRGAS at [www.sirgas.org](http://www.sirgas.org)

SIRGAS is the Geocentric Reference System for the Americas. The web site ([www.sirgas.org](http://www.sirgas.org)) is operated by the IGS Regional Network Associate Analysis Centre for SIRGAS (IGS RNAAC SIRGAS), which is under the responsibility of DGFI-TUM since 1996.

The SIRGAS web site provides (see Fig. 4.2)

- a scientific description of definition, realization, and kinematics of the SIRGAS reference frame,
- an organizational overview (operational structure and functions of the different components of SIRGAS),
- a bibliographic compilation related to SIRGAS activities (articles, reports, presentations).

## EUROLAS Data Centre (EDC)

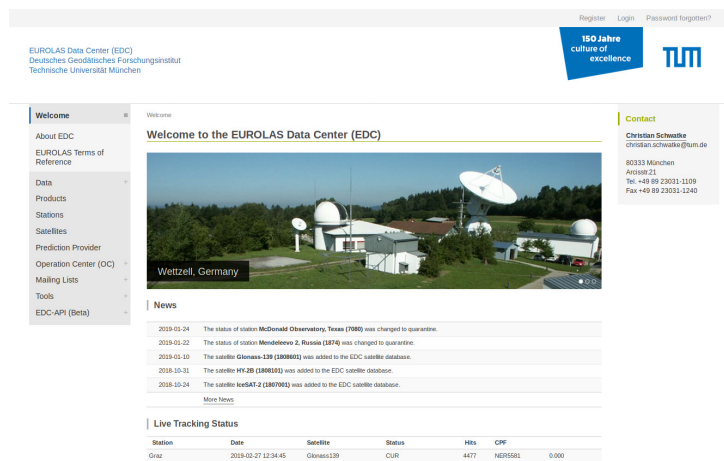


Figure 4.3: Web site of EDC at [edc.dgfi.tum.de](http://edc.dgfi.tum.de)

The EUROLAS Data Center (EDC) provides access to the database of SLR observations and derived products (see Fig. 4.3).

The web site at [edc.dgfi.tum.de](http://edc.dgfi.tum.de) informs about the data flow within the Operation Centre (OC) and the data holding of the Data Centre (DC).

## Open Altimeter Database (OpenADB)

OpenADB is a database for multi-mission altimeter data and derived high-level products. It is designed for both non-expert users and scientific users who are interested in the analysis and application of altimetry data in order to determine new products, models and algorithms. OpenADB allows for fast parameter updates and for extracting data and parameters in user-defined formats. OpenADB is open to the public at no charge after registration. The web site is available at [openadb.dgfi.tum.de](http://openadb.dgfi.tum.de).

## Database for Hydrological Time Series of Inland Waters (DAHITI)

The Database for Hydrological Time Series of Inland Waters (DAHITI) is a public repository of more than 1600 water level time series of globally distributed lakes, rivers, reservoirs, and wetlands derived at DGFI-TUM from multi-mission satellite altimetry. For a variety of the lakes, also time series of surface water extents are available that have been extracted from optical Landsat and Sentinel-2 images. The web site of DAHITI is available at [dahiti.dgfi.tum.de](http://dahiti.dgfi.tum.de) (see Fig. 4.4).

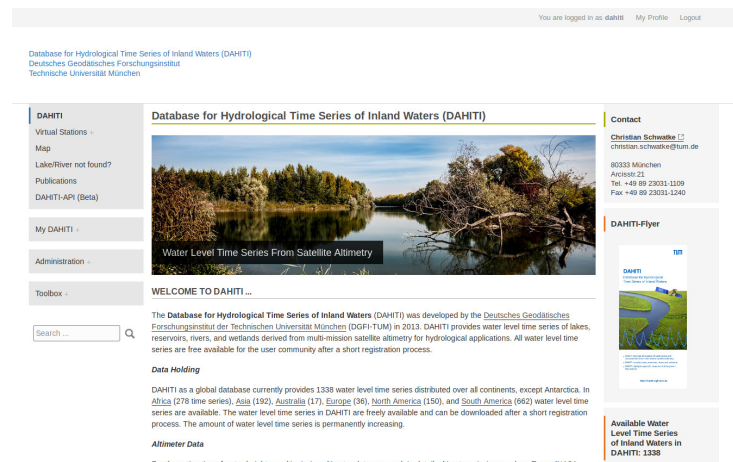


Figure 4.4: Web site of DAHITI at [dahiti.dgfi.tum.de](http://dahiti.dgfi.tum.de)

## GGOS Bureau of Products and Standards (BPS)

The GGOS Bureau of Products and Standards (BPS) was established as a component of IAG's Global Geodetic Observing System (GGOS) in 2009. The BPS is chaired by DGFI-TUM and operated jointly with partners from the Forschungsgruppe Satellitengeodäsie (FGS), the German Aerospace Centre (DLR) and the German Research Centre for Geosciences (GFZ). The GGOS BPS web site is located at [ggos-bps.dgfi.tum.de](http://ggos-bps.dgfi.tum.de)

## GGOS Focus Area Unified Height System

DGFI-TUM chairs the GGOS Focus Area *Unified Height System* for the term 2015–2019. Its website is available at [ihrs.dgfi.tum.de](http://ihrs.dgfi.tum.de). The immediate objectives of this GGOS component are (1) the outlining of detailed standards, conventions, and guidelines to make the IAG Resolution on the International Height Reference System (IHR) applicable, and (2) to establish the realization of the IHR, i.e. the International Height Reference Frame (IHRF). The web page informs about current activities and achievements.

## Office of the International Association of Geodesy (IAG)

Since the 24th General Assembly of the IUGG (2007) in Perugia, Italy, the DGFI has been hosting the Office of the International Association of Geodesy (IAG Office). For the same period, the former director of the DGFI, H. Drewes, has been holding the position of the IAG Secretary General. In this context, DGFI-TUM has taken the responsibility for the administration of the IAG budget. The web site of the IAG Office is available at [iag.dgfi.tum.de](http://iag.dgfi.tum.de)

## 4.2 Membership in scientific bodies

### **Ausschuss Geodäsie der Bayerischen Akademie der Wissenschaften (Deutsche Geodätische Kommission, DGK)**

- *Member: Seitz F.*

### **Centre National d'Etudes Spatiales (CNES) / National Aeronautics and Space Administration (NASA)**

- Ocean Surface Topography Science Team,  
*Member: Dettmering D., Passaro M., Schwatke C.*

### **Coastal Altimetry Workshop**

- Organizing Committee,  
*Member: Passaro M.*

### **Coastal Waters Research Synergy Framework (CoReSyf)**

- User Board,  
*Member: Passaro M.*

### **Deutsche Gesellschaft für Geodäsie, Geoinformation und Landmanagement (DVW)**

- Working Group 7: Experimentelle, Angewandte und Theoretische Geodäsie,  
*Member: Schmidt M., Seitz F.*

### **European Commission (EC) / European Space Agency (ESA)**

- Copernicus POD Quality Working Group,  
*Member: Dettmering D.*

### **European Space Agency (ESA)**

- CryoSat Expert Group,  
*Member: Passaro M.*

### **European Space Agency (ESA) / Centre National d'Etudes Spatiales (CNES)**

- Scientific Committee of "25 Years of Progress in Radar Altimetry Symposium",  
*Member: Passaro M.*

### **European Space Agency (ESA) / European Organisation for the Exploitation of Meteorological Satellites (EUMETSAT)**

- Sentinel-3 Validation Team, Altimetry sub-group,  
*Member: Dettmering D.*

### **Forschungsgruppe Satellitengeodäsie (FGS)**

- *Deputy Speaker: Seitz F.*

### **International Association of Geodesy (IAG)**

- Commission 1 Joint Working Group 1.3 Troposphere Ties,  
*Member: Kwak Y.*
- Commission 1 Working Group 1.3.1 Time dependent transformations between reference frames,  
*Member: Sánchez L.*



- Commission 1, Sub-Commission 1.4: Interaction of celestial and terrestrial reference frames,  
*Member: Seitz M.*
- Commission 1, Working Group 1.1.1 Co-locations using Clocks and New Sensors,  
*Member: Kwak Y.*
- Commission 1.2 / ICCT Joint Working Group Definition of next generation terrestrial reference frames,  
*Member: Bloßfeld M., Seitz M.*
- Commission 4, Joint Working Group 4.3.3 Combination of Observation Techniques for Multi-dimensional Ionosphere Modelling,  
*Member: Erdogan E., Schmidt M.*
- Commission 4, Sub-Commission 4.3 Atmosphere Remote Sensing,  
*Chair: Schmidt M.*
- Commission 4, Working Group 4.3.1 Real Time Ionosphere Monitoring,  
*Member: Dettmering D., Erdogan E.*
- Commission 4, Working Group 4.3.2 Ionosphere Predictions,  
*Vice-Chair: Erdogan E.*
- Commission 4, Working Group 4.3.5 Ionosphere Scintillations,  
*Member: Schmidt M.*
- Global Geodetic Observing System (GGOS) Bureau of Products and Standards,  
*Director: Angermann D., Member: Sánchez L.*
- Global Geodetic Observing System (GGOS) Coordinating Board,  
*Member: Angermann D., Sánchez L., Schmidt M.*
- Global Geodetic Observing System (GGOS) Executive Committee,  
*Member: Angermann D.*
- Global Geodetic Observing System (GGOS) Focus Area Geodetic Space Weather Research,  
*Lead: Schmidt M.*
- Global Geodetic Observing System (GGOS) Focus Area Unified Height System,  
*Lead: Sánchez L.*
- Global Geodetic Observing System (GGOS) Joint Working Group on the Realization of the IHRs,  
*Chair: Sánchez L.*
- Global Geodetic Observing System (GGOS) Working Group on Performance Simulations and Architectural Trade-Offs (PLATO),  
*Member: Bloßfeld M., Kehm A., Seitz M.*
- ICCT Joint Study Group 0.20 Space weather and ionosphere,  
*Member: Goss A.*
- ICCT Joint Study Group 0.19 Time series analysis in geodesy,  
*Member: Schmidt M.*
- ICCT Joint Study Group 0.20 Space weather and ionosphere,  
*Member: Erdogan E., Lalgudi Gopalakrishnan G., Schmidt M.*
- ICCT Study Group 5: Fusion of multi-technique satellite geodetic data,  
*Member: Bloßfeld M.*

- Joint Working Group for the establishment for the Global Geodetic Reference Frame (GGRF),  
*Member: Angermann D.*
- Symposia Series,  
*Assistant Editor-in-Chief: Sánchez L.*
- Working Group for the establishment of the Global Geodetic Reference Frame (GGRF),  
*Member: Angermann D., Sánchez L.*

#### **International Association of Geodesy (IAG) and International Earth Rotation and Reference Systems Service (IERS)**

- Joint Working Group on Site Survey and Co-location,  
*Member: Angermann D., Seitz M.*

#### **International Astronomical Union (IAU)**

- Commission A.2, Rotation of the Earth,  
*President: Seitz F., Member: Seitz M.*
- Division A Working Group: Third Realisation of International Celestial Reference Frame,  
*Member: Seitz M.*

#### **International Astronomical Union (IAU) and International Association of Geodesy (IAG)**

- Joint Working Group Theory of Earth Rotation and Validation,  
*Member: Seitz F.*

#### **International DORIS Service (IDS)**

- DORIS Analysis Working Group,  
*Member: Rudenko S.*
- Governing Board,  
*Member: Dettmering D.*
- Scientific Committee of the IDS workshop 2018,  
*Member: Dettmering D.*
- Working Group on NRT DORIS data,  
*Chair: Dettmering D., Member: Erdogan E., Schmidt M.*

#### **International Earth Rotation and Reference Systems Service (IERS)**

- Directing Board,  
*Associate member: Angermann D., Bloßfeld M.*
- ITRS Combination Centre,  
*Chair: Seitz M., Member: Bloßfeld M.*
- Working Group on Combination at the Observation Level,  
*Co-Chair: Seitz M., Member: Angermann D., Bloßfeld M.*
- Working Group on SINEX Format,  
*Member: Seitz M.*
- Working Group on Site Coordinate Time Series Format,  
*Member: Seitz M.*

#### **International GNSS Service (IGS)**

- Governing Board,  
*Network Representative: Sánchez L.*

- GPS Tide Gauge Benchmark Monitoring – Working Group,  
*Member: Sánchez L.*
- Ionosphere Working Group,  
*Member: Schmidt M.*
- Regional Network Associate Analysis Centre for SIRGAS,  
*Chair: Sanchez L.*

#### **International Laser Ranging Service (ILRS)**

- Analysis Standing Committee,  
*Member: Bloßfeld M., Kehm A., Müller H., Schwatke C.*
- EUROLAS Data Centre (EDC),  
*Chair: Schwatke C., Member: Müller H.*
- Data Formats and Procedures Standing Committee,  
*Chair: Müller H., Schwatke C.*
- Governing Board,  
*Member: Müller H., Schwatke C.*
- LARGE (LAser Ranging to GNSS s/c Experiment) Study Group,  
*Member: Müller H.*
- Networks and Engineering Standing Committee,  
*Member: Schwatke C.*
- ILRS-Operation Center,  
*Chair: Schwatke C.*
- Quality Control Board,  
*Member: Müller H.*
- Study Group on Data Format Update,  
*Member: Schwatke C.*
- Study Group on ILRS Software Library,  
*Member: Schwatke C.*

#### **International Service for the Geoid (ISG)**

- *Scientific advisor: Sánchez L.*

#### **International Union of Geodesy and Geophysics (IUGG)**

- *Representative to the Panamerican Institute for Geodesy and History (PAIGH):  
Sánchez L.*

#### **International VLBI Service for Geodesy and Astrometry (IVS)**

- IVS Working Group on Satellite Observations with VLBI,  
*Member: Kwak Y.*
- Operational Analysis Centre,  
*Member: Seitz M.*

#### **Sistema de Referencia Geocéntrico para las Américas (SIRGAS)**

- Scientific Committee,  
*Member: Sánchez L.*

- SIRGAS Analysis Centre,  
*Chair: Sánchez L.*

#### United Nations Global Spatial Information Management (UN-GGIM)

- Subcommittee “Geodesy” (Working Group for a Global Geodetic Reference Frame, GGRF)  
*IAG Representative for the Working Group “Data Sharing and Development of Standards”:*  
*Angermann D.*

### 4.3 Publications

- Androsov A., Nerger L., Schnur R., Schröter J., Albertella A., Rummel R., Savcenko R., Bosch W., Skachko S., Danilov S.: *On the assimilation of absolute geodetic dynamic topography in a global ocean model: impact on the deep ocean state.* Journal of Geodesy, 93(2), doi:[10.1007/s00190-018-1151-1](https://doi.org/10.1007/s00190-018-1151-1), 2018
- Angermann D., Bloßfeld M., Seitz M., Kwak Y., Rudenko S.: *ITRS Combination Centres: Deutsches Geodätisches Forschungsinstitut der TU München (DGFI-TUM).* In: Dick W.R., Thaller D. (Eds.), IERS Annual Report 2017, Verlag des Bundesamts für Kartographie und Geodäsie, 2018
- Angermann D., Gruber T., Gerstl M., Heinkelmann R., Hugentobler U., Sánchez L., Steigenberger P.: *GGOS Bureau of Products and Standards: Recent Activities and Future Plans.* International Association of Geodesy Symposia, 149, doi:[10.1007/1345\\_2018\\_28](https://doi.org/10.1007/1345_2018_28), 2018
- Bloßfeld M., Angermann D., Seitz M.: *DGFI-TUM analysis and scale investigations of the latest Terrestrial Reference Frame realizations.* International Association of Geodesy Symposia, 149, doi:[10.1007/1345\\_2018\\_47](https://doi.org/10.1007/1345_2018_47), 2018
- Bloßfeld M., Rudenko S., Kehm A., Panafidina N., Müller H., Angermann D., Hugentobler U., Seitz M.: *Consistent estimation of geodetic parameters from SLR satellite constellation measurements.* Journal of Geodesy, 92(9), doi:[10.1007/s00190-018-1166-7](https://doi.org/10.1007/s00190-018-1166-7), 2018
- Boergens E.: *Water Level Modelling of the Mekong River Based on Multi-Mission Altimetry,* Ausschuss Geodäsie (DGK), Series C 821, Verlag der Bayerischen Akademie der Wissenschaften, ISBN 978-3-7696-5233-8, 2018
- Dettmering D., Wynne A., Müller F.L., Passaro M., Seitz F.: *Lead Detection in Polar Oceans — A Comparison of Different Classification Methods for Cryosat-2 SAR Data.* Remote Sensing 10(8), 1190, doi:[10.3390/rs10081190](https://doi.org/10.3390/rs10081190), 2018
- Esselborn S., Rudenko S., Schöne T.: *Orbit-related sea level errors for TOPEX altimetry at seasonal to decadal timescales.* Ocean Science, 14, 205-223, doi:[10.5194/os-14-205-2018](https://doi.org/10.5194/os-14-205-2018), 2018
- Gómez-Enri J., González C.J., Passaro M., Vignudelli S., Álvarez O., Cipollini P., Mañanes R., Bruno M., López-Carmona M.P., Izquierdo A.: *Wind-induced cross-strait sea level variability in the Strait of Gibraltar from coastal altimetry and in-situ measurements.* Remote Sensing of Environment, 221, doi:[10.1016/j.rse.2018.11.042](https://doi.org/10.1016/j.rse.2018.11.042), 2018
- Göttl F., Schmidt M., Seitz F.: *Mass-related excitation of polar motion: an assessment of the new RL06 GRACE gravity field models.* Earth, Planets and Space, 70(1), doi:[10.1186/s40623-018-0968-4](https://doi.org/10.1186/s40623-018-0968-4), 2018

- Gruber C., Rudenko S., Groh A., Ampatzidis D., Fagiolini E.: *Earth's surface mass transport derived from GRACE, evaluated by GPS, ICESat, hydrological modeling and altimetry satellite orbits*. *Earth Surface Dynamics*, 6(4), 1203-1218, doi:[10.5194/esurf-6-1203-2018](https://doi.org/10.5194/esurf-6-1203-2018), 2018
- Kwak Y., Bloßfeld M., Schmid R., Angermann D., Gerstl M., Seitz M.: *Consistent realization of celestial and terrestrial reference frames*. *Journal of Geodesy*, 92(9), doi:[10.1007/s00190-018-1130-6](https://doi.org/10.1007/s00190-018-1130-6), 2018
- Legeais J.-F., Ablain M., Zawadzki L., Zuo H., Johannessen J.A., Scharffenberg M.G., Fenoglio-Marc L., Fernandes M.J., Andersen O.B., Rudenko S., Cipollini P., Quartly G.D., Passaro M., Cazenave A., Benveniste, J.: *An improved and homogeneous altimeter sea level record from the ESA Climate Change Initiative*. *Earth System Science Data*, 10(1), 281–301, doi:[10.5194/essd-10-281-2018](https://doi.org/10.5194/essd-10-281-2018), 2018
- Männel B., Thaller D., Rothacher M., Böhm J., Müller J., Glaser S., Dach R., Biancale R., Bloßfeld M., Kehm A., Herrera Pinzon I., Hofmann F., Andritsch F., Coulot D., Pollet A.: *Recent Activities of the GGOS Standing Committee on Performance Simulations and Architectural Trade-Offs (PLATO)*. *International Association of Geodesy Symposia*, 149, doi:[10.1007/1345\\_2018\\_30](https://doi.org/10.1007/1345_2018_30), 2018
- Noll C.E., Rinklefs R., Horvath J., Müller H., Schwatke C., Torrence M.: *Information resources supporting scientific research for the international laser ranging service*. *Journal of Geodesy*, doi:[10.1007/s00190-018-1207-2](https://doi.org/10.1007/s00190-018-1207-2), 2018
- Nothnagel A., Angermann D., Heinkelmann R.: *Investigations of reference systems for monitoring global change and for precise navigation in space: preface to the special issue on reference systems*. *Journal of Geodesy*, 92(9), doi:[10.1007/s00190-018-1179-2](https://doi.org/10.1007/s00190-018-1179-2), 2018
- Otsubo T., Müller H., Pavlis E., Torrence M.H., Thaller D., Glotov V., Wang X., Sośnica K., Meyer U., Wilkinson M.J.: *Rapid response quality control service for the laser ranging tracking network*. *Journal of Geodesy*, doi:[10.1007/s00190-018-1197-0](https://doi.org/10.1007/s00190-018-1197-0), 2018
- Panafidina N., Hugentobler U., Krásná H., Schmid R., Seitz M.: *Mechanism of error propagation from the subdaily Universal Time model into the celestial pole offsets estimated by VLBI*. *Advances in Space Research*, 63(1), doi:[10.1016/j.asr.2018.08.007](https://doi.org/10.1016/j.asr.2018.08.007), 2018
- Panafidina N., Hugentobler U., Seitz M.: *Influence of subdaily model for polar motion on the estimated GPS satellite orbits*. *Journal of Geodesy*, 93(2), doi:[10.1007/s00190-018-1153-z](https://doi.org/10.1007/s00190-018-1153-z), 2018
- Panzetta F., Bloßfeld M., Erdogan E., Rudenko S., Schmidt M., Müller H.: *Towards thermospheric density estimation from SLR observations of LEO satellites – A case study with ANDE-Pollux satellite*. *Journal of Geodesy*, 93(3), doi:[10.1007/s00190-018-1165-8](https://doi.org/10.1007/s00190-018-1165-8), 2018
- Passaro M., Rose S.K., Andersen O.B., Boergens E., Calafat F.M., Dettmering D., Benveniste J.: *ALES+: Adapting a homogenous ocean retracker for satellite altimetry to sea ice leads, coastal and inland waters*. *Remote Sensing of Environment*, 211, doi:[10.1016/j.rse.2018.02.074](https://doi.org/10.1016/j.rse.2018.02.074), 2018
- Passaro M., Zulfikar Adlan N., Quartly G.D.: *Improving the precision of sea level data from satellite altimetry with high-frequency and regional sea state bias corrections*. *Remote Sensing of Environment*, 218, doi:[10.1016/j.rse.2018.09.007](https://doi.org/10.1016/j.rse.2018.09.007), 2018
- Piccioni G., Dettmering D., Passaro M., Schwatke C., Bosch W., Seitz F.: *Coastal Improvements for Tide Models: The Impact of ALES Retracker*. *Remote Sensing*, 10(5), doi:[10.3390/rs10050700](https://doi.org/10.3390/rs10050700), 2018

- Restano M., Passaro M., Benveniste J.: *New Achievements in Coastal Altimetry*. EOS, 99, doi:[10.1029/2018eo106087](https://doi.org/10.1029/2018eo106087), 2018
- Rudenko S., Bloßfeld M., Müller H., Dettmering D., Angermann D., Seitz M.: *Evaluation of DTRF2014, ITRF2014 and JTRF2014 by Precise Orbit Determination of SLR Satellites*. IEEE Transactions on Geoscience and Remote Sensing, 56(6), doi:[10.1109/TGRS.2018.2793358](https://doi.org/10.1109/TGRS.2018.2793358), 2018
- Rudenko S., Schmidt M., Bloßfeld M., Xiong C., Lühr H.: *Calibration of empirical models of thermospheric density using Satellite Laser Ranging observations to Near-Earth orbiting spherical satellites*. In: Freymueller J., Sánchez L. (Eds.), International Association of Geodesy Symposia, 149, doi:[10.1007/1345\\_2018\\_40](https://doi.org/10.1007/1345_2018_40), 2018
- Sánchez L.: *SIRGAS Regional Network Associate Analysis Centre, Technical Report 2017*. In: Villiger A., Dach R. (Eds.), International GNSS Service Technical Report 2017 (IGS Annual Report), doi:[10.7892/boris.116377](https://doi.org/10.7892/boris.116377), 2018
- Sánchez L., Völksen Ch., Sokolov A., Arenz H., Seitz F.: *Present-day surface deformation of the Alpine region inferred from geodetic techniques*. Earth System Science Data, 10(3), doi:[10.5194/essd-10-1503-2018](https://doi.org/10.5194/essd-10-1503-2018), 2018
- Schwatke C.: *EUROLAS Data Center (EDC) - Status Report 2016-2018*. Proceedings of the 21th International Workshop on Laser Ranging, Canberra, Australia, 2018
- Schwatke C.: *EUROLAS Data Center (EDC) – Recent Developments (Site Logs, Station History Logs, and Data Transfer)*. Proceedings of the 21th International Workshop on Laser Ranging, Canberra, Australia, 2018
- Xiong C., Lühr H., Schmidt M., Bloßfeld M., Rudenko S.: *An empirical model of the thermospheric mass density derived from CHAMP satellite*. Annales Geophysicae, 36(4), doi:[10.5194/angeo-36-1141-2018](https://doi.org/10.5194/angeo-36-1141-2018), 2018

## 4.4 Posters and oral presentations

- Andersen O.B., Rose S.K., Passaro M., Benveniste J.: *A 25-year Arctic Sea-level Record (1991-2016) and first look at Arctic Sea Level Budget Closure*. Altimetry Cal/Val Review and Applications 2018, Chania, Crete, Greece, 2018
- Angermann D.: *Lecture “Geodäsie – Die Vermessung der Erde im Wandel der Zeit”*. Seminarvortrag am Schyren-Gymnasium Pfaffenhofen, Pfaffenhofen an der Ilm, 2018
- Angermann D.: *Geodetic Reference Systems*. Delegation visit from the Chinese Academy of Sciences (CAS) to DGFI-TUM, Munich, 2018
- Angermann D.: *GGOS BPS und FGS in den Diensten*. FGS Workshop, Bad Kötzting, 2018
- Angermann D.: *Literature survey and review of IERS EOP determination..* CDR meeting to ESA project “Independent Generation of Earth Orientation Parameters”, Darmstadt, 2018
- Angermann D.: *Lecture “Geodäsie und Geoinformation”*. Berufsinformationsveranstaltung am Ignaz-Günther-Gymnasium Rosenheim, Rosenheim, 2018

- Angermann D., Bloßfeld M., Seitz M.: *Report from the ITRF Combination centre at DGFI-TUM*. IERS Directing Board Meeting No. 66, Vienna, Austria, 2018
- Angermann D., Bloßfeld M., Seitz M., Bouman J.: *ITRF Realisierung, GGRF*. FGS Workshop, Bad Kötzing, 2018
- Angermann D., Gruber T., Gerstl M., Heinkelmann R., Hugentobler U., Sanchez L., Steigenberger P.: *The GGOS Bureau of Products and Standards*. American Geosciences Union Fall Meeting, Washington, 2018 (Poster)
- Angermann D., Gruber T., Gerstl M., Hugentobler U., Sánchez L., Heinkelmann R., Steigenberger P.: *The Bureau of Products and Standards and its key role within GGOS*. EGU General Assembly, Vienna, Austria, 2018
- Angermann D., Gruber T., Gerstl M., Hugentobler U., Sánchez L., Heinkelmann R., Steigenberger P.: *BPS: Overview, status and future plans*. GGOS Days 2018, Tskuba, Japan, 2018
- Angermann D., Müller F.: *Lecture "Geodäsie und Geoinformation"*. Berufsinformationsveranstaltung am Gymnasium Raubling, Raubling, 2018
- Benveniste J., Legeais J.-F., Cazenave A., Ablain M., Larnicol G., Johannessen J., Scharffenberg M., Timms G., Mbajon Njiche S., Andersen O., Cipollini P., Roca M., Rudenko S., Fernandes J., Balmaseda M., Quartly Q., Fenoglio-Marc L., Meyssignac B., Passaro M., Ambrozio A., Restano M.: *Accurate estimation of regional sea level changes with the ESA CCI sea level Essential Climate Variable*. 42nd COSPAR Scientific Assembly, Pasadena, CA, United States of America, 2018
- Bloßfeld M.: *Integration geodätischer Weltraumbeobachtungsverfahren zur Bestimmung geodätischer und geophysikalischer Parameter*. Zwischenevaluierung Habilitationsverfahren, 2018
- Bloßfeld M.: *Status and future plans of the ILRS Analysis Center at DGFI-TUM*. ILRS ASC meeting, Vienna, Austria, 2018
- Bloßfeld M., Angermann D., Seitz M.: *Report of the ITRS CC at DGFI-TUM*. IERS Directing Board Meeting, Washington D.C., USA, 2018
- Bloßfeld M., Jäggi A., Kehm A., Meyer U., Sosnica K.: *Evaluating the potential of combined SLR gravity field solutions*. 21st International Workshop on Laser Ranging, Canberra, Australia, 2018
- Bloßfeld M., Kehm A.: *Simulation studies for Satellite Laser Ranging at DGFI-TUM*. GGOS Standing Committee PLATO meeting, Vienna, Austria, 2018
- Bloßfeld M., Kehm A., Seitz F.: *Definition of the interface between rapid and final combination and common software layout*. Progress meeting 2a to ESA project "Independent Generation of Earth Orientation Parameters", 2018
- Bloßfeld M., Kehm A., Seitz F.: *Preliminary assessment of EOP combination using ESA products*. Progress meeting 2a to ESA project "Independent Generation of Earth Orientation Parameters", 2018
- Bloßfeld M., Kehm A., Angermann D.: *Determining 'essential' geodetic variables using Satellite Laser Ranging*. AGU Fall Meeting, Washington D.C., USA, 2018

- Bloßfeld M., Kehm A., Rudenko S.: *Status report of the DGFI-TUM ILRS AC*. 21st International Workshop on Laser Ranging – ILRS Analysis Standing Committee meeting, Canberra, Australia, 2018
- Bloßfeld M., Kehm A., Rudenko S., Angermann D.: *The Role of Laser Ranging for the Global Geodetic Observing System GGOS*. 21st International Workshop on Laser Ranging, Canberra, Australia, 2018
- Bloßfeld M., Kehm A., Thaller D.: *Konsistente Verknüpfung der Raumverfahren*. FGS Workshop, Bad Kötzing, 2018
- Bloßfeld M., Rudenko S., Lemoine F. G.: *Status of the IDS data processing at DGFI-TUM*. DORIS Analysis Working Group (AWG) meeting of the International DORIS Service, Toulouse, France, 2018
- Boergens E., Dettmering D., Seitz F.: *Multi-Mission Altimetry: Observing Water Level Extremes in the Mekong River Basin*. EGU General Assembly, Vienna, Austria, 2018
- Boergens E., Dettmering D., Seitz F.: *Observing Extreme Water Levels in the Mekong Basin with Multi-mission Altimetry*. International Review Workshop on Satellite Altimetry Cal/Val Activities and Applications, Chania, Crete, Greece, 2018
- Boergens E., Schwatke C., Dettmering D.: *Performance of Sentinel-3A for the Observation of Water Level Variations of Rivers and Lakes*. Ocean Surface Topography Science Team (OSTST) Meeting, Ponta Delgada, Azores, Portugal, 2018 (Poster)
- Börger K., Agena J., Erdogan E., Forootan E., Goss A., Hinrichs J., Löcher A., Mrotzek N., Schmidt M.: *On the Impact of Space Weather*. IX Hotine-Marussi, Rome, Italy, 2018
- Brunini C., Sánchez L., Galván R., Drewes H., Gende M.: *Modelling seasonal station motions by combining GNSS and GRACE data at the normal equation level*. International Symposium on Gravity, Geoid and Height Systems (GGHS2018), Copenhagen, Denmark, 2018
- Chereskin T., Rocha C., Gille S., Menemenlis D., Passaro M.: *Characterizing the transition from balanced to unbalanced motions in the Southern California Current system*. 25 Years of Progress in Radar Altimetry, Ponta Delgada, Azores, Portugal, 2018
- Craymer M., Angermann D.: *Activities of Focus Group "Data Sharing, Policies and Standards"*. UN-GGIM "GGRF" Subcommittee of Geodesy Meeting, Vienna, 2018
- De Freitas S.R.C., Martínez W., Mackern M.V., Cioce V.J., Rodino R.P., Sánchez L.: *Advances in the modernization of the height reference systems in Latin America and their integration to the International Height Reference System (IHR)*. International Symposium on Gravity, Geoid and Height Systems (GGHS2018), Copenhagen, Denmark, 2018
- Dettmering D.: *Wie verändert sich der Meeresspiegel? Eine wissenschaftliche Analyse von Satellitenbeobachtungsdaten der letzten 25 Jahre*. Förderverein Geodätisches Informationszentrum Wettzell (GIZ), 2018
- Dettmering D.: *Altimetrie*. FGS Workshop 2018, Bad Kötzing, 2018
- Dettmering D.: *Die Veränderung des Meeresspiegels: Wissenschaftliche Beobachtungsergebnisse statt „Fake News“*. Tag der offenen Tür, TUM, 2018
- Dettmering D.: *Monitoring surface water heights by satellite altimetry*. DFG Forschergruppe GlobalCDA, 2.Lecture Day, Frankfurt am Main, Germany, 2018



- Dettmering D., Schwatke C.: *Multi-Mission Cross-Calibration of Satellite Altimeters: Constructing a Long-Term Data Record for Sea Level Change Studies*. International Review Workshop on Satellite Altimetry Cal/Val Activities and Applications, Chania, Crete, Greece, 2018
- Dettmering D., Schwatke C.: *Relative range bias drifts revealed by a multi-mission crossover analysis: from TOPEX to Sentinel-3*. Ocean Surface Topography Science Team (OSTST) Meeting, Ponta Delgada, Azores, Portugal, 2018 (Poster)
- Erdogan E., Dettmering D., Schmidt M., Goss A.: *The impact of low-latency DORIS data on near real-time VTEC modeling*. IDS Workshop, Ponta Delgada, Portugal, 2018
- Erdogan E., Hoque M., Garcia-Rigo A., Cueto Santamaría M., Schmidt M., Jakowski N., Berdermann J., Hernández-Pajares M., Monte-Moreno E.: *Recent activities of IAG working group "Ionosphere Prediction"*. EGU General Assembly, Vienna, Austria, 2018 (Poster)
- Garcia-Rigo A., Erdogan E., Dettmering D., IAG's RTIM-WG: *Assessment of global and regional VTEC ionospheric maps within IAG's RTIM-WG*. EGU General Assembly, Vienna, Austria, 2018
- Gille S., Masich J., Chereskin T., Passaro M., Soares S.: *Assessing high-wavenumber spectral slopes (and effective resolution) in new altimeter products*. OSTST Meeting 2018, Ponta Delgada, Azores, Portugal, 2018
- Gille S., Mazloff M., Wang J., Chereskin T., Cornuelle B., Menemenlis D., Passaro M., Rocha C.: *High-frequency and high-wavenumber variability in the California Current: Evaluating model requirements for SWOT assimilation*. AGU - Fall Meeting, Washington D.C., USA, 2018
- Glomsda M., Gerstl M., Kwak Y., Angermann D., Seitz F.: *Recent developments of the VLBI analysis software DOGS-RI at DGFITUM*. EGU General Assembly, 2018, Vienna, Austria (Poster)
- Glomsda M., Gerstl M., Kwak Y., Angermann D., Seitz F.: *DOGS-RI: The VLBI Software of DGFITUM*. IVS 2018 General Meeting, 2018 (Poster)
- Glomsda M., Kwak Y., Gerstl M., Angermann D., Seitz F.: *New VLBI Solutions at Analysis Center DGFITUM*. IVS 2018 General Meeting, Longyearbyen, Norway, 2018
- Glomsda M., Kwak Y., Gerstl M., Angermann D., Seitz F.: *VLBI Analysis with DOGS-RI at DGFITUM*. Geodätische Woche 2018, Frankfurt a.M., Germany, 2018
- Gomez-Enri J., Aldarias A., Vignudelli S., Cipollini P., Laiz I., Passaro M., Tejedor B.: *Lessons learned after 10 years of validation of coastal altimetry products in the Gulf of Cadiz and the Strait of Gibraltar (Southwestern Iberian Peninsula)*. 25 Years of Progress in Radar Altimetry, Ponta Delgada, Azores, Portugal, 2018 (Poster)
- Gomez-Enri J., Vignudelli S., Izquierdo A., Passaro M., Gonzalez C.J., Cipollini P., Bruno M., Alvarez O., Mañanes R. : *Sea level variability in the Strait of Gibraltar from along-track high spatial resolution altimeter products*. Altimetry Cal/Val Review and Applications 2018, Chania, Crete, Greece, 2018
- Gomez-Enri J., Vignudelli S., Izquierdo A., Passaro M., Gonzalez C.J., Cipollini P., Bruno M., Alvarez O., Mañanes R.: *Coastal Altimetry for Ocean applications in the Strait of Gibraltar*. 11th Coastal Altimetry Workshop, Frascati (ESA-ESRIN), Italy, 2018
- Goss A., Börger K., Schmidt M., Zeitler L. : *The Impact of Space Weather on the Ionosphere*. COSPAR 42. Assembly, Pasadena, CA, USA, 2018

- Goss A., Erdogan E., Schmidt M.: *Comparison of Global Ionosphere Maps Using Different Basis Functions*. COSPAR 42. Assembly, Pasadena, CA, USA, 2018 (Poster)
- Goss A., Erdogan E., Schmidt M., Dettmering D., Seitz F., Börger K., Brandert S., Görres B., Kersten W., Bothmer V., Hinrichs J., Mrotzek N.: *Mapping and Predicting Ionospheric Conditions Based on Geodetic Space-Techniques and Solar Observations*. Frühjahrstagung der Deutschen Physikalischen Gesellschaft, 2018
- Goss A., Erdogan E., Schmidt M., Dettmering D., Seitz F., Börger K., Brandert S., Görres B., Kersten W.F.: *Modelling the Ionosphere: Global and Regional High-Resolution VTEC Representation by Means of B-Splines*. COSPAR 42. Assembly, Pasadena, CA, USA, 2018
- Göttl F., Schmidt M., Seitz F.: *Minimizing filter effects in GRACE-derived effective angular momentum functions*. EGU General Assembly, Vienna, Austria, 2018
- Kehm A., Bloßfeld M.: *ESA-EOP combination scenarios and software design*. Progress Meeting 3 to ESA project "Independent Generation of Earth Orientation Parameters", 2018
- Kehm A., Bloßfeld M.: *ESA-EOP product contributions (model inventory): current status/ESA contribution to the ILRS: comparison between the ILRS Analysis Centers*. Progress Meeting 2 to ESA project "Independent Generation of Earth Orientation Parameters", 2018
- Kehm A., Bloßfeld M.: *EOP combination scenario and software design*. Progress Meeting 2 to ESA project "Independent Generation of Earth Orientation Parameters", 2018
- Kehm A., Bloßfeld M., König P., Angermann D., Seitz F.: *Satellite Laser Ranging und sein Potential für das Globale Geodätische Beobachtungssystem GGOS – ein Blick in die Zukunft*. Geodätische Woche 2018, Frankfurt am Main, 2018
- Kehm A., Bloßfeld M., Seitz F.: *Optimization of the current SLR tracking network: potential for SLR-derived reference frames*. 21st International Workshop on Laser Ranging, Canberra, Australia, 2018
- Kehm A., Bloßfeld M., Seitz F.: *Extension of the SLR tracking network and its potential for the realization of Terrestrial Reference Frames*. 21st International Workshop on Laser Ranging, Canberra, Australia, 2018
- Knudsen P., Andersen O.B., Ludwigsen C.A., Rose S.K., Passaro M.: *Arctic sea level. Satellite and in-situ observations for more than 25 years*. AGU - Fall Meeting, Washington D.C., USA, 2018
- König P., Kehm A., Bloßfeld M., Seitz F.: *Erweiterung des Bodensegments von Satellite Laser Ranging (SLR) – Realisierung einer Simulationsstudie*. Geodätische Woche 2018, Frankfurt am Main, 2018
- Kusche J., Döll P., Bolch T., Van Dam T., Dettmering D., Eicker A., Engels O., Foglia L., Geßner U., Güntner A., Künzer C., Müller Schmied H., Seitz F., Sneeuw N., Tourian M.: *The GlobalCDA Project - Understanding the global freshwater system by combining geodetic and remote sensing information with modelling, using a calibration/data assimilation approach*. EGU General Assembly, Vienna, Austria, 2018
- Kwak Y., Bloßfeld M., Angermann D., Gerstl M., Seitz M., Schmid R.: *Consistent Realization of CRF, TRF, and EOP*. The 42nd COSPAR Scientific Assembly, Pasadena, CA, USA, 2018
- Kwak Y., Glomsda M., Gerstl M., Angermann D.: *Comparison of CONT17 Networks*. IVS 2018 General Meeting, Longyearbyen, Norway, 2018

- Kwak Y., Seitz M., Bloßfeld M., Angermann D., Gerstl M., Glomsda M.: *Contribution of satellite techniques to CRS realization*. XXXth General Assembly of the International Astronomical Union, Vienna, Austria, 2018
- Kwak Y., Seitz M., Bloßfeld M., Angermann D., Gerstl M., Glomsda M.: *Impact of geodetic satellite techniques on the CRS realization*. EGU General Assembly, Vienna, Austria, 2018 (Poster)
- Lalgudi Gopalakrishnan G., Schmidt M.: *Expressing the Thermosphere as an Affine Transformation of the Ionosphere*. IX Hotine-Marussi, Rome, Italy, 2018
- Lalgudi Gopalakrishnan G., Schmidt M.: *Comparison between thermospheric neutral density and ionospheric electron density from TIEGCM and empirical models*. EGU General Assembly, Vienna, Austria, 2018 (Poster)
- Lalgudi Gopalakrishnan G., Schmidt M., Rudenko S., Bloßfeld M.: *Towards the calibration of empirical and physics based neutral density models*. 7th IAGA/ICMA/SCOSTEP Workshop on Vertical Coupling in the Atmosphere-Ionosphere System, Potsdam, Germany, 2018
- Lalgudi Gopalakrishnan G., Schmidt M., Seitz F., Vielberg K., Kusche J., Börger K.: *Development of an operational prototype for the determination of the thermospheric density on the basis of a thermosphere-ionosphere coupling model (TIK)*. EGU General Assembly, Vienna, Austria, 2018 (Poster)
- Leger F., Birol F., Niño F., Fleury S., Passaro M.: *X-TRACK regional altimeter products for coastal applications*. 11th Coastal Altimetry Workshop, Frascati, Italy, 2018 (Poster)
- Leger F., Birol F., Niño F., Fleury S., Passaro M.: *Last developments and perspectives of the X-TRACK regional altimeter products*. 25 Years of Progress in Radar Altimetry, Ponta Delgada, Azores, Portugal, 2018 (Poster)
- Leger F., Birol F., Niño F., Passaro M., Cazenave A., Ablain M.: *Toward a new multi-mission altimetry product at high rate for coastal application, combining the ALES reprocessing, the X-TRACK editing algorithms and a dedicated set of correction..* AGU - Fall Meeting, Washington D.C., USA, 2018 (Poster)
- Müller F. L., Wekerle C., Dettmering D., Bosch W.: *Die Meerestopographie der Grönland See – ein Vergleich zwischen Satellitenaltimetrie und Ozeanmodellierung*. Geodätische Woche 2018, Frankfurt am Main, Germany, 2018
- Müller F. L., Wekerle C., Dettmering D., Bosch W., Seitz F.: *Arctic Ocean Topography from Ocean Modeling and Satellite Altimetry: Correspondence, discrepancies and prospects for combination*. 27th International Polar Conference 2018, Rostock, Germany, 2018 (Poster)
- Müller F., Wekerle C., Dettmering D., Bosch W., Seitz F.: *Arctic Ocean Topography from Ocean Modeling and Satellite Altimetry: Correspondence, discrepancies and prospects for combination*. International Review Workshop on Satellite Altimetry Cal/Val Activities and Applications, Chania, Crete, Greece, 2018 (Poster)
- Passaro M., Boergens E., Barbieri E.: *Status of the algorithm development*. CCI Sea State Project Progress Meeting 2, Southampton, UK, 2018
- Passaro M., Boergens E., Quartly G.D., Nencioli F., Quilfen Y., Roca M., Makhoul E., Taposeea C.A., Thibaut P., Arduin F., Donlon C., Cipollini P., Ash E.: *Sea State Climate Change Initiative: first steps of the Algorithm Development Team*. OSTST Meeting 2018, Ponta Delgada, Azores, Portugal, 2018 (Poster)

- Passaro M., Cipollini P., Quartly G.D., Smith W.H.F., Dettmering D., Schwatke C.: *From the open ocean to the coast and back with ALES: Bypassing waveform tail artefacts to observe the coastal sea level variability*. 25 Years of Progress in Radar Altimetry, Ponta Delgada, Azores, Portugal, 2018
- Passaro M., Nuñez A., Schwatke C.: *ALES dataset in OpenADB*. OSTST Meeting 2018, Ponta Delgada, Azores, Portugal, 2018
- Passaro M., Smith W., Schwatke C., Piccioni G., Dettmering D.: *Validation of a global dataset based on subwaveform retracking: improving the precision of pulse-limited satellite altimetry*. 11th Coastal Altimetry Workshop, Frascati (ESA-ESRIN), Italy, 2018
- Passaro M., Zulfikar Adlan N., Quartly G.D.: *Improving the precision of sea level data from satellite altimetry with high-frequency and regional sea state bias corrections*. OSTST Meeting 2018, Ponta Delgada, Azores, Portugal, 2018
- Piccioni G., Dettmering D., Bosch W., Seitz F.: *A new set of in-situ tidal constants based on the GESLA dataset*. Ocean Surface Topography Science Team (OSTST) Meeting, Ponta Delgada, Azores, Portugal, 2018 (Poster)
- Piccioni G., Dettmering D., Passaro M., Schwatke C., Bosch W., Seitz F.: *Coastal Improvements for Tide Models: the Impact of ALES retracker*. 11th Coastal Altimetry Workshop, 2018
- Piccioni G., Dettmering D., Schwatke C., Bosch W., Seitz F.: *An updated EOT model: first impressions from the North Sea*. Ocean Surface Topography Science Team (OSTST) Meeting, Ponta Delgada, Azores, Portugal, 2018 (Poster)
- Quartly G.D., Smith W., Passaro M.: *Better than averaging: empirical correction for intra-1Hz correlations*. OSTST Meeting 2018, Ponta Delgada, Azores, Portugal, 2018
- Rose S.K., Andersen O.B., Passaro M., Benveniste J.: *Review: 25 years of Sea Level Records from the Arctic Ocean using radar altimetry*. 25 Years of Progress in Radar Altimetry, Ponta Delgada, Azores, Portugal, 2018
- Royston S., Watson C., King M., Passaro M., Legresy B., Church J.: *Observed Sea-Level Trends and Variability from the Coast to Open Ocean: An Australian Case-Study*. AGU Ocean Sciences Meeting, Portland, Oregon, USA, 2018 (Poster)
- Royston S., Watson C., King M., Passaro M., Legresy B., Church J.: *Sea-level trends in the Australian region*. AMOS-ICSHMO 2018, Sidney, Australia, 2018 (Poster)
- Royston S., Watson C., Passaro M., Legresy B., King M.: *Variability in sea-level trends from open ocean to the coast: An Australian case-study*. Sea Level Futures Conference, Liverpool, 2018
- Rudenko S., Bloßfeld M., Dettmering D.: *Status of SLR and DORIS data processing of Jason satellites at DGFI-TUM*. IDS workshop, Ponta Delgada, Portugal, 2018
- Rudenko S., Bloßfeld M., Dettmering D., Kehm A., Zeithöfler J., Angermann D.: *Impact of various models on orbits of Jason satellites*. 42nd COSPAR Scientific Assembly, Pasadena, CA, United States of America, 2018
- Rudenko S., Bloßfeld M., Müller H., Dettmering D., Angermann D., Seitz M.: *Evaluation of the International Terrestrial Reference System 2014 realizations by Precise Orbit Determination of SLR satellites*. 42nd COSPAR Scientific Assembly, Pasadena, CA, United States of America, 2018

- Rudenko S., Bloßfeld M., Schmidt M.: *Using SLR observations to Low Earth Orbiting satellites to scale neutral thermospheric density values*. 21st International Workshop on Laser Ranging, Canberra, Australia, 2018 (Poster)
- Rudenko S., Dettmering D., Bloßfeld M., Esselborn S., Schöne T.: *On the long-term stability of altimetry satellites orbits*. “25 Years of Progress in Radar Altimetry” Symposium, Ponta Delgada, Portugal, 2018 (Poster)
- Rudenko S., Schmidt M., Bloßfeld M.: *Estimation of scaling factors of thermospheric density from the analysis of satellite laser ranging observations to spherical low Earth orbiting satellites*. INSIGHT project progress meeting, Munich, Germany, 2018
- Rudenko S., Schmidt M., Bloßfeld M., Erdogan E., Goss A.: *Scaling thermospheric density of thermospheric empirical models using satellite laser ranging measurements to spherical low orbit Earth satellites*. Frühjahrstagung der Deutschen Physikalischen Gesellschaft, Würzburg, Germany, 2018
- Rudenko S., Schmidt M., Bloßfeld M., Lalgudi Gopalakrishnan G.: *Thermospheric density estimation using Satellite Laser Ranging observations of low Earth orbiting satellites*. 42nd COSPAR Scientific Assembly, Pasadena, CA, United States of America, 2018
- Rudenko S., Schmidt M., Bloßfeld M., Xiong C., Lühr H.: *Investigation of temporal change of thermosphere density scale factors derived from SLR observations to LEO satellites*. EGU General Assembly, Vienna, Austria, 2018 (Poster)
- Sánchez L.: *GGOS Focus Area Unified Height System: Ongoing activities*. GGOS Coordinating Board Meeting, Vienna, Austria, 2018
- Sánchez L.: *Implementierung des Internationalen Höhenreferenzrahmens (IHRF)*. Forschungsgruppe Satellitengeodäsie Workshop 2018, Bad Kötzting, Germany, 2018
- Sánchez L.: *GGOS Focus Area Unified Height System: Status report, ongoing activities, outlook*. GGOS Days 2018, Tskuba, Japan, 2018
- Sánchez L.: *SIRGAS and the implementation of the International Height Reference System (IHR)*. Symposium SIRGAS2018, Aguascalientes, Mexico, 2018
- Sánchez L.: *Strategy for the establishment of the International Height Reference System (IHR)*. Symposium SIRGAS2018, Aguascalientes, Mexico, 2018
- Sánchez L.: *22 years of IGS RNAAC SIRGAS – IGS Regional Network Associate Analysis Centre for SIRGAS*. Symposium SIRGAS2018, Aguascalientes, Mexico, 2018
- Sánchez L.: *SIRGAS reference frame data in the Internet*. Symposium SIRGAS2018, Aguascalientes, Mexico, 2018
- Sánchez L., Ågren J., Huang J., Véronneau M., Wang Y.M., Roman D., Vergos G., Abd-Elmotaal H., Amos M., Barzaghi R., Blitzkow D., Matos A.C.O.C., Denker H., Filmer M., Claessens S., Oshchepkov I., Marti U., Matsuo K., Sideris M., Varga M., Willberg M., Pail R.: *Advances in the establishment of the International Height Reference Frame (IHRF)*. International Symposium on Gravity, Geoid and Height Systems 2018 (GGHS2018), Copenhagen, Denmark, 2018
- Sánchez L., Cioce V., Drewes H., Brunini C., de Almeida M. A., Gaytan G., Guagni H., Mackern V., Martínez W. A., Morillo A., Moya J., Parra H., Rodríguez O., Suárez N., Rudenko S.: *Time evolution of the SIRGAS reference frame*. 42nd COSPAR Scientific Assembly, Pasadena, CA, United States of America, 2018 (Poster)

- Sánchez L., Madzak M.: *GGOS activities related to the implementation of the International Height Reference System (IHRIS)*. EGU General Assembly, Vienna, Austria, 2018
- Sánchez L., Sideris M.: *Vertical Datum Unification for the International Height Reference System (IHRIS)*. International Symposium on Gravity, Geoid and Height Systems 2018 (GGHS2018), Copenhagen, Denmark, 2018
- Scherer D., Schwatke C.: *Automated Extraction of Time-Variable Water Surfaces based on Google Earth Engine*. Geodätische Woche, Frankfurt a. M., Germany, 2018
- Schmidt M.: *Combination of space-geodetic observation techniques for ionosphere modelling and space weather research*. Colloquium, 2018
- Schmidt M.: *Combination of Space-Geodetic Observation Techniques for Ionosphere Monitoring and Space Weather Research*. Geodetic Colloquium, 2018
- Schmidt M.: *Combination of space-geodetic observation techniques for ionosphere modelling and space weather research*. Astronomical Seminar, Bern, Switzerland, 2018
- Schmidt M., Börger K.: *Focus Area 04 – Geodetic Space Weather Research – Basic Ideas*. IX Hotine-Marussi, Rome, Italy, 2018
- Schmidt M., Börger K.: *GGOS Focus Area on Geodetic Space Weather Research*. EGU General Assembly, Vienna, Austria, 2018 (Poster)
- Schmidt M., Erdogan E., Farzaneh S., Forootan E.: *Assessing properties for near real-time estimations of the vertical total electron content of the ionosphere from GNSS data*. EGU General Assembly, Vienna, Austria, 2018
- Schmidt M., Erdogan E., Goss A., Dettmering D., Seitz F., Börger K., Brandert S., Goerres B., Kersten W.F.: *Ionospheric VTEC Modelling From Various Observation Techniques With Different Latencies by Means of Parallel Filtering and B-splines*. IX Hotine-Marussi, Rome, Italy, 2018
- Schmidt M., Erdogan E., Goss A., Dettmering D., Seitz F., Börger K., Brandert S., Görres B., Kersten W.F.: *Modelling of ionospheric parameters from various observation techniques considering different latencies*. SGI Workshop – Berlin, Berlin, 2018
- Schmidt M., Erdogan E., Goss A., Dettmering D., Seitz F., Börger K., Brandert S., Görres B., Kersten W.F.: *High-precision and high-resolution VTEC maps based on B-spline expansions and GNSS data*. IGS Workshop 2018, Wuhan, 2018
- Schmidt M., Erdogan E., Goss A., Dettmering D., Seitz F., Börger K., Brandert S., Görres B., Kersten W.F.: *VTEC modelling using multi-technique observations with different latencies: a parallel filtering approach*. EGU General Assembly, Vienna, Austria, 2018
- Schwatke C.: *EUROLAS Data Center (EDC) – Status Report 2016–2018*. 21th International Workshop on Laser Ranging, Canberra, Australia, 2018 (Poster)
- Schwatke C.: *EUROLAS Data Center (EDC) – Recent Developments (Site Logs, Station History Logs, and Data Transfer)*. 21th International Workshop on Laser Ranging, Canberra, Australia, 2018
- Schwatke C., Dettmering D.: *Database for Hydrological Time Series of Inland Waters (DAHITI)*. 2nd Mapping Water Bodies from Space Conference, Frascati, Italy, 2018 (Poster)

- Schwatke C., Scherer D.: *Automated Extraction of Time-Variable Water Surfaces based on Google Earth Engine*. 2nd Mapping Water Bodies from Space Conference, Frascati, Italy, 2018
- Seitz F.: *Plattentektonik, Erdbeben und Klimawandel: Wie bestimmt man ein stabiles Koordinatensystem auf einer sich ständig verändernden Erde?*. Förderverein Geodätisches Informationszentrum Wettzell (GIZ), 2018
- Seitz F.: *Forschungsprogramm 2016–2020 der Forschungsgruppe Satellitengeodäsie: Schwerpunkt Raumbezug*. Workshop der Forschungsgruppe Satellitengeodäsie, Bad Kötzing, 2018
- Seitz F.: *IAU Commission A2 'Rotation of the Earth': Upcoming period 2018-2021*. IAU General Assembly, Vienna, Austria, 2018
- Seitz F.: *Geodetic Earth Observation from Space: Research Activities at the Deutsches Geodätisches Forschungsinstitut (DGFI-TUM)*. Delegation visit from the Chinese Academy of Sciences (CAS) to DGFI-TUM, Munich, 2018
- Seitz F.: *Die Vermessung der Welt: Millimetergenaues Monitoring von Geodynamik, Plattentektonik und Erdbeben*. Tag der offenen Tür, Technische Universität München, Munich, 2018
- Seitz F.: *Geodätische Erdbeobachtung aus dem Weltraum: Aktuelle Arbeiten am Deutschen Geodätischen Forschungsinstitut*. DGK Annual Meeting, Munich, 2018
- Seitz F.: *Independent Generation of Earth Orientation Parameters: Work plan and achievements in project phase 1*. Critical Design Review to ESA project "Independent Generation of Earth Orientation Parameters", Darmstadt, 2018
- Wang Y.M., Forsberg R., Sánchez L., Ågren J., Huang J. : *Report on Colorado geoid comparisons*. International Symposium on Gravity, Geoid and Height Systems 2018 (GGHS2018), Copenhagen, Denmark, 2018

## 4.5 Participation in meetings, symposia, conferences

- 2018-01-29/31 : **SWARM Winter School (ESA SWARM Mission), Kühlungsborn, Germany**  
*Lalgudi Gopalakrishnan G.*
- 2018-02-07 : **Google Earth Engine Workshop, Munich, Germany**  
*Schwatke C.*
- 2018-02-02/03 : **Retreat of the Faculty of Civil, Geo and Environmental Engineering of the TUM, Berg, Germany**  
*Seitz, F.*
- 2018-02-19 : **ESA EOP project meeting, Munich, Germany**  
*Angermann D., Bloßfeld M., Kehm A., Seitz, F.*
- 2018-03-05 : **Coordination meeting, DFG RU NEROGRAV, Karlsruhe, Germany**  
*Seitz, F.*

- 2018-03-06 : **Annual meeting of DGK Section Geodesy, Karlsruhe, Germany**  
*Seitz, F.*
- 2018-03-08 : **Demonstration Definition Meeting, H2020 project Auditor, Athens, Greece**  
*Goss A.*
- 2018-03-09 : **Milestone meeting of Project TIK, IGG, Bonn, Germany**  
*Lalgudi Gopalakrishnan G., Schmidt M.*
- 2018-03-09 : **Thermosphere-Ionosphere Coupling (TIK) project meeting, Institute for Geodesy and Geoinformation, University of Bonn, Germany**  
*Lalgudi Gopalakrishnan G.*
- 2018-03-13 : **Geodetic Colloquium, TU Vienna, Austria**  
*Schmidt M.*
- 2018-03-19 : **Frühjahrestagung der Deutschen Physikalischen Gesellschaft (DPG), Würzburg, Germany**  
*Goss A.*
- 2018-03-20 : **FGS Board Meeting, Munich, Germany**  
*Schmidt M., Seitz F.*
- 2018-03-22 : **Review of SPP 1788 "Dynamic Earth", DFG, Potsdam, Germany**  
*Schmidt M.*
- 2018-03-23 : **Colloquium of the GFZ Department 1 'Geodesy', Potsdam, Germany**  
*Schmidt M.*
- 2018-03-25/29 : **27th International Polar Conference, German Society for Polar Research, Rostock, Germany**  
*Mueller F.*
- 2018-03-27/28 : **2nd Mapping Water Bodies from Space Conference, ESA-ESRIN, Frascati, Italy**  
*Schwatke C.*
- 2018-04-07 : **GGOS Coordinating Board Meeting, Vienna, Austria**  
*Angermann D., Sánchez L., Schmidt M.*
- 2018-04-09 : **GGOS PLATO Standing Committee Meeting, Vienna, Austria**  
*Bloßfeld M.*
- 2018-04-09/13 : **European Geosciences Union (EGU) General Assembly 2018, Vienna, Austria**  
*Angermann D., Bloßfeld M., Börgens E., Glomsda M., Göttl F., Schmidt M., Seitz F.*
- 2018-04-12 : **ILRS Analysis Standing Committee Meeting, Vienna, Austria**  
*Bloßfeld M.*
- 2018-04-12 : **UN-GGIM "GGRF" Subcommittee of Geodesy, Vienna, Austria**  
*Angermann D.*



- 2018-04-23/26 : **International Review Workshop On Satellite Altimetry Cal/Val Activities & Applications, Chania, Crete, Greece**  
*Dettmering D.*
- 2018-04-25/27 : **Workshop on Knowledge Gaps of Cryospheric Extremes, Finnish Meteorological Institute, Helsinki, Finland**  
*Müller F.*
- 2018-05-16 : **ESA EOP project meeting, Munich, Germany**  
*Angermann D., Bloßfeld M., Kehm A., Seitz, F.*
- 2018-05-28 : **Status Seminar of Project OPTIMAP, Uedem, Germany**  
*Erdogan E., Schmidt M., Seitz F.*
- 2018-06-03/08 : **10th IVS General Meeting, IVS, Longyearbyen, Svalbard, Norway**  
*Glomsda M.*
- 2018-06-11 : **DORIS Analysis Working Group (AWG) meeting of the International DORIS Service, Toulouse, France**  
*Rudenko S.*
- 2018-06-12/15 : **11th Coastal Altimetry Workshop and Coastal Altimetry Training, ESA/ESRIN, Frascati, Italy**  
*Passaro M., Piccioni G.*
- 2018-06-13/15 : **FGS-Workshop 2018, Bad Kötzting, Germany**  
*Angermann D., Bloßfeld M., Dettmering D., Sánchez L., Schmidt M., Seitz F.*
- 2018-06-15 : **DFG RU GlobalCDA, Kick-off meeting, Bonn, Germany**  
*Schwatke C.*
- 2018-06-18 : **ESA Sea State Climate Change Initiative, Kick-off meeting, ESA/ESRIN, Frascati, Italy**  
*Passaro M.*
- 2018-06-19 : **IX Hotine-Marussi Symposium, Rome, Italy**  
*Schmidt M.*
- 2018-06-28 : **SGI Workshop 2018, Berlin, Germany**  
*Schmidt M.*
- 2018-07-15/21 : **42nd COSPAR Scientific Assembly, Pasadena, USA**  
*Goss A., Rudenko S.*
- 2018-07-25 : **AUDITOR Final Review Meeting, Prague, Czech Republic**  
*Schmidt M.*
- 2018-08-27/29 : **XXXth General Assembly of the International Astronomical Union (IAU), Vienna, Austria**  
*Seitz, F.*
- 2018-09-11/13 : **VieVS User Workshop, TU Vienna, Vienna, Austria**  
*Glomsda M.*

- 2018-09-17/21 : **International Symposium on Gravity, Geoid and Height Systems 2018 (GGHS2018), Copenhagen, Denmark**  
*Sánchez L.*
- 2018-09-18 : **IDS Governing Board Meeting, Paris, France (via telephone)**  
*Dettmering D.*
- 2018-09-20 : **Kick-off meeting INSIGHT II, Munich, Germany**  
*Schmidt M., Goss A.*
- 2018-09-24/25 : **IDS Workshop, Ponta Delgada, Azores Archipelago**  
*Dettmering D., Rudenko S.*
- 2018-09-24/26 : **25 Years of Progress in Radar Altimetry Symposium, Ponta Delgada, Azores Archipelago**  
*Dettmering D., Passaro M., Piccioni G., Rudenko S.*
- 2018-09-25 : **Kick-Off Meeting TIPOD, Bonn, Germany**  
*Schmidt M., Zeitler L.*
- 2018-09-26 : **IDS Governing Board Meeting, Ponta Delgada, Azores Archipelago**  
*Dettmering D.*
- 2018-09-27/28 : **Ocean Surface Topography Science Team Meeting (OSTST), Ponta Delgada, Azores Archipelago**  
*Dettmering D., Passaro M., Piccioni G., Rudenko S.*
- 2018-09-27/28 : **FGS Retreat, Frankfurt a.M., Germany**  
*Bloßfeld M., Schmidt M., Seitz F.*
- 2018-10-02/05 : **GGOS Days 2018, Tsukuba, Japan**  
*Angermann D., Sánchez L.*
- 2018-10-05 : **Review Meeting, DFG RU NEROGRAV, Berlin, Germany**  
*Dettmering D.*
- 2018-10-08/12 : **Symposium SIRGAS2018, Aguascalientes, Mexico**  
*Sánchez L.*
- 2018-10-16/18 : **INTERGEO/Geodätische Woche 2018, Frankfurt a. M., Germany**  
*Mueller F., Glomsda M., Kehm A., Scherer D., Koenig P., Seitz F.*
- 2018-10-19 : **ESA EOP Critical Design Review, Darmstadt, Germany**  
*Angermann D., Bloßfeld M., Kehm A., Seitz, F.*
- 2018-11-04 : **ILRS Analysis Standing Committee Meeting, Canberra, Australia**  
*Bloßfeld M., Kehm A., Schwatke C.*
- 2018-11-04 : **ILRS Governing Board Meeting, Canberra, Australia**  
*Schwatke C.*
- 2018-11-05/09 : **21st International Workshop on Laser Ranging, Canberra, Australien**  
*Bloßfeld M., Schwatke C., Kehm A.*

- 2018-11-07 : **ILRS Data Formats & Procedures Standing Committee Meeting, Canberra, Australia**  
*Schwatke C.*
- 2018-11-07/09 : **DGK Annual Meeting, Munich, Germany**  
*Seitz, F.*
- 2018-11-26 : **Astronomical Seminar, Bern, Switzerland**  
*Schmidt M.*
- 2018-12-07 : **DFG RU GlobalCDA, First Status Meeting, Frankfurt am Main, Germany**  
*Dettmering D., Ellenbeck L.*
- 2018-12-08 : **IERS Directing Board Meeting, Washington D.C., USA**  
*Bloßfeld M.*
- 2018-12-10 : **GGOS BNO Meeting, Washington D.C., USA**  
*Bloßfeld M.*
- 2018-12-10/14 : **AGU Fall Meeting, Washington D.C., USA**  
*Bloßfeld M.*
- 2018-12-18 : **ESA CCI Sea State project meeting 2, Southampton, UK**  
*Boergens E., Passaro M.*

## 4.6 Guests

- 2018-02-05 : Prof. Dr. Eicker A., HCU Hamburg, Germany
- 2018-02-06 : Prof. Dr. Güntner A., GFZ Potsdam, Germany
- 2018-06-06 : Roggenbuck O. with a group of students, Jade University, Oldenburg, Germany
- 2018-07-03 : 25 heads of Chinese research institutions, Delegation of the Chinese Academy of Sciences (CAS), Beijing, China
- 2018-09-20/12-31 : Dr. Ren X., Wuhan University, China
- 2018-10-15/12-31 : Kanwal S., Department of Land Surveying and Geo-Informatics, Hong Kong Polytechnic University, China
- 2018-11-01/12-31 : Dr. Peng C., College of Geomatics, Xian University of Science and Technology, China
- 2018-12-11 : Doglioni F., Alfred Wegener Institut, Bremerhaven, Germany

## 5 Projects

*A large part of DGFI-TUM's research activities is financed through third-party funds from various sources. Funding of the following projects is gratefully acknowledged (in alphabetic order):*

- AUDITOR** Advanced multi-constellation EGNSS Augmentation and Monitoring Network (EU Horizon2020)
- CIEROT** Combination of space geodetic observations for the determination of mass transports in the cryosphere and their impact on Earth rotation (DFG)
- DAAD Thematic Network** Modern Geodetic Space Techniques for Global Change Monitoring (DAAD)
- DIGERATI** Direct geocentric realisation of the American reference frame by combination of geodetic observation techniques (DFG)
- ESA-EOP** Independent generation of Earth Orientation Parameters (ESA)
- FOR 1503, PN6-2** Consistent dynamic satellite reference frames and terrestrial geodetic datum parameters-2 (DFG)
- NEG-OCEAN** Variations in ocean currents, sea ice concentration and sea surface temperature along the North-East coast of Greenland (DFG)
- OPTIMAP** Operational Tool for Ionospheric Mapping And Prediction (ZGeoBw)
- ORG4Heights** Optimally combined regional geoid models for the realization of height systems in developing countries (DFG)
- REWAP** Monitoring and Prediction of Regional Water Availability for Agricultural Production under the Influence of Climate Anomalies and Weather Extremes (DFG/IGSSE)
- SPP 1788, INSIGHT-1** Interactions of low-orbiting satellites with the surrounding ionosphere and thermosphere (DFG)
- SPP 1788, INSIGHT-2** Interactions of low-orbiting satellites with the surrounding ionosphere and thermosphere (DFG)
- SPP 1788, MuSE** Multi-satellite reconstruction of the electron density in ionosphere and plasmasphere (DFG)
- SPP 1788, TIPOD** Development of high-precision thermosphere models for improving precise orbit determination of Low-Earth-Orbiting satellites (DFG)
- SLCCI** Sea Level Climate Change Initiative, Bridging Phase: Improvement of coastal sea level (ESA)
- SLCCI Plus** Sea Level Climate Change Initiative Plus (ESA)
- SSCCI Plus** Sea State Climate Change Initiative Plus (ESA)
- TIK** Entwicklung eines operationellen Prototyps zur Bestimmung der thermosphärischen Dichte auf Basis eines Thermosphären-Ionosphären Kopplungsmodells (BMW/DLR)
- WALESA** Refined estimates of absolute water levels for inland waters from multi-mission satellite altimetry (DFG)

## 6 Personnel

### 6.1 Lectures and courses at universities

**Angermann D. :** Lecture “Satellite Geodesy: Global Geodata for Society and Politics”, TUM, SS 2018

**Bloßfeld M. :** Lecture “Realization and Application of Global Geodetic Reference Systems”, TUM, SS 2018

**Bloßfeld M. :** Lecture “Earth System Dynamics”, TUM, WS 2017/18 and WS 2018/19

**Passaro M. :** Lecture “Oceanography and Satellite Altimetry”, TUM, WS 2017/18 and WS 2018/19

**Dettmering D. :** Lecture “Hydrogeodesy: Monitoring Surface Waters from Space”, TUM, WS 2017/18 and WS 2018/19

**Sánchez L. :** Lecture “Advanced Aspects of Height Systems”, TUM, WS 2017/18 and WS 2018/19

**Schmidt M. :** Lecture “Numerical Modelling”, TUM, WS 2017/18 and WS 2018/19

**Schmidt M. :** Lecture “Numerical Methods in Satellite Geodesy”, TUM, SS 2018

**Schmidt M. :** Lecture “Ionosphere Monitoring and Modeling”, TUM, WS 2017/18 and WS 2018/19

**Seitz F. :** Lecture “Seminar ESPACE”, TUM, SS 2018

**Seitz F. :** Seminar for Doctoral Candidates at the DGFI-TUM, TUM, WS 2017/18, SS 2018 and WS 2018/19

**Seitz F. :** Lecture “Earth Rotation”, TUM, WS 2017/18 and WS 2018/19

### 6.2 Lectures at seminars and schools

**Angermann D. :** Lecture “Geodäsie und Geoinformation”. Berufsinformationsveranstaltung, Gymnasium Raubling, 2018-03-08

**Seitz F. :** “Plattentektonik, Erdbeben und Klimawandel: Wie bestimmt man ein stabiles Koordinatensystem auf einer sich ständig verändernden Erde?” Förderverein Geodätisches Informationszentrum Wettzell (GIZ), 2018-03-22

**Angermann D. :** Lecture “Geodäsie - Die Vermessung der Erde im Wandel der Zeit”. Seminarvortrag, Schyren-Gymnasium, Pfaffenhofen a. d. Ilm, 2018-04-23.

**Dettmering D. :** “Wie verändert sich der Meeresspiegel? Eine wissenschaftliche Analyse von Satellitenbeobachtungsdaten der letzten 25 Jahre.” Förderverein Geodätisches Informationszentrum Wettzell (GIZ), 2018-06-15

**Angermann D. :** Lecture “Geodäsie und Geoinformation”. Berufsinformationsveranstaltung, Ignaz-Günther-Gymnasium, Rosenheim 2018-10-11.

**Schmidt M. :** Lecture “Combination of space-geodetic observation techniques for ionosphere modelling and space weather research”. Astronomical Seminar, University of Berne, Switzerland, 2018-11-26.

## 6.3 Thesis supervision

### Master Theses

**Seitz F., Passaro M.:** Master Thesis Wang Q., TUM/Wuhan University: Regional coastal altimetry in China based on multi-missions. 2018-06-01

**Seitz F., Passaro M.:** Master Thesis Tikhenko A., TUM: Retrieving coastal sea level from early satellite altimeters. 2018-09-14

**Seitz F., Dettmering D.:** Master Thesis Schaffhauser T., TUM: Analysis of extreme droughts in East Brazil based on satellite altimetry and other remote sensing techniques. 2018-09-17

**Seitz F., Passaro M.:** Master Thesis Nuñez Olivas A., TUM: Does the coastal mean sea level variability differ from the global trend? 2018-10-23

**Schmidt M.:** Master Thesis Zeitler L., TUM: Einfluss des Weltraumwetters auf geodätisch bestimmbare Ionosphärenparameter. 2018-11-30

**Seitz F., Passaro M.:** Master Thesis Barbieri E., TUM: Design and test of a scheme for performance assessment of Significant Wave Height data. 2018-12-04

### Doctoral Theses

**Seitz F.** (supervisor): Doctoral Thesis Börgens E., TUM: Water Level Modelling of the Mekong River Based on Multi-Mission Altimetry. 2018-03-14

## 6.4 Conferral of Doctorates

**Börgens E.:** *Title:* Water Level Modelling of the Mekong River Based on Multi-Mission Altimetry. *Supervisors:* Prof. Dr.-Ing. F. Seitz (TUM), Prof. Dr.-Ing. N. Sneeuw (University of Stuttgart), Prof. Dr. P. Knudsen (Technical University of Denmark). *Day of defense:* 2018-07-10. *Institution:* TUM

## 6.5 International Research Stays

**Bloßfeld M.:** Academic Institution: NASA Goddard Space Flight Center, USA  
Duration: 2018-02-06 until 2018-03-25

### TUM Graduate School

**Müller F.:** Academic Institution: Finnish Meteorological Institute, Finland  
Duration: 2018-04-03 until 2018-05-11  
Supervisor: Dr. Eero Rinne